Title

Penetration of horseradish peroxidase into the optic nerve after vitreal or vascular injection in the developing chick

Author

Kistler, Henry B

Publication Date

1981

Peer reviewed|Thesis/dissertation

PENETRATION OF HORSERADISH PEROXIDASE INTO THE OPTIC NERVE AFTER VITREAL OR VASCULAR INJECTIONS IN THE DEVELOPING CHICK

by

Henry Blackmer Kistler, Jr.

DISSERTATION

Submitted in partial satisfaction of the requirements for the degree of

DOCTOR OF PHILOSOPHY

in

Anatomy

in the

GRADUATE DIVISION

of the

UNIVERSITY OF CALIFORNIA

San Francisco

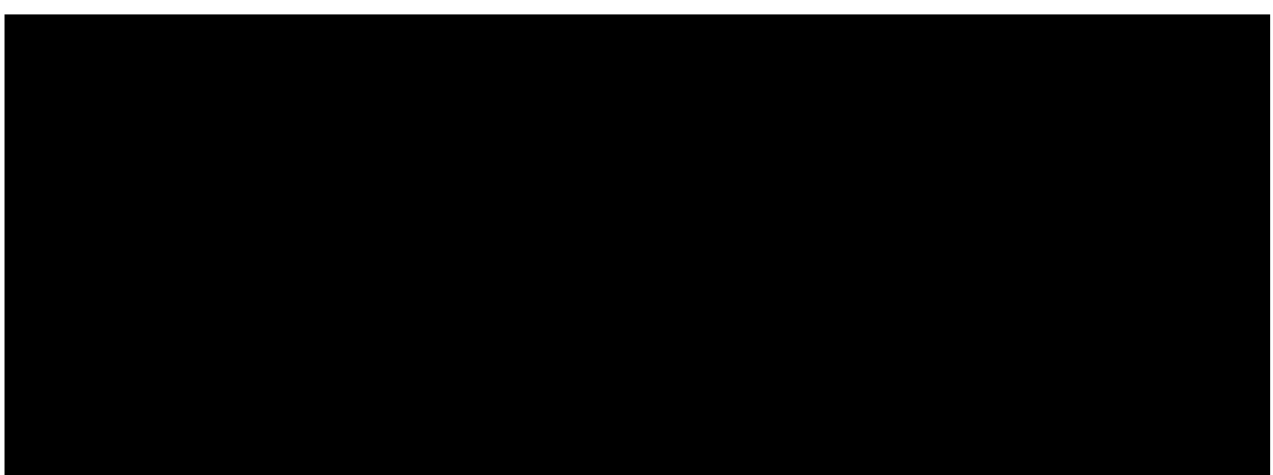

Date) University Librarian

APR 5 1981

Degree Conferred: . . . . . .

DEDICATION

I wish to express my deepest gratitude and appreciation to

Jennifer LaVail, for her patient support, guidance, and friendship

Ilene Sugino, a constant source of technical wisdom, moral support, and the best friend I ever hope to have

Edith Brown, for helping me to find the courage to meet myself

Cyndi Devlin Kistler, for the love and support that formed the foundation for the entire endeavor

The completion of this project is a tribute to the efforts of these people, I dedicate it to them.

TABLE OF CONTENTS

ABSTRACT

One of the critical assumptions made in many anterograde and retrograde axonal transport studies is that the spread of vitreally injected tracers into the optic nerve is limited. As a foundation for subsequent studies on retrograde axonal transport in the visual system of chick embryos, the spread of vitreally injected horseradish peroxidase (HRP) into the optic nerve was examined in chicks ranging in age from embryonic day 5 (E5), to 3 days posthatching (P3).

At E5.5, E13, and P3, HRP was found in the extracellular spaces surrounding optic nerve axons after intravitreal injections. Vitreally injected HRP was found to enter the periaxonal spaces of the optic nerve via two routes: 1) the marker passed directly across the inner limiting membrane and percolated through the extracellular spaces of the nerve, and 2) the marker spread within pericapillary spaces that surround the vessels of the nerve.

At E13 and P3 the spread of HRP from the vitreal surface in the pericapillary spaces exceeded the distance spread in the periaxonal spaces. Spread of vitreally injected tracer in the pericapillary spaces is dependent on the presence of a vascular plexus in the nerve. Vascular India ink injections demonstrated that the vascular invasion of the optic nerve begins on E8 and an extensive vascular plexus extending from the vitreal surface to the optic chiasm exists by E16. Thus, periaxonal spread from the inner limiting membrane accounted for HRP spread into the nerve prior to E8, and was subsequently supplemented by pericapillary spread after formation of the vascular plexus in the nerve.

To determine whether pericapillary HRP deposits might result from leakage of tracer from capillaries in the nerve, the distribution of HRP in the optic nerve after vascular injection was determined. Tracer leaked into the laminar region of the nerve from the space surrounding choroidal capillaries at E14 and P2. In addition, tracer leaked directly from capillaries in the nerve into the pericapillary and periaxonal spaces at E14 but not at P2. Thus, capillary impermeability that comprises a crucial component of the adult blood-brain barrier was not present at E14 but did exist at P2 in the optic nerves of developing chicks.

These results confirm previous findings of an apparent restriction in the spread of HRP percolating through the periaxonal space at all ages. The limited spread of HRP is thought to be a function of glial endocytosis of extracellular materials and not an occlusion of the extracellular space. The leakage of tracer into the nerve after vitreal or vascular injection is a potential source of artifact for studies utilizing the chick visual system.

ABBREVIATIONS

BBB	blood brain barrier
CNS	central nervous system
CSF	cerebrospinal fluid
DAB	diaminobenzidine
EBA	Evans blue-labeled albumen
ECS	extracellular space
EDTA	ethylenediamine tetraacetate
EM	electron microscopy
HRP	horseradish peroxidase
ILM	inner limiting membrane
ION	isthmo optic nucleus
IOP	intraocular pressure
MOPC	membrane associated orthagonal particle complexes
MP	microperoxidase
PE	pigment epithelium
TEM	transmission electron microscopy

I. INTRODUCTION

The composition of the fluids surrounding the parenchyma of the central nervous system (CNS) is influenced by barriers which prevent the free diffusion of materials. The blood-brain barrier (BBB) physically restricts the passage of large polar molecules from the circulation into the parenchymal extracellular space. At the same time, blood gasses, certain electrolytes, lipid-soluble non-electrolytes and certain ligands with affinity for endothelial carrier-mediated transport systems pass from the circulation and equilibrate quickly with the perivascular interstitial fluids of the CNS. Although the significance of this selective barrier is not clear, its presumed function is to provide metabolic necessities and to exclude extraneuronal and blood plasma constituents that might interfere with the normal functioning of the CNS.

The optic nerve and the retina originate from an embryonic outgrowth of the developing diencephalon. Numerous studies indicate that capillaries of the optic nerve and retina participate as barriers, similar to the BBB present in the majority of the CNS. Thus, the optic nerve and retinal fluid environment are similarly protected (with exceptions to be discussed later) from circulating and extraneuronal substances.

Little is known about the presence and location of barriers within the CNS that may compartmentalize the CNS fluid space by restricting the flow of macromolecules from one region to another. Such compartmentalization of CNS fluids might serve to maintain specialized environments for regions with specific metabolic requirements. Evidence suggests that the lamina cribrosa region of

the optic nerve may be the site of such an intra-CNS barrier to the equilibration of extracellular materials between the vitreous and optic nerve, the vitreal-optic nerve barrier. However, the paths of extracellular fluid movement and the factors responsible for blocking fluid movement in that region are poorly understood.

Clarification of the pathways of fluid movement in the optic nerve head and the extent of extracellular passage of soluble materials from the vitreous into the nerve would be useful for several neurobiological and clinical reasons. A variety of axonal transport studies are based on the premise that there is limited spread of tracers into the optic nerve after vitreal injections. It is therefore assumed that tracers subsequently localized in the nerve by scintillation counting, autoradiography, or histochemical reaction are transported intraaxonally. From recent studies, however, it is clear that a variety of materials pass from the vitreous into the extracellular spaces of the optic nerve of adult animals, as well as being transported intraaxonally. It is crucial, therefore, for the interpretation of axonal transport studies that the extracellular spread of tracers be considered. Understanding fluid movement in embryonic optic nerves is a similar prerequisite for evaluation of axonal transport by developing neurons.

An understanding of normal vitreal-optic nerve fluid movement may be significant clinically for studies of vitreal fluid movement under conditions of altered intraocular, intracranial, or intravascular pressure. Numerous studies suggest that anterograde and retrograde axonal transport are blocked under conditions of papilledema caused by increases in intracranial or intraocular pressure, but changes in

extracellular fluid movement and drainage of vitreal fluids under these conditions and their possible contributions to the observed pathological changes are largely unknown.

Further, a vitreal-optic nerve barrier might affect the accumulation of toxins which diffuse into the optic nerve from intraocular lesions. Accumulation of toxins in a particular region of the nerve might result in secondary pathological foci forming at the site of blockage. This might explain the common occurrence of optic neuritis occurring secondarily to primary intraocular inflammations of bacterial, viral, fungal, or parisitic origin. In addition, such a barrier might restrict the movement of a variety of blood-borne toxins or infectious agents once deposited in the nerve, and might explain the common occurrence of visual system pathologies after systemic exposure to a number of environmental contaminants (heavy metals, hydrocarbons), drugs or medications (quinine) or other infectious agents.

Although the presence of the blood-brain barrier during development has been studied in the past (see Saunders, '77 for review) the developing vitreal-optic nerve barrier has not been studied. I have therefore conducted a series of studies to define the vitreal-optic nerve barrier in the adult and developing visual system.

BACKGROUND

Blood-brain barrier - vascular permeability

In 1885, Erlich observed that intravenously injected acidic dyes penetrated freely into most tissues of the body, but not the brain or testes. Erlich presumed that the brain had failed to take up the

dyes. Later, the concept of a barrier preventing influx of substances into the brain, became popular. In 1950, Tschirgi showed that acidic dyes such as those used in vascular permeability studies quickly bound to plasma proteins in the blood. Thus, it was clear that the blood-brain barrier was restricting the passage of large protein-dye complexes and not simply the small dye molecules themselves.

Subsequent studies have shown that the blood-brain barrier, which protects the integrity of the fluid environment of the CNS, results from the blockage of substances at two distinct sites. Materials circulating in the blood-vascular system are blocked from the spaces surrounding neuronal constituents by specialized features of cerebral capillaries. In addition, substances are blocked from entering the neuronal parenchyma by the arachnoid membrane of the meningeal sheaths that surround and cover the surface of the CNS.

Investigators have appreciated the impermeability of cerebral capillaries for many years without understanding its structural bases. Substances pass from extraneuronal capillaries by diffusion, either across the cleft separating adjacent endothelial processes, or across open fenestrae, pores, or transendothelial channels in the luminal wall (Simionescu et al., '75; Wissig, '79). In addition, substances may cross the capillary wall by facilitated transport or within plasmalemmal vesicles. Studies with ultrastructural tracers such as horseradish peroxidase (HRP) or smaller heme peptides such as microperoxidase (MP) demonstrate that both the passive diffusion and facilitated movement of substances were blocked at cerebral capillaries (Reese and Karnovsky, '67; Brightman et al., '70a). The passive extracellular passage of tracer from cerebral capillaries was

blocked by a series of continuous occludens-type junctions between adjacent endothelial cell processes. Although tracer-filled vesicles were observed at the luminal surface of these capillaries, transendothelial movement and subsequent fusion at the abluminal surface was not observed.

Vessels of the optic nerve and retinae of species having vascularized retinae resemble the cerebral capillaries described by Reese and Karnovsky ('67). These vessels have reduced vesicular activity, have occludens-type endothelial junctions (Ishikawa, '63; Shakib and Cunha-Vaz, '66; Lasansky, '67) and they are impermeable to large tracer molecules. Light microscopically, substances such as trypan blue (Schnaudigel, '13; Palm, '47; Ashton, '65) colloidal carbon (Cunha Vaz et al., '66) Evans blue-labeled albumin (Olsson and Kristensson, '73) fluorescent diaminoacridines (Rodriguez-Peralta, '63, '66) and HRP (Olsson and Kristensson, '73) fail to pass from optic nerve or retinal capillaries after intravenous injection. After similar injections, electron microscopy studies showed that electron-dense tracers such as thorium dioxide (Shakib and Cunha Vaz, '66) microperoxidase (Smith and Rudt, '75) and HRP (Shiose, '70; Peyman and Bok, '72; Peyman and Apple, '72; Olsson and Kristensson, '73; Yamashita et al., '74; Tsukahara and Yamashita, '75; Tso et al., '75) failed to pass from these capillaries. From these tracer studies the permeability characteristics of optic nerve capillaries are seen to be similar to those of cerebral capillaries.

The avian retina is avascular but possesses a highly vascularized, fan-shaped structure, the optic pecten. The pecten is thought to play a nutritional role for the avian retina (Mann, '24a; Walls, '42) but

physiological evidence to support this contention is lacking. Although the light and electron microscopic structure of the pecten has been studied (Mann, '24a,b; Fischlschweiger and O'Rahilly, '66; Raviola and Raviola, '67), no one has yet studied the permeability of pecten capillaries after vitreal or vascular injections of tracer.

Blood-brain barrier - meningeal sheaths

A second component of the blood-brain barrier is the series of meningeal sheaths covering the optic nerve (Anderson, '69; Hogan, '71; Fine and Yanoff, '79). These are extensions of the cerebral meninges, the dura, the arachnoid, and the pia.

The dura covers the optic nerve. At the level of the globe it fuses with the outer layers of the sclera. Subjacent to the dura, and separated from it by the potential sub-dural space, is a highly cellular layer, the arachnoid membrane. The arachnoid is composed of a central, largely collagenous, core, covered on its free surfaces by stacks of flattened fibroblasts. Subjacent to the arachnoid, and superimposed on the surface of the nerve is a thin, vascularized sheath of fine collagen and elastic fibers, the pia. Numerous extensions of the pia, pial septae, containing collagenous and cellular connective tissue elements, surround blood vessels as they penetrate into the nerve. The pial sheath at the surface of the nerve and invading pial septae are separated from neuronal elements in adult optic nerves by a continous series of astrocytic foot processes.

The arachnoid sheath functions as a barrier to the entry of protein-bound tracers into the CNS (Tschirgi, '50). The layers of flattened fibroblasts are joined by occludens junctions which

presumably prevent the passage of extraneuronal substances into the nerve and similarly prevent constituents of the CNS fluid environment from escaping (Nabeshima et al., '75). At the optic nerve, diaminoacridines leaking from dural and extradural vessels after intravenous injections in a variety of species, fail to pass beyond the dura into the nerve (Rodriguez-Peralta, '66). After similar injections of Evans blue-labeled albumen (EBA) in rats and mice the extradurally leaking tracer "stopped abruptly at a level corresponding to the inner part of the optic nerve sheath," regardless of the duration of extraneuronal exposure. A similar barrier to intravenously injected sodium fluorescein has been reported by Grayson and Laties ('71).

Neither the pial sheath nor its subjacent astrocyte layer prevent passage of materials into the extracellular space surrounding neuronal elements of the CNS or specifically the optic nerve. When injected into the subarachnoid space, ferritin (Brightman, '65), fluorescent diaminoacridines (Rodriguez-Peralta, '66), iodinated bovine albumin (Lee and Olszewski, '60), HRP (Shabo and Maxwell, '71; Wagner et al., '74; Tsukahara and Yamashita, '75), fluorescein (Hayreh, '77), and fluorescein-labeled dextran (de la Motte, '78) pass the pia and subpial astrocytic layers and enter the perivascular spaces and extracellular space of the nerve (Cserr et al., '77).

Thus, it is clear that tracer materials circulating in the cerebrospinal fluid penetrate into the extracellular space of the optic nerve. Hayreh ('77) reports that 2 hrs after sodium fluorescein was injected into the cisterna magna of rhesus monkeys, the fluorescent tracer diffused forward from the subarachnoid space of

the optic nerve to the vitreous. From this study it is reasonable to assume that cerebrospinal fluid also enters the interstitial space of the optic nerve from the subarachnoid space, as has been shown in the CNS (Davson, '72).

Blood-brain barrier breach in optic nerve

Of crucial importance to this discussion of the origin and movement of fluid in the optic nerve is the possibility that the arachnoid barrier does not exist at the base of the optic nerve surrounding the lamina cribrosa. In fact, a variety of tracer studies, now suggest that a considerable amount of fluid flows from the peripapillary connective tissue into the lamina cribrosa and the prelaminar optic nerve.

Cohen ('73) described a potential disruption in the blood-retinal barrier at the lamina cribrosa in rhesus monkeys. He noted that the space surrounding connective tissue elements in the choroid was continuous with the space surrounding the glial processes (border tissue of Elschnig) that enclose the optic nerve elements. These glial processes were similar to those identified in nerve pia, in that they were not joined by junctions which might impede the extracellular passage of substances. Therefore, Cohen concluded that materials in the extracellular matrix of the choroid might be free to penetrate directly into the extracellular space surrounding elements of the nerve.

Tso and co-workers ('75) demonstrated experimentally that the anatomical breach that Cohen described was a functional breach as well. They showed that after its intravenous injection, HRP leaked into the choroidal connective tissue from capillaries of the choriocapillaris,

penetrated the border tissue of Elschnig, and surrounded elements within the nerve. Experiments appropriate to show such a breach in chicks have never been reported, but due to the consistency of this finding in other animals, it seems reasonable to assume that materials may leak into the optic nerves of posthatching chicks from perineurial capillaries in the choroid.

Vitreal-optic nerve fluid movement

Investigators have examined the posterior drainage of materials from the vitreous into the optic nerve for nearly a century (Hayreh, '66, for review). Original studies involve localizing tracers such as trypan blue, colloidal carbon or colloidal iron at various intervals following vitreal injections. The majority of early work was performed on rabbits and can be summarized as follows: 1) tracers penetrated into the optic nerve head and moved along vascular septae located close to the vitreal surface. 2) The tracer in the optic nerve head was located in the large connective tissue space surrounding the central retinal vessels. Tracer followed the course of these central vessels and extended along their length to their point of entry into the retrobulbar nerve. 3) Tracer could also be seen in small caliber offshots of septae, following small vessels which branched radially from the central vessels. Such tracer-containing septae often radiated out from the central vessels, extending to the pial surface of the nerve. 4) Tracer did not spread further from the vitreous into the nerve than the level at which the central vessels enter the retrobulbar nerve.

The use of ultrastructurally identifiable extracellular tracers such as HRP aided in demonstrating the posterior movement of vitreal

substances. HRP was found to pass freely beyond the inner limiting membrane and filled the extracellular spaces surrounding neural and glial elements of the retina and prelaminar region of the optic nerve head (Lasansky, '67; Peyman et al., '71; Peyman and Apple, '72; Peyman and Bok, '72). Peroxidase was also present within the perivascular spaces of septae which surrounded capillaries of the nerve head. Within these septae, tracer penetrated the vascular basement membrane of the nerve capillaries but was apparently blocked from entering the capillary lumen by endothelial junctions. The authors did not indicate how far the peroxidase penetrated along the nerve. Okinami and co-workers ('76) found that vitreally injected lanthanum nitrate spread into the optic nerve from the inner limiting membrane to the level of the retinal pigment epithelium. The lanthanum was also found in the extracellular and perivascular spaces of the nerve. These studies indicate that molecules as large as 40,000 MW (HRP) may pass from the vitreal space across the inner limiting membrane and its basal lamina into the optic nerve head.

Vitreal-optic nerve barrier

Rodriguez-Peralta ('66), was first to suggest that the penetration of substances from the vitreous into the optic nerve might be impeded by a barrier in the nerve. After vitreal injections of fluorescent diaminoacridines in rabbits, cats, dogs, guinea pigs, and primates, the tracer was densely distributed in the anterior prelaminar segment of the nerve. Tracer could not be detected in the laminar or postlaminar nerves of these animals. Bunt and co-workers ('74), also commented that no HRP was found in the optic nerves of rats after vitreal injections. When Kristensson and Wisniewsky ('76) injected

either HRP or fluorescein-labeled globulin into the vitreous in rabbits, they demonstrated a more extensive penetration of both tracers from the vitreous, beyond the lamina cribrosa and into the retro-laminar segment of the nerve. In their experiments, the extent of tracer spread did not vary after 2 or 27 hrs and did not vary in 11 day or adult animals.

In chicks, LaVail and LaVail ('74) detected a concentration gradient in HRP reaction product in the proximal segment of optic nerves 2, 11.5, and 42.5 hrs after vitreal injection. In addition, a barrier to materials moving from the brain to the eye was suggested from the observation that 25.5 hrs after optic tectum injections that diffusely filled the tecta, the optic tracts, optic chiasm, and distal optic nerves, HRP could not be detected in the extracellular space of the retina.

The studies mentioned above have shown that ultrastructural tracers such as HRP enter the optic nerve across the inner limiting membrane. As a whole, they also suggest that the movement of the tracer into the retrobulbar optic nerve may be impeded just beyond the level of the lamina cribrosa.

Several questions regarding the movement of tracers from the vitreous remain unanswered.

1) By precisely what routes do vitreally injected macromolecules penetrate into the optic nerve?
2) What is the rate that macromolecules travel from the vitreal surface and does the rate depend on which route the tracers take?

3) What factors are responsible for the concentration gradient of periaxonal tracer into the retrobulbar nerve?

In addition, a study of the vitreal-optic nerve barrier during the development of the optic nerve (not yet reported) might address these additional questions.

1) Do macromolecules penetrate into the optic nerve throughout development?
2) Does the distance a macromolecule spreads into the nerve vary for different developmental stages?
3) Is the spread of tracers into the optic nerve impeded throughout the development of the nerve?

To address these and other questions, I have studied the movement of intravitreally injected tracers during the development of the optic nerve. Specifically, I studied the extracellular spread of HRP from the vitreous into the optic nerves of embryonic and posthatching chicks by light and electron microscopy. In addition, to clarify questions of possible vascular contributions to optic nerve fluid and of the possible vascular conveyance of tracers into the optic nerve, I also studied the spread of HRP into the nerve after vascular injections.

I chose to study the chick visual system for several reasons. Primarily, the retina of chicks (in addition to other ground feeding birds and turtles) receives a projection from the isthmo-optic nucleus in the midbrain. Questions concerning the development of this projection may be addressed by experiments utilizing intravitreal injections of HRP. Understanding the vitreal-optic nerve movement of vitreally injected HRP during development is a crucial prerequisite

for analyzing those experiments. Technical advantages such as segregation of embryos from their mothers, and the easy accessibility of the embryos in their own protective compartments, also made the chick an attractive system for this study.

II. ANATOMY OF THE DEVELOPING CHICK OPTIC NERVE AND PECTEN

INTRODUCTION

Throughout this discussion of the development of the optic nerve head, pecten and retrobulbar optic nerve, I will concentrate on specific cellular structures or cellular relationships that might affect the spread of tracers within the optic nerve. Following this descriptive introduction, I will discuss experiments involving a) vitreal and b) vascular injections of HRP.

MATERIALS AND METHODS

A. Animals

White leghorn chicks and embryos were maintained in a forced draft incubator at 38°C. All embryos were staged at the time of fixation by the external morphological criteria described by Hamburger and Hamilton ('51). A series of embryos from embryonic day 5 (E5) to embryonic day 20 (E20) and posthatching chicks were prepared by a number of histological procedures and examined by light and electron microscopy.

B. Histological procedures

1.) Embryos at E6, E10, E13, E16, and E20 were fixed by immersion in either Bouin's fixative or in a 0.1 M Na cacodylate buffered (pH 7.4) fixative containing 2.5% paraformaldehyde, 3% glutaraldehyde, 0.12% $CaCl_2$ and 10% sucrose. The samples were dehydrated, cleared in toluene, embedded in Paraplast, sectioned at 8-10 μm thickness, and stained with thionine.

2.) Embryos at E8, E10, E14, E16 were perfused through a vitelline vein with an undiluted, undialized solution of India ink

(Higgins) immediately before decapitation and immersion fixation as described above. The corneas of these embryos were split but no further dissection was performed. After overnight fixation, the heads were rinsed in 0.1 M Na cacodylate buffer (pH 7.2) with 5% sucorse, frozen and sectioned at 150-200 μm on a freezing microtome. Serial sections were mounted on gelatin-coated slides, stained with thionine.

3.) All embryonic materials prepared for electron microscopy were fixed after decapitation in the cacodylate-buffered immersion fixative described above. Post-hatching birds were anesthetized with ether or Avertin (Lumb, '63) and perfused through the heart with 20 ml of 0.1 M cacodylate-buffer containing 0.9% NaCl, followed immediately by 150-300 ml of the 0.1 M cacodylate-buffered perfusion fixative (pH 7.4) containing 1% paraformaldehyde, 2% glutaraldehyde, and 0.12% $CaCl_2$, described above. After perfusion, the birds were decapitated, their corneas split, calvaria opened and the heads placed in fresh fixative. After an initial period of fixation (2-4 hrs), the optic chiasm was cut at the midline and the eys and attached optic nerves were removed and placed in fresh fixative. After an additional period of fixation, extraocular muscles and cartilagenous sheaths were removed from the back of the eye, and a 1 cm^3 segment including retina, optic disc, optic nerve, and pecten was removed from the eye. The optic nerves of all but the E6 eyes were bissected along the vertical meridian and replaced in fixative. Following a total period of fixation of 6-20 hrs the tissue was rinsed in 0.1 M Na cacodylate

buffer (pH 7.2) with 10% sucrose. The tissue was subsequently post-fixed in either a) 2% OsO_4 on 0.1 M Na cacodylate buffer (pH 7.2) plus 10% sucrose for 2 hrs on ice, or b) 1% OsO_4 plus 1.5% potassium ferricyanide in 0.1 M phosphate buffer (pH 7.4) with 10% sucrose either 2 hrs at room temperature or overnight at 4°C. Some tissue post-fixed in (a) was then stained en bloc in 2% aqueous uranyl acetate for 40-48 hours at 37-40°C. The hyperosmotic immersion and perfusion fixatives used undoubtedly caused shrinkage in the tissue. However, in comparisons with tissue fixed in lower aldehyde concentrations and with reduced osmolarity, these fixatives gave the most reproducible, informative, and visually appealing ultrastructural preservation.

All EM samples, except those stained en bloc with uranyl acetate were dehydrated in a series of graded ethanol and embedded in Epon-Araldite. Uranyl acetate stained tissue was dehydrated in a series of graded acetone and embedded in Epon-Araldite. 1-3 μm sections were cut with glass knives, stained with toluidine blue, and examined by light microscopy. Ultrathin sections, 700-1000 Å thick (as determined by interference refraction colors) were cut with a diamond knife, collected on 1-2 mm oval slot or 100 mesh formvar-coated copper grids and stained 10-20 min with 2% aqueous uranyl acetate and 1-2 min with lead citrate.

OBSERVATIONS

1) Retina

The light microscopic histological appearance of the developing retina was consistent with previous descriptions by Weysse and

Burgess ('06); Mann ('28); Coulombre ('55), and Romanoff ('60). Therefore, most attention will be paid to specific details rather than repeating the features already described.

The retina at E6, the youngest stage examined in the present study, consisted of a compact stratum of cells extending from the inner limiting membrane at the vitreal surface to the ventricular surface adjacent to the pigment epithelium.

End feet of Müller cell processes formed the inner limiting membrane (ilm) at the vitreal surface (fig. 1). The glial processes extended from the vitreal surface into the substance of the developing nerve. Membranes of the processes, although closely apposed were apparently not attached by junctional specializations near the vitreal surface. The lack of membrane specializations between processes of the inner limiting membrane and the patency of intercellular space between the glial end feet were consistent features of the inner limiting membrane throughout development. Electron dense particles, presumably glycogen, were present in these processes in samples not stained en bloc with uranyl acetate (fig. 1A). A continuous basal lamina was present adjacent to the inner limiting membrane, and was a consistent feature at all subsequent stages.

A proliferative zone, with occasional dense mitotic figures (fig. 2A) was present at the ventricular surface of the neural retinal layer. Cells of this zone were joined near the ventricular space by a series of zonulae adhaerentes (fig. 2B). These junctions (described previously by Sheffield and Fischman, '70) consisted of regions of close membrane apposition featuring cytoplasmic densities subjacent to both apposed membranes. The apposition of neural and

pigment epithelial layers appeared incomplete and the ventricular space was still distinguishable by light and electron microscopy (fig. 2A,B). The patent ventricular space was partially filled by cytoplasmic extensions from both the neural and pigment epithelial cells (fig. 2A,B).

At the vitreal surface on E13 the processes forming the inner limiting membrane had become flattened and elongated. As a result, the inner limiting membrane appeared as a thin, sheet-like series of processes at the vitreal surface (fig. 1B). At the ventricular surface adherens junctions and gap junctions were present at the ventricular surface. The arrangement of structures at this surface was interrupted in regions where photoreceptor outer segments had grown through the zone, projecting toward the pigment epithelium.

At P3, the inner limiting membrane resembles that of E13 embryos, a closely apposed but apparently unattached series of glial end feet. The terminal bar zone of the ventricular surface was present as the outer limiting membrane located at the base of the photoreceptor outer segments.

2) Pigment Epithelium

The pigment epithelium (PE) forms from cells of the primary optic vesicle after collapse of the vesicle to form the concave, two-layered optic cup. Immediately after the formation of the optic cup the PE is separated from the inner, neural retina, layer of the cup by a continuation of the ventricular cavity that once filled the primary optic vesicle. The ventricular space remains continuous with the ventricular space in the optic stalk and thus with the

intracerebral ventricular space for a brief period after formation of the optic cup (fig. 4A).

The pigment epithelium of the retina at E6 was a sheet of cuboidal epithelial cells containing a few scattered pigment granules. The apical surface of these cells (facing the ventricular space and the neural retina) featured numerous cytoplasmic extensions radiating from the cell body into the ventricular space (fig. 2). The flattened basal surface of the pigment epithelium was situated adjacent to a distinct basal lamina. Junctional complexes were present near the apical surface of adjacent PE cells. Gap junctions, tight junctions, and apparent desmosomal contacts were present at E6. The junctional complexes joining adjacent PE cells were more clearly defined at later stages. Tight junctions (as characterized by a series of membrane fusion sites) were detected next to gap junctions present near the apical surface of adjacent cells (fig. 3A). The convoluted nature of these PE cells and their joined lateral surfaces, made unambiguous identification of the occludens junctions difficult. Nevertheless, suitably sectioned, clear examples of tight junctions were found.

No space separated neural and pigment epithelia of the retina at E13. The apical cytoplasmic extensions of the PE cells enveloped the differentiating photoreceptors and undifferentiated neuroblasts at the proliferative zone.

The basal surface of the pigment epithelium was marked by a series of infoldings at E13. The resulting foot-like extensions formed roughly planar array adjacent to a basal lamina. A basal lamina (which along with surrounding connective tissue elements

comprise Bruch's membrane) was a consistent feature separating the basal processes of the PE from adjacent choroid capillary bed.

3) Pecten

In the adult chicken, the pecten consists of a series of 18 folds or pleats composed of vascular elements and pigmented interstitial cells. The folds are anchored along the course of the embryonic choroid fissure. The unanchored ends are bound to a strip of tissue that bridges the fibrillar elements of the vitreous.

The histologic appearance of the pecten during development was consistent with previous studies of the development and histology of the structure (Mann, '24a,b; Romanoff, '60; O'Rahilly and Meyer, '61; Raviola and Raviola, '67; Fischlschweiger and O'Rahilly, '66; Seaman and Storm, '63). Again, only selected features will be discussed here.

At E6, a small cluster of cells was apparent in the trough formed at the choroid fissure. These cells, Bergmeister's papilla (Mann, '24a) were destined to become the optic pecten. Small blood vessels of unknown origin were present in this cellular cluster (fig. 6A). A strand of tissue was occasionally present extending from the vitreal surface of the eye across the vitreal chamber, and terminating at Bergmeister's papilla. It was not clear whether the strand represented the vestigial remains of the arteria cupulae opticae as suggested by Mann. The cluster of cells representing Bergmeister's papilla was covered at the vitreal surface by a basal lamina.

By E13, the pecten had become a series of elongated hollow folds of tissue extending into the vitreous. These folds were composed of immature vascular elements interspersed in roughly equal numbers with sparsely pigmented interstitial cells (fig. 6B). A basal lamina,

continuous with that adjacent to the inner limiting membrane of the retina, surrounding each of the pecten folds. A similar basal lamina also surrounded the interstitial cells within the folds (fig. 7A). The surface of the pecten folds was made up of numerous cell bodies and foot processes of the interstitial cells. Adjacent processes were not joined by junctional specializations and did not form a continuous sheath surrounding the folds. Thus, at E13 and subsequent ages the basal lamina surrounding the entire surface of each pecten fold was the sole continuous physical structure separating the vitreal space, the extracellular space within the pecten folds, and the contents of the pecten capillaries.

At the base of the pecten was a region of scattered cellular and vascular elements which extended from the vitreal surface. Axonal profiles were never seen within the base tissue at any stage, although no physical barrier separated the neural tissue from the base tissue.

Although the folded appearance of the pecten did not change between E13 and P3, the distribution of cellular constituents changed considerably. At P3, the pecten folds contained more vascular than interstitial cells (fig. 6C). Numerous longitudinally and transversely sectioned capillary profiles filled the pecten folds. Stellate, pigmented interstitial cells (previously scattered throughout the folds) were compressed into intersticies of the pecten capillaries. The cytoplasm of these pigmented cells had changed from one characterized by numerous mitochondria and polysomal arrays to one containing enlarged Golgi complexes, and rough endoplasmic reticulum whose cisternae were dilated and filled with flocculant material. Large surfaces of interstitial cells were in close

apposition, and occasionally junctional specializations were identified between these cells (fig. 7B).

4) Optic Nerve

The optic nerve at E6 was composed of scattered cellular and axonal profiles surrounded by extensive extracellular spaces. A proliferative zone of densely packed cells surrounded the patent ventricular channel connecting the remnants of the primary optic vesicle lumen and diencephalic ventricular cavity. The proliferating cells of the optic stalk are thought to differentiate exclusively into glial cells (Vaugn, '69) and it is presumed therefore, that the cells within the nerve are either glioblasts, differentiating glial precursors, or invading vascular elements from the surrounding extraneural vascular plexus.

Occasionally, the cells of the optic stalk were arranged in loose, longitudinally-oriented strands (fig. 4B), that were partially surrounded by an incomplete and poorly organized chain of glycogen-containing foot processes. The system of processes resembled astrocytic foot processes that were seen in later development surrounding vascular elements. However, the clustered cells formed no lumina at this stage, and collagen fibrils were never present within the space defined by the foot processes. By these criteria, the cellular clusters failed to qualify as vascular elements. The nerve was occupied principally by unmyelinated axonal profiles at E6, with the appearance of myelinated fibers by E13. No vascular structures were seen in the retrobulbar optic nerve at E6.

By E13, the nerve had lengthened considerably. Chains or clusters of vascular cells were enwrapped by glial processes. Collagen bundles

were present within the perivascular spaces. Thus, they were identified as developing vascular elements.

At the back of the eye, bundles of collagen and other cellular connective tissue elements formed scleral trabeculae surrounding vascular elements as they entered the nerve (fig. 5A). A sheath of glial foot processes was interposed between the contents of the trabeculae and the surrounding neural elements.

Two groups of glial cells were distinguished on the basis of their location in relation to vascular bundles (fig. 12). The first group, located perivascularly, was composed of large cells with pale staining nuclei and cytoplasmic matrix. The second group was a mixed population of cells arranged in longitudinal clusters and situated further from vascular septae than the first group. The clusters were composed of cells identical to the presumptive astrocytes of the first group and smaller, densely stained cells presumed to be developing oligodendrocytes. From random observations of 1-4 μm thick plastic sections, it appeared that these clusters of cell bodies did not border vascular bundles. Between E6 and E13 a considerable reduction in extracellular space occurred in the optic nerve.

The optic nerve underwent a period of considerable growth between E13 and P3. The extracellular space was drastically reduced and the density of neural, glial and vascular elements increased in the nerve. Light microscopically, the scleral trabeculae first seen at E13 in the retrobulbar nerve trabeculae appeared more attenuated and more sharply defined than at E13 (fig. 5B). The trabeculae were also more densely packed with collagen and cellular connective tissue elements.

5) Vasculature

a) Optic Nerve

Although the timing of the vascular invasion of the optic nerve was not the principle concern of this study, I have followed this in the series of embryos receiving vascular India ink injections. At E6 and E8, the only ink-filled vessels in the nerve were anastomotic branches of the short posterior ciliary arteries extending from the perineurial connective tissue to Bergmeister's papilla at the base of the developing pecten (fig. 8A,B). By E10, numerous vessels entered the lamina cribrosa from the surrounding connective tissue (fig. 8C). These vessels formed a net-like vascular complex in that region. Branches from that network extended longitudinally within the nerve, joining with branches of pial vessels emanating from the surrounding meninges along the length of the nerve. At E13 and E16 ink-filled vessels formed a progressively more complex vascular plexus within the nerve. The only difference was in the increase in vessel branching and the resulting, increased density of the vascular net in the nerve (fig. 8D).

By EM it was impossible to identify vascular elements until adjacent cells within a vascular sprout had joined to form a lumen. At E6, such vascular cells, present in Bergmeister's papilla, were not detected in the retrobulbar region of the optic nerves. By E13, endothelial cells, identified by this criterion, were present in all regions of the nerve (fig. 9A,B). Where adjacent processes forming a capillary lumen came in close apposition, specialized sites were present, often taking the form of amorphous cytoplasmic densities beneath the apposed membranes. When appropriately sectioned, sites

of apparent membrane fusion (in which the hydrophobic regions of the two adjacent membranes joined to form a single region) were detected at these sites (fig. 9C).

At E13 and P3 the lumens formed by such fused endothelial processes varied considerably in shape. Some appeared as thin, convoluted "collapsed" channels surrounded by thick regions of endothelial cytoplasm. Numerous cytoplasmic processes protruded from the endothelial walls into the lumens. In contrast, other capillaries had rounded open lumens formed by attenuated endothelial walls with few, if any, cytoplasmic extensions projecting into the luminal spaces. The thickened endothelial processes forming the capillary walls of the "collapsed" capillaries are filled with a variety of cytoplasmic components, most prominently, arrays of ribosomes, mitochondria, RER, and Golgi complexes. By contrast, the thin attenuated walls of "open" capillaries were relatively devoid of organelles and the cytoplasmic constituents mentioned above were concentrated in the perinuclear cytoplasm adjacent to a thin, sickle-shaped nucleus (fig. 10A).

At E13, most capillaries had "collapsed" lumina while at P3, the majority were "open" and rounded. Whenever a lumen was present within endothelial cell processes at E13 or P3, no matter how attentuated its boundary, it was bounded and closed by junctional specializations (fig. 10B). From my thin-sectioned transmission electron microscopy (TEM) views of these capillaries, no instances were identified in which the apposed membranes of such junctions clearly <u>lacked</u> points of fusion.

Capillaries in the optic nerve were enclosed within a pericapillary space, bounded by a series of astrocytic foot processes. At E13, these processes appeared often as a disorganized system of attenuated end feet (fig. 9A,B). The processes were often separated by gaps, sometimes as large as 0.5 μm that connected the periaxonal and pericapillary extracellular spaces. By P3, this astrocyte sheath consisted of several layers of processes, prominently filled with bundles of astrocytic filaments. Gap junctions and desmosomes were present between processes of the astrocyte sheath (most prominently at P3 and older stages) (fig. 10C,D). Although some processes at E13 and all processes at P3 were closely apposed, the extracellular space was not apparently occluded.

The pericapillary space situated between the endothelial cells and the surrounding astrocytic sheath, contained presumptive fibroblasts, pericytes, and bundles of collagen (fig. 10A). In addition, two basal laminae formed in this space, one adjacent to the astrocyte sheath processes, and another, surrounding the vascular and extravascular cells of the pericapillary space. The glial basal lamina was detectable first as a discontinuous lamina at E13. By P3, both glial and vascular laminae were present.

b) Retina

The chick retina is an avascular structure that is principally supplied with nutrients via the fenestrated capillaries of the choriocapillaris. A second source, the capillaries of the highly folded and vascularized pecten, has also been proposed.

c) Choriocapillaris

At E6, mesenchymal elements have congregated near the basal surface of the PE in the future choroid. Endothelial cells were found among these disorganized cells and cytoplasmic extensions. The cytoplasmic extensions which form the capillary lumens were almost devoid of vesicular profiles, pores or channels which span the width of the wall and few fenestrae were detected.

As in the nerve, endothelial processes were joined by junctional complexes between the adjacent processes to form a lumen (fig. 11D). Due to the relative scarcity of capillaries at E6 and the difficulty in obtaining views with junctions sectioned precisely perpendicular to their opposed membranes, only a few endothelial junctions of these immature capillaries have been examined. However, of those studied, no junction clearly lacked membrane fusions characteristic of tight junctions. A consistent characteristic of these capillaries throughout development therefore is the presence of at least one point of membrane fusion at the junctional site.

At E13, the choriocapillaris was composed of a series of rounded or oval capillaries arranged in a linear array and running parallel to the PE and its basal lamina. The cytoplasmic extensions are thicker along the capillary surface adjacent to the PE. Again, few cytoplasmic inclusions such as vesicles or pores, were present in the capillary walls. Fenestrations were also rare. The endothelial cell bodies of these capillaries were more often found at either end of the capillary lumen rather than within the luminal wall which faces the pigment epithelium at this age. As was seen at E6, the endothelial junctions were characterized by 1-4 points of apparent membrane fusion between the apposed membranes.

At P3, several new features of the choriocapillaries were apparent. First, the capillaries had obviously elongated, along the plane of the choroid. Second, the capillaries were polarized, in that the cell body and majority of the cytoplasmic organelles were congregated within the wall opposite the PE and the wall adjacent to the PE was much thinner and depleted of organelles.

A third new feature of these capillaries at P3 was the appearance of a variety of openings spanning the luminal wall facing the PE. These openings seem to be of two distinct types. One opening was a fenestrae similar to those described previously by a number of workers (a, in fig. 11A) (Maul, '71; Raviola, '77; Spitznas and Reale, '75; Hudspeth and Yee, '73). These fenestrae consisted of a distinct gap in the luminal wall. The luminal wall on either side of the gap narrowed to a point at the edge of the gap. The gap was spanned by a single fuzzy "diaphram" which often contained a small globular particle or central knob half way from its lateral edges.

The second opening, a vesicular pore, was possibly the product of the simultaneous fusion and opening of a cytoplasmic vesicle at the luminal and abluminal surfaces of the capillary wall. As previously described (Maul, '71; Palade and Bruns, '68; Kuwabara, '79), these pores were easily distinguishable from the fenestrae in that their lateral walls formed a concave, rather barrel-shaped configuration (b, in fig. 11A). In addition, there were often two distinct fuzzy diaphrams spanning the luminal and abluminal openings of the same pore. Occasionally, a central globular particle could be distinguished in each diaphram of a single pore.

In a fortuitous tangential section through a portion of the capillary wall containing these openings, circular openings with a dense spot in their center (fig. 11B) were clearly seen. Previous reports of freeze-fractured endothelial cells had assumed these circular tangential profiles and similar circular openings to be fenestrae but due to the similarity between the fenestrae and pores as demonstrated in figure 11A, it is unclear whether the structures seen in figure 11B constitute views of one opening and/or the other.

d) Pecten

Since the structure of pecten capillaries in a P3 chick was similar to that previously described in adult pigeon (Raviola and Raviola, '67) once again I shall concentrate on selected features. In this section I shall begin discussing features of the P3 pecten and compare these observations with those on E13 animals.

Profuse slender processes extended radially from both the luminal and abluminal surfaces of P3 pecten capillaries (fig. 7A,C). The processes extending from the basal, abluminal surface of the capillary wall were shorter than those extending into the lumen. The cytoplasmic extensions forming the walls of the capillary were joined by tight junctions and contained a number of vesicular profiles and sites where similar vesicles (some coated) were either pinching off from or fusing with the luminal surface in the trough between adjacent radial processes (fig. 7C). These junctions were conspicuous by the cytoplasmic density adjacent to the two joined membranes. On fortuitous sectioning it was clear that the adjacent membranes were joined by one or more discrete points of membrane fusion. The perinuclear cytoplasm contained many free ribosomes and

well developed Golgi complexes. The basal processes of the capillaries were surrounded by a basal lamina which separated the vascular from extravascular elements within the folds.

Pecten capillaries in E13 embryos by contrast were similar to the "collapsed" capillaries intrinsic to the nerve were present with their tortuous, attenuated lumens. Regardless of the luminal configuration, adjoining endothelial processes forming the lumen walls were invariably joined by tight junctions as described above.

DISCUSSION

In this anatomical introduction, I described several anatomical features that might form the basis for control of the movement of soluble materials in the developing chick retina and optic nerve. Appreciation of the structure and arrangement of these elements and how they change during development will be useful for evaluating data from experiments involving tracer injections into the vitreous or the blood vascular system. In lieu of a prolonged, detailed evaluation of each aspect of the developing nerves, I will summarize my observations on specific, important elements.

The extracellular space, thought to be occluded by points of membrane fusion at tight junctions, is not blocked at gap junctions or desmosomes (McNutt and Weinstein, '73). Thus, regardless of the configuration of junctional complexes between PE cells, until tight junctions are present the transepithelial movement of materials between the retina and choroid is directly affected by the appearance of tight junctions during development. The presence of these

junctions at E6, the earliest stage examined, suggests that the passage of materials across the PE is blocked, or at least impeded from an early stage onward.

The inner limiting membrane (ilm), a discontinuous series of astrocytic foot processes and its associated basal lamina, are continuous, situated at the vitreal surface of the neural retina. They form the boundary between the vitreal fluid and the interstitial space of the retina and optic nerve head.

The inner limiting membrane is present throughout the developmental period of my study. As described by Coulombre ('55) it first appears at the fundus region of the developing retina at E4. The processes comprising the ilm changed from large, bulbous profiles at E6 to extremely thin, attenuated structures at P3.
Regardless of variations in the shape of the component processes, an extracellular space is always discernible between adjacent processes of the ilm. Thus, a physical continuity between the vitreal space and the interstitial space of the retina and optic nerve is present throughout development.

A basal lamina was also present at all ages examined. It lines the vitreal surface of the inner limiting membrane. The basal lamina extended to cover the surface of the pecten. The thickness of the lamina, its filamentous appearance, and its separation from the inner limiting membrane at the retinal surface varied slightly during development.

The developmental expansion of vascular basal laminae in other studies and sites has been reported previously (Donahue and Pappas, '61; Bär and Wolff, '72). These basal laminae consist of acidic

muccopolysaccharides, glycosaminoglycans and various forms of filamentous proteins. However, it is not clear whether certain of these components are deposited sequentially or if the lamina expands by gradual accumulation of all components. An organized substructure of anionic sites can be demonstrated in basal laminae of rat renal glomeruli using cationic substrates such as lysosyme, cationized ferritin, and ruthenium red, that bind to anionic sites within the laminae rarae. A lattice-like arrangement of anionic sites is revealed (Kanwar and Farquar, '79; Rennke et al., '75; Rennke and Venkatachalam, '77). It is not clear if this lattice-like substructure has any significance either for the integrity of the basal lamina or for its functional properties as a potential molecular seive (see chapter 3, discussion).

The filamentous nature of the basal lamina at the retinal surface, in addition to its possible influence on solute passage, is also important for interacting with structural elements of the vitreous body. The vitreous is not simply a fluid mass but is actually a connective tissue with a distinct topography, structure, and population of cells (hyalocytes) (Balazs et al., '65; Jaffe, '69). The vitreous consists of a dilute solution of salts with low concentrations of plasma proteins, acidic glycoproteins, and the muccopolysaccharide hyaluronic acid, contained in a fine meshwork of residual protein collagen. At the periphery or cortical region of the vitreous these collagenous elements condense and interact with the basal lamina near the ora seratta and at the base of the pecten, anchoring the vitreous at those sites (Warwick, '76).

The vitreous exists as both gel and fluid states. The gel phase develops first. The liquid phase appears at E10 and forms at the base of the developing pecten (Balazs et al., '65). The liquid phase subsequently expands and assumes a central position in the vitreal chamber, surrounded by gel. Although no physical barriers separate the anterior and vitreous compartments of the eye, many solutes show significant concentration differences between these compartments and the blood plasma or plasma dialysate (Bito and deRousseau, '79).

The "mature" capillaries of P3 chick optic nerves show the same structural specializations described by Reese and Karnovsky for cerebral capillaries and by Ishikawa ('63), Lasansky ('67), and Shakib and Cunha-Vaz ('66), for mammalian optic nerve capillaries. Specifically, the capillary walls are composed of attenuated endothelial processes containing few vesicular profiles, and adjacent processes are joined by occludens junctions marked by multiple sites of fusion between the apposed membranes.

The intrinsic capillaries of P3 nerves are the central element of the vascular unit composed of endothelial cell and a surrounding basal lamina. It is contained within a pericapillary space, bounded by a series of astrocytic foot processes and their adjacent basal lamina. The structure of the basal laminae (after conventional EM processing) associated with a) capillary endothelia, b) perivascular glial processes, or c) inner limiting membrane of the retina are all similar. Obviously, however, the composition, anionic substructure, or permeability characteristics of these different structures may vary.

The space separating the glial and endothelial basal laminae, the perivascular space, contains collagen and other connective tissue elements. As one follows cerebral vessels from the pial surface, the glial and endothelial basal luminae apparently fuse, thus occluding the perivascular space (Woolam and Millen, '54; Jones, '70; Davson, '72). In the laminar and retrobulbar regions of the chick optic nerve, however, this occlusion of perivascular space is rarely seen.

Although the appearance of many optic nerve capillaries of E13 and P3 was variable in several ways, these capillaries were similar to optic nerve and cerebral capillaries in mammals. Specifically, few vesicles were seen within the often bulbous endothelial walls outlining all discernible capillary lumens, no matter how small or contorted the luminae appeared. In addition, the endothelial processes were invariably joined by junctional specializations. Although the specific interrelationships of the apposed membranes were not always obvious due to inappropriate planes of sectioning, in cases where the membranes were clearly visualized, the junctional region was marked by at least one point of apparent fusion of the apposed membranes.

In contrast to the capillaries of P3 optic nerves, the concentrically layered structures of the vascular unit are either absent or incomplete at earlier stages. My observations are consistent with a sequence of events which has been described previously in other developing and regenerating systems (Sandison, '32; Clark and Clark, '39; Cliff, '63; Schoefl, '64). Vascular cells sprout from existing blood vessels and form chains which

extend from the surface of the CNS into the neuronal parenchyma. Adjacent cells of these chains form junctions which mark the boundaries of the convoluted lumens of immature capillaries. A number of the features of the "collapsed" capillaries found predominantly at E13 such as the large, rounded, nuclei, the convoluted luminal spaces, and the thickened capillary walls resemble previous descriptions of growing vascular sprouts. A series of glial processes subsequently forms around the vascular sprouts, interposed between vascular and neuronal structures (Donahue and Pappas, '61; Caley and Maxwell, '70; Phelps, '72). Finally, as the capillary lumens expand, the luminal walls attenuate, and the glial sheath becomes complete, the maturing vascular and glial elements deposit basal laminae which line the inner surfaces of the pericapillary space (Caley and Maxwell, '70; Phelps, '72).

As in any anatomical study, the conclusions drawn from experimental observations are subject to the limitations of the procedures and conditions employed in the study. The timing of optic nerve vascularization, location of initial vascular invasion, and hypothetical sequence of steps involved in the process depends on several assumptions. The thin plastic sections necessary to achieve useful resolution in TEM offer a drastically reduced sample of any given piece of tissue. Using such sections is quite useful in identifying structures by their ultrastructural features but are of limited assistance in surveying a large volume of tissue for the initial appearance of a specific structure. Once the feature is present the same sampling problems make it equally difficult to map out the feature's distribution within the host

structure. In an effort to circumvent this sampling problem I sought to highlight the vascular structures by filling them with colloidal carbon particles visible by light microscopy. In this way, I could examine the entire developing nerve in a limited number of sections, and could simultaneously ascertain the presence and distribution of the filled vessels.

An additional uncertainty of these experiments lies in the degree to which the vascular plexus in the nerve was filled by the India ink perfusions. Images of the filled vascular plexus at E16 suggest that small caliber cerebral and optic nerve vessels are filled extensively but this does not preclude the possibility that spasms of established vessel walls or occlusion by the accumulation of carbon particles might prevent the complete filling of the optic nerve's vasculature. Moreover, the possibility exists that growing vessels are not filled. Growing vascular sprouts are described as closed ended tubes which fuse with adjacent vessels and establish continuity between their lumen and that of the "target" vessel. It is unclear whether materials such as tracer substances enter into the blind, tubular, vascular sprouts before those sprouts fuse with another sprout. If filling is variable or incomplete, then the distribution of vessels "labeled" by India ink would not accurately reflect the total population of vessels present in the nerve and would not be a reliable gauge for the initial appearance of new sprouts in the nerve.

A great deal of uncertainty in the size, shape, distribution and inter-relation of cellular structures is generated by a variety of the preparative processes associated with electron microscopy.

One example of such uncertainty comes in the estimation of extracellular space in the developing nerve. My electron micrographs clearly show a reduction in the extracellular space during the development of the optic nerve. This reduction in extracellular space (ECS) corresponds to similar findings in different systems using physiological (Flexner and Flexner, '49; Flexner and Flexner, '50; Lajtha, '57; Vernadakis and Woodbury, '65; Barlow et al., '61) and anatomical (Karlsson, '69; Sumi, '69; Caley and Maxwell, '70; Pysh, '69) techniques.

Whether the representation of ECS in electron micrographs at each age is accurate or whether the relative spaces at different ages can be compared is unclear. Considerable swelling of neuronal elements (and reciprocal shrinkage of ECS) occurs during asphixiation, anoxia, and also during immersion or perfusion fixation with hyperosmotic mixtures of glutaraldehyde (Van Harreveld, '72; Pappius, '75). Sumi ('69) found that immature rat CNS was particularly sensitive to such fixation conditions. Van Harreveld suggests that under these conditions, cellular membranes become permeable to Na^+ resulting in the influx of NaCl and an osmotic equivalent of water from the extracellular space into the intracellular space. Thus, extracellular material is taken up by cellular elements which then swell. These examples point out that not only do fixation conditions affect tissue but that developing tissue may be affected differently at different stages. This situation obviously necessitates caution when comparing tissue from different stages of development.

III. PENETRATION OF HORSERADISH PEROXIDASE INTO THE OPTIC NERVE AFTER VITREAL INJECTION.

INTRODUCTION

In mammalian species, the extracellular spaces of the optic nerve head are continuous with the vitreal space of the eye as determined by the diffusion of extracellular tracers. However, beyond the optic nerve head the concentration of markers such as horseradish peroxidase (HRP) is markedly reduced with distance from the lamina cribrosa to more distal points along the nerve. Whatever the physical or physiological cause for the reduction in concentration in the adult nerve, such a barrier regulates the concentration of retinally synthesized extracellular molecules within the optic nerve. During development, diffusible trophic substances might also be controlled, thus affecting the timing or coordination of differentiation in the retina or optic nerve.

Thus far, the presence of a barrier to diffusion of extracellular markers from the eye has not been confirmed in embryos. Its existence and the timing of its appearance would have an important influence not only on our understanding of the differentiation of the retina and optic nerve, but also on the interpretation of axonal transport studies in embryonic systems.

I have, therefore, studied the extracellular spread of HRP from the vitreous to the optic nerve in developing chick embryos by light and electron microscopy. In addition, I compared the spread of HRP with the spread of a larger colloidal tracer, colloidal carbon, after injections at the same ages. At those times when I found the extracellular passage of marker to be blocked, I examined the optic

nerve for specialized membrane contacts, or other evidence of a physical obstruction within the nerve.

MATERIALS AND METHODS

Animals

White leghorn chicks were used in all experiments. Embryos of age E6 (N=12), E13 (N=12), P3 (N=6), P60 (N=6) were examined after intravitreal injections of HRP or colloidal carbon. All embryos were staged at the time of fixation according to external morphological criteria described by Hamburger and Hamilton ('51).

Extracellular Markers

HRP (Type VI, Sigma) was used in all experiments. For intravitreal injections in embryos, 30% solutions of HRP in 0.1 M phosphate buffer (pH 7.4) containing 0.9% NaCl were injected at room temperature in volumes ranging from 1-5 µl. For both P3 and P60 birds 25 µl of a 20% solution of HRP in 0.1 M phosphate buffer plus 0.9% NaCl (pH 7.4) was injected.

India ink, an aqueous solution of 10% soot, 9.5% gelatin, 1.3% phenol, was used (Pelikan special biological ink, C11-1431A). Samples of ink were dialized at least 24 hr against distilled water and then overnight against 0.1 M phosphate buffer plus 0.9% NaCl (pH 7.4) at room temperature. Undiluted, dialyzed ink was injected intravitreally in embryos in volumes ranging from 1-5 µl and at P3 and P60 in 10 µl and 25 µl volumes respectively.

Injections

Embryonic chicks received HRP or India ink through an opening made in the egg shell and extraembryonic membranes. The loose skin

surrounding the forming cornea was grasped with forceps and a hole was made in the right eye with a 27 guage needle. Through this hole, the beveled tip of a 26 guage needle on a 10 µl Hamilton syringe was inserted toward the temperoinferior quadrant of the orbit. After injection the eggs were sealed with adhesive tape and returned to a forced draft incubator at 38°C. The animals survived 1 or 4 hours after injection.

P3 and P60 birds were anesthetized with ether and injected intravitreally through a previously opened hole at the corneal-scleral junction. After 1 or 4 hours, the birds were reanesthetized and killed.

Fixation

All embryos were killed by decapitation, their corneas split, and the head immersed in 0.1 M Na cacodylate buffered (pH 7.2) fixative containing 2.5% paraformaldehyde, 3% glutaraldehyde, 0.12% calcium chloride and 10% sucrose for 3-4 hr at room temperature. The eyes were then removed and a $1cm^3$ region containing the optic nerve, optic disc and retina were then dissected and immersed in fresh fixative. After a total period of 6-7 hr fixation, the optic nerves were split along the verticle meridian and rinsed in 0.1 M Na cacodylate buffer (pH 7.2) plus 10% sucrose overnight.

P3 and P60 birds were anesthetized with ether, perfused with 20 ml of 0.1 M cacodylate buffer plus 0.9% NaCl through the left cardiac ventricle, and then perfused with 150-300 ml of 0.1 M cacodylate buffered (pH 7.2) fixative containing 1% paraformaldehyde, 2% glutaraldehyde and 0.12% calcium chloride. After fixation, the birds were decapitated, their corneas slit, calvarium opened, and

the head immersed in fresh fixative. After 3 hours the eyes were dissected as described above. In some cases, optic nerves were either bissected as before or cut longitudinally into 200 μm thick slabs with a Vibratome.

Histological Procedures

All tissues prepared for HRP histochemistry were rinsed in 0.1 M phosphate-buffer (pH 5.5) plus 10% sucrose. The tissue was subsequently incubated for three hours on ice in 0.1 M Po_4 buffer (pH 5.5) containing 0.5% diamino benzidine (DAB), 0.01% H_2O_2 and 10% sucrose. After incubation, the tissue was washed in 0.1 M Po_4 buffer (pH 5.5) plus 10% sucrose and then post-fixed in 2% O_sO_4 in 0.1 M Po_4 buffer plus 10% sucrose. The tissue was rinsed in buffered sucrose, dehydrated in a graded series of ethanol, cleared in propylene oxide, and embedded in Epon-Araldite. Serial 10 μm thick sections were cut from the optic nerves with glass knives. These sections were examined to determine the presence or absence of HRP throughout the nerve and to be sure that I was examining regions in which the substrate had fully penetrated. Selected sections were reembedded in Epon-Araldite and thin sectioned for EM. Sections were collected on 1-2 mm oval slot or 100 mesh Formvar-coated copper grids. Some, but not all, thin sections were stained with uranyl acetate and lead citrate as described previously, before examination using a Zeiss EM10 microscope.

Those embryos and birds receiving intravitreal India ink injections were treated in an identical manner, except their tissue was not incubated in the histochemical substrate.

CONTROLS

1) In many experimental animals, a small amount of HRP refluxed from the eye via the small hole through which the injection was made. To verify that HRP leaking around the eye did not pass extraocularly to the optic nerve head and cause the observed labeling, I injected a 30% solution of HRP in 0.1 M phosphate buffer plus 0.9% NaCl (pH 7.4) into the space separating the eyelid and the uninjured corneas of E13 (N=2) and P2 (N=2) animals. After 1 hour, the animals were sacrificed and processed identically to the experimental subjects.* These injections resulted in no labeling in the perineurial connective tissue or the scleral trabeculae in the laminar region of the optic nerve.

2) A major site of fluid drainage from the eye is the canal of Schlemm at the angle of the anterior chamber of the eye (Sherman et al., '78; Bill, '79). Because there is no physical barrier to intermixing vitreal fluids and aqueous humor generated by the ciliary epithelium, it was possible that vitreally injected substances might pass from the eye via this anterior drainage route, and gain access to the leaky perineurial vasculature surrounding the lamina cribrosa. To control for this possibility, I made injections of 30% HRP in 0.1 M phosphate buffer plus 0.9% NaCl (pH 7.4) into the anterior chamber of E13 (N=2) and P2 (N=2) animals and followed the drainage of tracer from this site. 1 hr after injection, there was a faint deposit of HRP reaction product

---

*Since the distribution of HRP in experimental animals varied slightly between 1 and 4 hour survival times, control experiments were only conducted at 1 hour survival intervals.

at the vitreal surface of these animals, presumably resulting from posterior leakage of HRP through the vitreous. However, there was no detectable "staining" of the perineurial connective tissue in these animals nor was there any detectable reaction product in the laminar or retrobulbar regions of the nerve.

3) Changes in intraocular pressure (IOP) affect a variety of parameters such as blood flow in intrinsic vessels (Geijer and Bill, '79), and intraaxonal transport in optic nerve fibers (Minckler and Tso, '76; Minckler et al., '77; Quigley et al., '79). Both acute and chronic vascular hypertension and elevations in IOP are also known to affect optic nerve vascular permeability (Radius and Anderson, '80). It was reasonable, therefore, to ask two questions about my experimental procedure; a) did the HRP injections result in an alteration in intraocular pressure? b) did the vitreal injections affect the permeability of blood vessels in the optic nerve? With the assistance of Dr. Robert Lisenmeier in the laboratory of Roy Steinberg, I measured the intraocular pressure of E13 (N=3) and P2 (N=4) animals before and after injections of phosphate buffered saline were made into the vitreal chamber of the eye with a 27 gauge needle at the corneoscleral junction. The pressure measurements were made by inserting a pressure sensitive electrode into the vitreal chamber via the same hole utilized for the fluid injections. The time interval between making the original hole and inserting the electrode for IOP measurements was similar to that between making the hole and injecting HRP in the experimental animals. From these measurements, it was clear that the injection procedure and injections themselves resulted in no change or a

slight reduction in intraocular pressure. Before injection the IOP of E13 and P2 animals was 3 mm and 10 mm Hg respectively, while after injection IOPs were 2.5 and 8 mm Hg respectively. To determine whether injections similar to the experimental injections might affect the permeability of intrinsic optic nerve capillaries to HRP, a 5.6 mM solution of bovine serum albumin (Fraction 5, Sigma) (equimolar to that of HRP in the experimental injections) in 0.1 M phosphate buffer plus 0.9% NaCl was injected into the right eye of E13 (N=3) and P2 (N=3) animals. Give min later, an injection of 4% HRP in phosphate buffered saline (pH 7.4) was made directly into the vasculature of the animal (see chapter 3 for details of injections). After 1 hr the animals were killed and processed as previously described. In these animals the effects of the injections could be seen by comparing the leakage of HRP in the right (injected) and the left (uninjected nerves). This comparison showed that although more HRP was deposited in the chorio-scleral connective tissue space of the injected eye, no difference in the pattern of leakage from intrinsic capillaries was apparent. It was obvious that my qualitative observations of these differences are limited in detecting subtle changes in the vascular permeability across these capillaries, although focal sites of leakage at the capillaries would certainly be detected.

4) In addition to these experimental controls, additional substrate controls were done. From all animals receiving vitreal HRP injections, the left, or uninjected eyes and optic nerves were processed in parallel with the right, injected tissue. Right nerves were also examined after processing which excluded diaminobenzidine

chromagen or H_2O_2 from the reaction substrate mixture. In addition, the right nerves from animals receiving injections of phosphate buffered saline (pH 7.4) and from uninjected animals were also examined after standard histochemical treatment.

Presentation of findings

I concentrated my attention principally on three regions in the optic nerve (fig. 2-1). Zone 1 included the lamina retinalis, a region extending from the junction of the vitreal surface with the optic pecten to the level of the pigment epithelium. Zone 2 included both laminae choroidalis and scleralis. This intermediate region extends from the level of the pigment epithelium to a level of the nerve defined by an imaginary line drawn across the nerve at the outer point of attachment of the cartilagenous cuff on the superior side of the nerve to the opposite side of the nerve. Zone 3, the retrolaminar or retrobulbar portion of the nerve, extended from the sclerad limit of Zone 2 to the optic chiasm.

The presence of HRP in the retinae and optic nerve of the experimental animals has been demonstrated by an enzymatic reaction involving the peroxidase and its substrate H_2O_2 and diaminobenzidine (DAB), followed by the reaction of the resultant DAB complex with O_sO_4 to form an electron dense product (Graham and Karnovsky, '66). This reaction, by comparison with other substrate reactions utilizing chromagens such as tetramethyl benzidine, and o-dianisidine, is relatively insensitive in generating visualizable product from low concentrations of peroxidase. Thus, it is important to emphasize that my conclusions dealing with the distance of HRP spread into the nerve from the vitreous are relative, and may not

represent the full extent of HRP spread into the nerve. In addition, peroxidase may be inactivated by aldehyde fixation and EM processing.

RESULTS

A summary of results of experiments in which HRP and colloidal carbon were injected intravitreally is presented in Table 1. Since differences were generally not found between 1 and 4 hour survivals, I shall concentrate on the 1 hour results and note in passing any exceptions at 4 hr.

E6

After intravitreal injection of HRP in E6 embryos, the reaction product was located at the inner limiting membrane and in the extracellular spaces of the neural retina (fig. 1A). The reaction product often obscured the basal lamina at the vitreal surface. Reaction product was also seen within the ventricular space between the neural retina and pigment epithelium (fig. 2A).

At the optic nerve head, reaction product was present across the vitreal surface and in the extracellular spaces surrounding the cellular elements of Bergmeister's papilla and developing neural and glial elements in the optic nerve (fig. 13A). The concentration of reaction product diminished with distance from the vitreal surface until only isolated pockets of marker were seen surrounding axons in Zone 2. In both Zones 1 and 2, glial cells containing HRP-positive inclusions ranging in size from 64 X 64 nm to 0.4 X 0.5 μm were found (fig. 13B). However, periaxonal HRP was absent from Zone 3 and the uninjected left eyes and nerves of E6 embryos.

E13

After intravitreal HRP injections at E13, as in E6, reaction product was most densely distributed along the vitreal surface and its concentration appeared to diminish with distance into Zone 1. The region of dark brown staining seen by light microscopy extended about 340 μm into the optic nerve and approached the boundary of Zones 2 and 3 (fig. 14A). Choroidal and scleral connective tissue spaces of E13 eyes were densely "stained" after vitreal HRP injections. In addition, the contiguous spurs of connective tissue radiating into the nerve from the perineurial connective tissue, were "stained" with DAB reaction product. HRP could be traced in these scleral spurs and their vascular extensions throughout Zone 2 and into the proximal portions of Zone 3.

One hour after injection HRP was present in the pericapillary periaxonal spaces of Zone 3 (fig. 14B). The amount of HRP adhering to membranes in the periaxonal space was less than seen in the periaxonal spaces of Zones 1 and 2, however. Rarely, I also found HRP-positive inclusions in the perinuclear cytoplasm of glial cells and in the astrocytic end feet surrounding vascular spaces. Three hours later, by contrast, HRP-positive inclusions were much more evident, while the periaxonal spaces were essentially free of label.

P3

After vitreal injections of HRP at P3, the distributions of HRP was qualitatively the same after 1 or 4 hours. Reaction product was dense throughout the retina and extended into and filled the extracellular space of the retina to the level of the pigment epithelium where it was blocked by tight junctions between pigment epithelial cells (fig. 3B).

Although the density of periaxonal reaction product diminished with distance from the vitreal surface by 4 hrs in P3 chicks it was still conspicuous 0.75 mm from the vitreal surface, through Zones 1 and 2 and into the proximal portion of Zone 3 (fig. 15A). In the proximal regions of Zone 3, discrete pools of HRP were distinct in the periaxonal spaces. In more distal regions, i.e. near the optic chiasm, scattered deposits of HRP were observed only in close proximity to "stained" pericapillary spaces (fig. 16B).

The pericapillary spaces of Zones 1 and 2 were heavily labeled in P3 animals. HRP labeling of the network of pericapillary spaces extended through Zone 3 to the optic chiasm and into the spaces surrounding anastomotically connected vessels of Zone 3 of the opposite optic nerve (fig. 15B). HRP-positive inclusions were prominent in both endothelial cells and astrocytes throughout the nerve and were more common in Zones 1 and 2 (fig. 16A).

At P60 the qualitative distribution of HRP in the nerve after intravitreal injection was the same as P3 and thus will not be discussed at length. HRP reaction product was present both periaxonally and in pericapillary spaces in the nerve in all zones.

The spread of HRP from the vitreous into the optic nerve was in stark contrast to the spread of colloidal carbon. Although clusters of dense, spherical particles were present in the vitreal space, and along the vitreal surface, of the retina and optic nerve head, they did not cross the basal lamina adjacent to the inner limiting membrane at any age examined. Neither were carbon particles readily detectable in the extracellular space of any zone of the optic nerve.

Left Nerves

In the left optic nerves, i.e. in the side opposite the intravitreal injection, neither extracellular HRP nor colloidal carbon were present in the pericapillary or periaxonal spaces in any zone of the nerve E6 or E13. At P3, however, HRP but not colloidal carbon was present in the left optic nerve. Reaction product was clearly visible in the scleral and choroidal extracellular space surrounding the back of the eye and was present in the pericapillary spaces of Zones 1, 2, and in the most proximal portion of Zone 3 (fig. 17A). Reaction product was recognized in Zone 2 near the basal lamina adjacent to glial foot processes bounding the pericapillary spaces in this zone, and surrounding axons near vascular septae (fig. 17B). In Zone 3, I failed to identify the marker in the periaxonal spaces outside the limits of the perivascular glial end foot boundary.

To summarize (Table 1), in E6 embryos HRP spread periaxonally through Zones 1 and 2 and was present in the incomplete perivascular spaces of the only zone containing vascular elements at that stage, Zone 1. In E13 and P3 animals, the periaxonal spread of HRP also extended through Zones 1 and 2 and in P3 partially into the proximal portion of Zone 3. In E13, when preliminary vascularization had occurred throughout the nerve, the spread of HRP in the perivascular network extended further, through Zones 1 and 2 and into the proximal portion of Zone 3. After more extensive vascularization, HRP was present in pericapillary spaces at all levels of the nerve extending into and beyond the optic chiasm.

The presence of HRP-positive inclusions in the perinuclear cytoplasm of extravascular glial cells, perivascular pericytes and endothelial cells and in the end feet forming the pericapillary space closely paralleled the presence of periaxonal HRP in E13 embryos, P3 and P60 birds. Moreover, as previously described, although I observed desmosomal and gap junctions between glial elements throughout the nerve, I found no suggestion of tight junctions that might serve as a barrier to the free diffusion of extracellular HRP.

DISCUSSION

When HRP is injected into fetal or posthatching chick vitreous, it may reach axons of the optic nerve by at least two routes (fig. 18). The first and most obvious route involves direct diffusion from the vitreal surface, past the inner limiting membrane, and around axons, glia and vascular cells of the nerve (large arrows). A second possible route involves the vascular system (small arrows). HRP may travel in the pericapillary spaces which surround the intrinsic vessels of the optic nerve head and the optic nerve. The tracer may enter the system of pericapillary spaces directly or indirectly. Direct access to these spaces is gained by flooding from the vitreous into the spaces surrounding the afferent and efferent vessels supplying the pecten. These spaces are continuous with pericapillary spaces surrounding the branching and anastomosing plexus of vessels which extends from the vitreous into the laminar region of the nerve. Traveling in these pericapillary spaces tracer may drain into and permeate the perineurial connective tissue

surrounding the lamina cribrosa. From this space, it may move through the scleral trabeculae which radiate into the lamina cribrosa and the retrobulbar optic nerve. The marker may then spread through the contiguous pericapillary spaces whence it escapes their glial foot process boundaries to reach the periaxonal spaces of the nerve.

The barrier to periaxonal spread of HRP has previously been described (LaVail and LaVail, '74; Kristensson and Wisniewski, '76). Once the marker reaches the periaxonal spaces of Zones 1 and 2 in P3 chicks, what might limit its continued spread into the retrobulbar nerve, and beyond? Several explanations for this blockage are possible.

One possibility is that the restriction of tracer movement may result from the physical arrangement of elements with the nerve. The extracellular diffusion of solute through intercellular clefts may be affected by the geometry of the spaces in which it is moving.

Fenstermaker and Patlak ('75) claim extracellular molecules such as sucrose, inulin and EDTA have diffusion rates in monkey, dog, and dogfish CNS that are 20-50% slower than their respective diffusion rates in water. These authors suggest that "a major factor which accounts for this reduction seems to be the tortuosity of the ECS."

This contention seems unlikely for several reasons. The most prominent is that the direct periaxonal spread of HRP from the vitreous (route 1) varied little during a period (E6-P3) in which the structural complexity of the nerve was vastly increased. During this period of pronounced ingrowth of tissue elements and proliferation of glial cells and their processes, there was a

reciprocal reduction of the size of the extracellular space and presumably an increase in the "tortuosity" of the extracellular channels. Even at P3, the extracellular spaces are extremely large compared to the ~50 Å radius of HRP. Thus, barring electrostatic or chemical interactions between HRP and surface constituents of neuronal and glial membranes or with substances in the extracellular matrix, it seems reasonable to assume very little hindrance to the diffusion of HRP in the extracellular spaces of the nerve.

The spread of materials in the nerve might, however, be impeded by a physical occlusion of the extracellular space. Such barriers are known to exist along the lateral borders of the prelaminar optic nerve. At this site a series of astrocytes (the border tissue of Kundt) surrounds the nerve and separates from surrounding retinal elements. From the level of the pigment epithelium to the level of the outer limiting membrane, the Kundt cells are joined by tight junctions which occlude the extracellular space and prevent the passage of tracers laterally from the optic nerve head into the retina (Okinami et al., '76; Tso et al., '75; Tsukahara and Yamashita, '75; Rodriguez-Peralta, '66).

The possibility that some sort of physical occlusion of the extracellular space might exist in the nerve itself was the basis for examination of embryos. Taking the possible existence of a series of membrane junctions as a hypothetical basis, I reasoned that at early developmental stages, the junctions forming the barrier might not yet exist, and no barrier would be detected. To my surprise, however, the periaxonal spread of HRP was restricted

at E6, the earliest stage examined. In fact, it was clear that at earlier stages, prior to vascularization of the nerve, the spread of tracer from the vitreous was limited, due to the absence of perivascular system of channels, as compared to the spread at later stages.

I also examined nerves of E6 and E13 embryos and P3 chicks for the presence of occluding junctions. This search was directed to a fairly broad region of the nerve near the limit of periaxonal spread of HRP for these three ages. The concentration of reaction product decreased gradually over considerable distance, suggesting that any possible structure acting as a barrier would not be confined to a narrow band across the nerve. Although junctional specializations such as gap junctions and desmosomes were occasionally observed, as described earlier in other species (Vaugn and Peters, '67; Brightman and Reese, '69; Morales and Duncan, '75; Peters et al., '76; Quigley, '77), no tight junctions (with the exception of those between endothelial cells) were recognized at any age. These findings were confirmed by examination of uninjected tissue (post-fixed with O_sO_4-potassium ferricyanide or <u>en bloc</u> stained with uranyl acetate, see chapter 2). In these samples, membrane structure was enhanced and yet no system of junctions was present in nerves of either age.

Assuming that neither sampling restrictions inherent in thin section electron microscopy, the tissue preparation itself, nor the plane of sectioning of the tissue were critical to the interpretation of my data, the fact that not a single occludens-type

junction was observed suggested that membrane junctional specializations were not a significant factor in impeding the passage of HRP.

My observations supported the proposition that endocytic uptake of HRP from the extracellular space of the optic nerve by glial and/or vascular elements served to limit the spread of vitreally injected tracer. Frequently, HRP-positive inclusions were seen in the perinuclear cytoplasm of glial cells and in the end feet boundary for the pericapillary space. The number of these HRP-positive profiles was directly related to the concentration of HRP reaction product in the extracellular space. The clearing of extracellular HRP by glial cells has been seen in several regions of the CNS (Brightman, '65; LaVail and LaVail, '74; Turner and Harris, '74; Bunt et al., '74; Decker et al., '68; Lane and Reherne, '70; Olsson and Hossman, '70; Sellinger and Petiet, '73). This phenomenon is not limited to the ingestion of the extrinsic protein HRP. Ferritin (Brightman, '65) and radiolabeled amino acids are also taken up by glial cells in the CNS and the optic nerve (Minckler et al., '76; Minckler and Tso, '76; Hayreh, '78).

The bulk flow of fluids from the vitreous into the optic nerve head may play a role in the spread of vitreally injected substances. If this is so, then factors influencing the bulk flow might affect the spread of tracers into the nerve. Bulk flow of fluid from one point to another in the vitreal chamber is very difficult to distinguish from diffusion because the vitreal chamber is small and the tracers (i.e. fluorescein) used to examine the question diffuse freely in the substance of the vitreous body (Suran and McEwen, '61).

Although Fowkes ('63) did report bulk flow of nitro blue tetrazolium in the vitreous, Maurice ('79) contends that the vitreal fluid is almost stagnant as revealed by the spread of vitreally injected ^{24}Na (Maurice, '57), ^{131}I (Maurice, '59), and fluorescein (Cunha-Vaz and Maurice, '67).

In contrast to the view of vitreal fluid as being relatively immobile, is the evidence that vitreally injected tracers do spread into the retina and optic nerve and that their spread is influenced by a pressure gradient between the vitreal space and the optic nerve (Hayreh, '78; Cunha-Vaz, '79). The tissue pressure of the retrolaminar optic nerve in cats and rhesus monkeys has been estimated experimentally (Ernest and Potts, '68; Hedges and Zaren, '73). These studies showed that elevated CSF pressure (caused by inflation of intracranial balloon) increased the pressure in the retrobulbar nerve but an acute rise in intraocular pressure had no affect on the nerve pressure. The results raise the possibility that the tissue pressure of the retrobulbar nerve (influenced by intracranial and/or CSF fluid pressure) may differ from the tissue pressure at the optic nerve head (influenced by intraocular pressure).

Since the intraocular pressure is normally higher than the CSF pressure, a gradient might exist which would result in the bulk flow of fluid from the vitreous into the nerve. In support of this, Hayreh ('66) compared the penetration of vitreally injected colloidal iron into the optic nerve head of rabbits with or without an increase in intracranial pressures produced by inflation of an intracranial balloon. He found that the penetration of tracer was diminished in the animals with elevated intracranial pressures. In

addition, the flow of vitreally injected diaminoacridines into the nerve (Rodriguez-Peralta, '66) and ^{3}H-leucine into the optic nerve and orbital meninges increased with the elevation of intraocular pressure (Minckler et al., '76; Minckler and Tso, '76).

The vitreal-optic nerve flow of materials has been suggested as a possible factor in impeding the movement of materials from the laminar region of the nerve (see chapter 3) towards the vitreal surface (Tso et al., '75; Okinami et al., '76). Conversely, Hayreh ('77) has shown that fluorescein leaking from the subarachnoid spaces of the retrobulbar nerve, travels to the vitreal surface. It is not clear whether this movement of tracer represents simple diffusion or the bulk flow drainage of this material into the vitreous analogous to the drainage of interstitial elements into the subarachnoid space. If such an optic nerve-vitreous flow of materials does exist it might act to impede passage of tracer from the vitreous in the opposite direction. Rodriguez-Peralta further suggests that the lamina cribrosa acts as a drain for fluids originating both in the vitreous and in the subarachnoid space of the nerve. The currents generated by the constant drainage of fluid at the lamina cribrosa might well impede the bidirectional flow of material across the laminar region of the nerve.

My findings are relevant to two broader aspects of developmental neurobiology. First, they bear directly on a variety of findings on the rates and composition of transported macromolecules found in the developing chick visual system. A major motivation of my work was to determine whether the eyes of developing chick embryos were similar to those of more mature birds

whose vitreal chamber has been considered a relatively closed system for injection of tracers. Although the periaxonal spread of HRP from the vitreous was in the main restricted to a region extending just distal to the laminar region of the nerve, as described earlier (LaVail and LaVail, '74; Kristensson and Wisniewski, '76) a second vascular channel for passage of HRP from the eye into the optic nerve was also observed. Materials introduced into the vitreous may move through this pericapillary conduit and subsequently leak between the boundary glial processes to collect in the extracellular space surrounding axons in Zones 2 and 3.

The importance of this leakage extends to a variety of studies. In biochemical studies of anterograde axonal transport, the possibility of confusing extraaxonal spread of radiolabeled precursors with labeled, intraaxonally-transported products is an important consideration. Distinguishing between labeled materials traveling by slow axonal transport and materials diffusing extracellularly in the optic nerve head may in fact be quite difficult unless transport blockers such as colchicine or vinblastine are used to distinguish the actively transported materials from those spreading passively (Chihara, '79; Haley et al., '79).

Second, the presence of HRP in the optic nerve and chiasm after intravitreal injections would have important consequences for the interpretation of results of axonal transport studies using HRP in embryonic optic nerves. One such study (Clarke and Cowan, '75), utilized the retrograde transport of vitreally-injected HRP to

study aspects of the development of the projection of axons from the isthmo-optic nucleus (ION) to the contralateral eyes of chick embryos. The authors sought to establish the time of arrival of ION fibers at the eye by determining when neuronal cell bodies in the ION were first "labeled" by retrogradely-transported HRP after vitreal injection. They also sought to estimate the rate at which HRP was transported by these embryonic neurons based on the time necessary for HRP to appear in ION neurons and the length of the isthmo-optic tract. They also identified and counted populations of labeled neurons in the ipsilateral ION and "ectopic" cells outside the histological confines of the ION nucleus on the contralateral side after vitreal HRP injections. In interpreting their findings, Clarke and Cowan assumed limited diffusion of the tracer from the vitreal injection sites. My studies showed this assumption to be incorrect. I demonstrated that vitreally injected tracer may spread into the retrobulbar nerve via pericapillary spaces by E13 and that the capillary invasion which precedes formation of pericapillary channels has begun by E10 (see chapter 2). From these studies it was clear that HRP was present in the retrobulbar nerves of these embryos after vitreal injections. Therefore, the growth cones of developing axons traveling through the nerve at these stages, were possibly exposed to tracer well outside the limits of the retina. Thus, the labeling of the developing ION neurons by accumulation of retrogradely-transported HRP was not unequivocal evidence of arrival of their fibers to the eye itself, but simply a reflection of when the growing fibers first encountered vitreally injected tracer. In addition, the transport

rate computations were affected by the presence of tracer in the nerve. Since it was unclear where the growing fibers first encountered the vitreally injected HRP, it therefore was uncertain how far the tracer has been transported and thus how fast it had gotten there. Lastly, my findings raised the possibility that the population of ipsilaterally projecting ION neurons may simply be an artifact caused by the filling of growth cones at the optic chiasm which are traveling to the uninjected eye.

The presence of HRP in the choroidal and scleral connective tissue surrounding the retrobulbar optic nerve coincides with the location of one of the important targets of retrogradely-transported substances from the iris and ciliary body of the eye, the ciliary ganglion. Substances such as wheat germ agglutinin, nerve growth factor, tetanus toxin (Max et al., '78) and HRP (Jaeger and Benevento, '80) accumulate in ciliary ganglion cells after intraocular injection in chick and rat (Max et al., '78) and monkey (Jaeger, '80). This parasympathetic ganglion is embedded in the connective tissue surrounding the optic nerve. Although the ganglion itself is covered by a tough capsule of connective tissue, the capsule does not completely prevent the influx of diffusible substances. Therefore, in experiments involving retrograde transport to the ciliary ganglion (Max et al., '78; Jaeger and Benevento, '80), control experiments such as those in which transection of the postganglionic branches of the ganglion blocks the retrograde transport of the marker are of particular relevance.

Table 1. Summary of results of HRP localization in the developing chick right optic nerve after intravitreal injection of the right eye or after intravascular injection.

AGE	ZONE	INJECTION SITE	PERICAPILLARY SPACE		ASTROCYTIC END-FEET		PERIAXONAL SPACE	
			1 hr	4 hr	1 hr	4 hr	1 hr	4 hr
E6	1	Vitreous	+	+	**	+	+	+
	2		+	+	NA	NA	+	+
	3		-	-	NA	NA	-	-
E13	1	Vitreous	+	+	+	+	+	+
	2		+	+	+	+	+	+
	3		+	+	+/-	+	+/-	-
P3	1	Vitreous	+	+	+	+	+	+
	2		+	+	+	+	+	+
	3		+	+	+	+	+	+

(Continued)

Table 1 (Continued).

AGE	ZONE	INJECTION SITE	PERICAPILLARY SPACE		ASTROCYTIC END-FEET		PERIAXONAL SPACE	
			1 hr	4 hr	1 hr	4 hr	1 hr	4 hr
E14	1	Vitelline Vein	+	+	+	+	+	+
	2		+	+	+	+	+	+
	3		+	+	+	+	+	+
P2	1	Left Ventricle	+	+	+	+/-	+	+/-
	2		+	+	+	+	+	+/-
	3		+	+	+	+/-	+	+/-

*NA, not applicable since astrocytes have not yet formed end-feet around the developing capillaries; -, no HRP observed; +/- HRP present in a minority of the fields examined; +, HRP present in a majority of the fields examined; ** not examined. Each value is based on observations of at least 10 fields each 178 μm^2 from at least two animals.

IV. PENETRATION OF HORSERADISH PEROXIDASE INTO THE OPTIC NERVE AFTER VASCULAR INJECTIONS

INTRODUCTION

After vitreal injections of HRP in E13, P3 and P60 nerves, the marker spread from the vitreal surface into Zone 3 of the nerve. However, it was unclear whether the HRP present in the pericapillary spaces of Zone 3 had reached that position by diffusing directly from the vitreous or by leaking from the intrinsic capillaries of the nerve.

To address this question I examined the spread of vascularly circulating HRP into the optic nerve during development. I sought to answer the following questions:

1) Does vascularly circulating HRP penetrate the optic nerve during development?
2) By what routes does HRP enter the nerve?
3) Does access via the different routes vary during development?

To accomplish this I injected HRP directly into the vasculature of E14 embryos and P2 and P60 chicks and examined the nerves 1 or 4 hrs later by light and electron microscopy.

MATERIALS AND METHODS

White leghorn embryos at E14 (N=8), and chicks at P2 (N=8) and P60 (N=6) were used for this study. All eggs were maintained in a forced draft incubator at 38°C before and after injections. All embryos were staged at the time of fixation by external morphological criteria of Hamburger and Hamilton ('51).

Extracellular Markers

HRP (Type VI, Sigma) was used in all experiments. 100-150 µl of a 4% solution of HRP in 0.1 M phosphate buffer plus 0.9% NaCl (pH 7.4) (PBS) was used in each embryo. 150-200 µl and 400-500 µl of 4% HRP in PBS (pH 7.4) was injected into P2 and P60 birds respectively.

Injections

A 1 cc syringe adapted with a pulled glass micropipette as its needle was used for all vascular injections. A vitelline vein of chick embryos was injected through a hole made in the shell and extraembryonic membranes. The eggs were sealed with adhesive tape and returned to their incubator for 1 or 4 hrs.

Under Avertin anesthesia, the hearts of P2 and P60 birds were exposed and HRP injected directly into the left cardiac ventricle. The birds were reanesthetized 1 or 4 hrs later and killed.

Fixation and Histological Procedures

All embryos and posthatching birds were killed, fixed, dissected, and histologically processed in an identical manner to that previously described for animals receiving vitreal injections.

RESULTS

After vascular injections, HRP was never found in the extracellular space of the retina at any age. At E14 slight deposits of reaction product were apparent by light microscopy at the vitreal surface and along the folds of the pecten. Similar deposits were not present at P2. These deposits and the extent of their spread into the retina from the vitreal surface were not discernible by EM.

After formation of the pecten folds, reaction product could be detected at the luminal surface of pecten capillaries but seldom in the extracellular space of the pecten folds. Numerous HRP-positive inclusions were present in the endothelial walls of pecten capillaries but the presence of such inclusions at the abluminal surface of those capillaries was rarely observed.

HRP was also present both within the lumens and in the pericapillary spaces surrounding many immature capillaries in the nerves of E14 embryos. Thus, it was difficult to assess the permeability of those capillaries. However, one observation was consistent in all profiles observed. In no case could HRP be traced in continuity across the junction joining two adjacent endothelial processes at a capillary lumen.

At E14, dense HRP reaction product filled periaxonal and pericapillary spaces in each zone of the nerve (fig. 19A). The concentration of reaction product was greatest in Zone 2 and diminished with distance toward Zones 1 and 3.

The perinuclear cytoplasm of glial cells and the astrocytic end feet bounding the pericapillary spaces at E14 contained HRP-positive inclusions in all zones of the nerve after 1 hr (fig. 19). After 4 hrs, the distribution of labeled glial processes and cell bodies in the nerve was the same but the number of organelles had greatly increased.

In P2 chicks, HRP was present in the choroidal, scleral, and perineurial connective tissue surrounding the back of the eye after vascular injections (fig. 20A). By EM, HRP reaction was easily detected both inside and outside the fenestrated capillaries of the

choroid. Reaction product was present within endothelial vesicles of these capillaries as well as filling pores (described in chapter 1) spanning the luminal wall (fig. 20B). Reaction product was present across the basal lamina of Bruch's membrane and surrounding the basal processes of the pigment epithelium. Reaction product was also present in the scleral septae entering the nerve head. In contrast to the nerves at E14, however, the concentration of reaction product in the pericapillary channels diminished rapidly with distance from Zone 2. For example, although HRP was clearly present in the pericapillary spaces of Zone 2 and the proximal portion of Zone 3, no discernible pericapillary reaction product was present in the distal portion of Zone 3 or the optic chiasm.

The presence of HRP in the periaxonal spaces of P2 nerves paralleled its distribution in the pericapillary spaces. Periaxonal spaces in Zone 2 were the most densely filled, and the concentration decreased with distance from Zone 2 toward the vitreal surface or the optic chiasm.

Although these animals were fixed by vascular perfusion, and HRP may have been washed away, reaction product remained at the luminal surface of many capillaries in the nerve (fig. 20C). In these cases, reaction product could be seen at the luminal entrance to the endothelial cleft in the luminal wall. In every case, the reaction product was blocked from passing between endothelial cells by a junctional specialization usually found at the luminal end of the cleft (fig. 21A). Very little vesicular activity was present in the luminal walls of these capillaries. HRP-filled profiles were occasionally present in capillary walls and in the perinuclear cytoplasm of cells in the pericapillary space (fig. 21B).

DISCUSSION

The findings of these studies can be summarized as follows:

1) There are two potential routes of entry of vascularly circulating substances into the optic nerve.
   a) by diffusion into the lamina cribrosa of the nerve from the choriocapillaris
   b) by extravasation from intrinsic capillaries of the nerve
2) At E14, both potential routes are open and HRP is deposited in pericapillary and periaxonal spaces throughout the nerve.
3) Between E14 and P2 the second route, leakage from intrinsic capillaries is eliminated by the closure of the capillaries.
4) The anatomical basis for the permeability of immature vessels at E14 has not been established. The sequence of events which results in decreased leakage from these vessels and the timing of these events are also unclear.

My observations on the distribution of vascularly circulating HRP in posthatching birds confirms the findings of numerous studies using different tracers on a variety of species. HRP apparently leaked from capillaries of the choriocapillaris into the surrounding choroidal and scleral connective tissue space. As pointed out by Cohen ('73) there was no physical barrier separating this connective tissue space from the extracellular space of the scleral septae which radiate into the nerve at the lamina cribrosa. Thus, materials leaking from the choriocapillaris may follow an unobstructed path from the choroidal extracellular space, to the extracellular space of the septae entering the nerve and their pericapillary extensions in the nerve. HRP leaked from these spaces

by passing between the astrocytic processes that form their boundaries.

Unlike the leakage of materials into the nerve from the choriocapillaris, the leakage of tracer from the intrinsic nerve capillaries apparent at E14 was insignificant at P2 and P60. These findings may reflect a change in optic nerve vascular permeability between E14 and P3.

Such a change in vascular permeability during development has also been reported for regions of the embryonic chick CNS. Delormē and co-workers ('70) found great differences in the permeability of chick cerebral capillaries during development. At embryonic day 5-6, 6.5-7,8, and 10, intravenously injected HRP was clearly seen in the developing telencephalic neuropile 1-20 minutes later. After E10, there was no extravascular HRP visible. The authors suggested that the reduction in permeability to HRP could be correlated with the "formation of all the tight junctions between outer leaflets of apposed plasma membranes at the level of the capillary endothelium."

Wakai and Hirokawa ('78) also noted altered capillary permeability during the development of chick cerebelum and spinal cord. The authors found that prior to E12, circulating peroxidase penetrated into the parenchyma. On E13 and E14, peroxidase could be detected in the medullary regions and not the surrounding cortical areas. After E15, there was no detectable penetration of HRP into the spinal cord or cerebellum from the vasculature. Despite such speculations (see above), the structural modifications that might account for the altered vascular permeability have never been elucidated.

Reese and Karnovsky ('67) established that the impermeability of cerebral capillaries was due to the lack of vesicular transport across the capillary wall and the presence of tight junctions between adjacent endothelial processes. Based on their hypothesis, the increased permeability at E14 might be due to 1) an increase in vesicular activity in the luminal walls of the immature capillaries or 2) the absence or modification of endothelial junctions in the capillaries.

Neither of these possibilities was borne out from a comparison of E14 and P2 capillaries by TEM. It seemed implausible that vesicular transport could be responsible for sufficient movement of tracer to account for the periaxonal deposits seen in my experimental nerves at E14. Anatomically, there was no drastic increase in the number of labeled vesicles in the E14 endothelial cells, and the luminal walls of these vessels were considerably wider than those of P2, thus increasing the distance and presumed energy expense necessary to move the materials.

From anatomical considerations, the endothelial junctions also seem to be unlikely candidates for the site of the increased permeability of immature capillaries. Throughout this study, whenever developing capillaries were encountered (identified by the presence of a central lumen) the walls of those capillaries were sealed by tight junctions between the two apposed membranes. Occasionally the membranes themselves could be resolved. In these cases, points of membrane fusion, characteristic of occludens junctions were evident. Thus, junctional specializations appear to

exist even at the earliest stages of capillary formation as has been previously reported (Delormē et al., '70; Caley and Maxwell, '70; Phelps, '72; Roy et al., '74).

The consistent finding of junctions between endothelial processes during development does not imply uniform permeability across the interendothelial cleft. Physiological studies indicate that epithelial tight junctions vary considerably with regard to the transepithelial ionic resistance they impart to a given epithelium. In addition, tight junctions in different tissues allow a variable degree of passage of extracellular tracer.

Transmission electron microscopy gives little indication of morphological differences that might account for the variability in their leakiness. Cross-sectioned views of the junctions show a series of points where the outer leaflets of adjacent membranes come together and fuse, occluding the extracellular space. Although HRP, MP, and lanthanum are apparently blocked at these points of membrane fusion (Reese and Karnovsky, '67; Brightman and Reese, '69; Brightman et al., '70), these results offer a deceptively simplistic two-dimensional view of these junctions.

As described earlier, the freeze-fracture method of preparing and examining membranes reveals the intramembranous particle arrangement within the membranes of a junctional region. At tight junctions prepared by freeze fracture, the sites of membrane fusion are correlated with a branching and anatomosing network of crests or strands of intramembranous particles on the P face and a complimentary set of grooves on the E face of the fractured membrane. The organization of particle strands within a junctional membrane has

been correlated with the physiologically determined resistance properties of that particular epithelium (Claude and Goodenough, '73). Claude and Goodenough assert that the tightness of epithelial tight junctions was related to the number of parallel particle strands and the apical-basal width of the complex of strands in a junctional membrane.

The correlation between tight junction morphology and its physiological characteristics may apparently be extended from epithelial to endothelial junctions as well. Wissig ('79) found that the junctional membrane of mouse diaphram capillaries (known to allow interendothelial passage of MP) contained few intramembranous particle strands. By contrast, Dermietzel ('75) found numerous parallel strands of particles in the junctional membranes of cat cerebral capillaries, known to be impermeable to a variety of tracers. These examples of the structural heterogeneity of epithelial or endothelial tight junctions have not been presented to defend the correlation proposed by Claude and Goodenough* but rather, to point out that the presence of endothelial occludens junctions in TEM is a qualitative indication of an impediment to diffusion in the interendothelial cleft, not a quantitative gauge of the degree to which materials are blocked.

From the freeze fracture view of tight junction structure, it is conceivable that the decreasing permeability of CNS capillaries

---

*In fact a number of studies exist which show that hyperosmotic treatments of epithelia which change the transepithelial electrical resistance do not effect the distribution of intramembranouse particles within the junctional membranes (Martinez-Polomo and Erlij, '75; Mollgard et al., '76).

during development reflects an ongoing process by which additional intramembranous particles are constantly added to the junctional membrane in a manner analogous to the development of epithelial tight junctions (Suzuki and Nagano, '79). By analogy to the contention of Claude and Goodenough, the addition of intramembranous particles resulting in the completion or interconnection of intramembranous strands might decrease the flux of substances across that junction.

Although the barrier to efflux of electron dense tracers such as HRP, MP, or lanthanum generally resides at the endothelium of the vascular unit [except at CNS capillaries in sharks (Brightman et al., '70b)] it is possible that other elements of the vascular unit may also be important as diffusion barriers or sites of active transport processes. The vascular basal lamina surrounding fenestrated capillaries of the intestine and renal glomerulus and unfenestrated capillaries of rat and mouse diaphram are thought to impede the passage of colloidal particles and anionic molecules larger than 40,000 MW (Majno and Palade; Cauffield and Farquar, '76; Simionescu et al., '78). However, studies have shown that the passage of HRP is not restricted by basal laminae surrounding capillaries of mammalian cerebrum (Brightman et al.,'70). It thus seems clear that the basal lamina is not a factor influencing CNS capillary permeability of HRP in some species, and is unlikely to be a factor for chicks as well.

Vascular basal laminae are known to increase in density and thickness during development. Whether their properties as a molecular size and charge-selective seive are consistent throughout

this developmental process is unknown. Acquisition of charge-selective character by the lamina might be directly linked to the deposition of these acidic components in the filamentous framework of the lamina. Clearly the sieve characteristics of a basal lamina might change during a period in which its ultrastructural appearance did not appreciably vary.

In addition, the sheath of astrocytic end feet bounding the CNS vascular unit may also influence the composition of perivascular fluid and the passage of substances into the surrounding interstitial space. Processes such as facilitated transport and ion secretion are functions thought to be effected by the astrocyte foot processes which surround all CNS vascular units (Bradbury, '75). In developing rat brain the physiological development of the barrier to influx of inulin, sucrose and Cl^- (Ferguson and Woodbury, '69) coincides with the development and completion of the astrocytic sheath and its basal lamina around the cerebral capillaries. During the same period the structural appearance of endothelial junctions by TEM does not change (Donahue and Pappas, '61; Bär and Wolff, '72; Phelps, '72).

Anatomical specializations have been found in the astrocytic end feet which make up the sheath surrounding mammalian CNS capillaries. Landis and Reese ('74), Brightman et al. ('78), and Dermietzel ('74), have described arrays of membrane associated orthagonal particle complexes (MOPC) in freeze fracture preparations of perivascular astrocytic end feet. Similar arrays of intramembranous particles are found in non-neuronal cells such as hepatocytes (Kreutziger, '68), intestinal epithelial cells (Staehelin, '72), skeletal muscle (Rush

et al., '74), trachea (Inoue and Hogg, '77), myocardial cells (McNutt, '75), and interestingly, on Müller glial cell end feet of the inner limiting membrane. In the retina these arrays consist of rectilinear assemblies of 4-60 globular subunits (Reale et al., '74; Raviola, '77). Although the function of these assemblies and the significance of their preferential localization in CNS within astrocytic membranes facing either vascular or subarachnoid spaces or in Müller cell processes of the inner limiting membrane are unclear, it is interesting to speculate that they might be involved in transport or permeability of substances across the astrocytic membrane.

Several features of these assemblies suggest indirectly that they may play a role in influencing their microenvironment. 1) The assemblies accumulate in membranes during development in rats coincident with the development of transport mechanisms (Anders and Brightman, '79). 2) They are known to disappear under conditions of low pH, anoxia, or treatments with oxidative phosphorylation uncouplers such as dinitrophenol just as transport functions decrease under these conditions (Cullen and Gulley, '80). 3) In addition, Wood and co-workers ('77) have determined by immunocytochemical localization techniques that a gradient in the distribution of $Na^+ - K^+$ ATPase exists in the perivascular astrocytic foot processes. The end feet were especially heavily labeled while other astrocytic surfaces were relatively lightly labeled. As discussed by Bradbury ('75), such as assymetric arrangement of ionic transfer machinery is analogous to the assymetric arrangement of components at the apical and basal surfaces of epithelial cells. Since the assymetric

arrangement in epithelia is thought to be crucial for the active transport of solutes between the apical and basal surfaces of the epithelia, a similar intracellular transport of solutes might also take place between the perivascular astrocytic surface and other regions of the cell. It is thought that such an intracellular flux of K^+ may be important for the spacial buffering of K^+ concentration away from sites of K^+ build-up in locations of high electrical activity (Kuffler, '67; Franck et al., '78). A recent finding consistent with this last idea of intracellular movement of materials from astrocytic end feet, was reported by White ('80), who showed that radiolabeled amino acids and/or protein were incorporated in perivascular astrocytic processes whence they were subsequently dispersed, presumably to other processes of the astrocytes.

Another possible explanation for the increased vascular permeability at E14 is that the neuronal vascular plexus is incomplete at that stage, and tracer may leak from the growing vascular elements. Very little ultrastructural evidence can be brought to bear on this possibility. Light microscopic examination of vessels growing in tadpole tail fins and regenerating vessels in rabbit ears (Sandison, '32; Clarke and Clarke, '39) have served as model systems for study of vascular growth processes. Vessels grow by a process of endothelial sprouting from pre-existing vessels. As the sprout advances, it is preceded by thread-like cytoplasmic extensions, a luminal opening continuous with the lumen of the pre-existing vessel follows behind the leading edge of the sprout. Cliff ('63) showed by EM of regenerating rabbit ear vessels that the lumen formed by consolidation of numerous small spaces that form

between cells of the growing sprout. From Cliff's description, it is still unclear whether the lumen forming within a growing vascular sprout has transient openings with the extracellular space that might allow efflux of tracer circulating in the established vascular bed. Moreover, these new vessel sprouts may be fragile and abnormally permeable. Clarke and Clarke ('39) noted that slight increases in vascular pressure caused red blood cells to be extruded from the tips of growing vessels. Spontaneous bursting of growing vascular tips has also been observed during the revascularization of injured rabbit cornea (Cogan, '49). An increase in the passage of dye has also been observed at the growing tips of regeneration rabbit ear vessels (Abell, '46) and in the rabbit cornea (Cogan, '49). Large colloidal particles also leaked from regenerating vessels in rat cornea and cremaster muscle (Schoefl, '64). The leaky tracers in these experiments only leaked from the very tips of the vessels in question suggesting that the conditions allowing efflux exist transiently and only at the earliest stages of vessel growth. From the above mentioned studies it seems likely that the increased permeability of optic nerve vessels at E14 results from leakage of tracer across immature, "leaky" endothelial junctions in addition to extravasation of tracer from growing vascular tips.

Whether this leakage is a normal phenomenon or is artifactually caused by my experimental procedures is unclear. A variety of pathological and experimentally induced conditions cause changes in the permeability across endothelial junctions and result in increased production of vesicles in the capillary walls of adult cerebral capillaries. Acute and chronic hypertension, hypertonic

external or internal conditions, and electrically or chemically induced seizures are all known to cause focal sites of tracer leakage from adult CNS capillaries* (see reviews by Rapoport, '79; Brightman, '77; Westergaard, '77).

The permeability of cerebral vessels may also be affected artifactually by the tracer substance and/or the injections themselves. Thorotrast, preparations of colloidal iron and cadmium-free ferritin have all been shown in different systems to cause vascular injury and increase permeability of vessels. Cotran and Karnovsky ('67) have similarly shown that commercial preparations of HRP induce increases in EBA permeability of small vessels (predominantly venules) after local or parenteral injection in adult Sprague-Dawley rats. The vascular leakage in rats caused by HRP or thorotrast was associated with the degranulation of mast cells and could be inhibited by a combination of histamine and serotonin antagonists.

The volume of injection has also been suggested as contributing to increased vascular permeability. Schneeberger and Karnovsky ('71) found that the amount of HRP leaking from endothelial clefts of alveolar capillaries was greatly reduced by reducing the volume of injection. Horton and Hedley-Whyte ('79) also found that increasing

---

*Laties and co-workers ('79) have produced evidence which indicates that the capillaries of vascularized primate retinae may differ from cerebral capillaries in their resistance to hypertension-induced permeability changes. The authors found that while cerebral capillaries showed focal leakage to circulating EBA at carotid pressures elevated to 160 mm Hg, the retinal capillaries remained closed even at pressures as high as 310 mm Hg. Whether these unique properties only apply to retinal capillaries in monkeys is unclear.

their injection bolus from 0.1 ml to 1.0 ml in mice (total blood volume of mice is 1.3 ml) resulted in focal leakage of tracer from vessels. The injections in my studies, however, were below 10% of total blood volume, to minimize such difficulties.

Returning to the original motivation for this study, what can now be said about the possibility of local leakage of tracer to account for pericapillary filling following vitreal HRP injection? First, it is clear that leakage of tracer from the immature capillaries of E13 optic nerve capillaries is plausible. However, it is not likely due to the lack of a site where HRP might enter the vascular system after vitreal injection. The pecten, with its rich vascular plexus offers a perfect combination of composition and location to serve such a purpose, but both anatomical and permeability results suggest that vitreal HRP may not enter the pecten capillaries. From my own observations and the report of Raviola and Raviola ('67) the specialized pecten capillaries contain tight endothelial junctions and have no fenestrations. In addition, in all the vascular injections of E14 and P2 animals, HRP was never seen in the vitreal space nor at the vitreal surface, further supporting the impermeability of these vessels. Thus, while the intrinsic capillaries of the nerve might allow passage of tracer, the lack of a viable site of HRP entrance into the bloodstream diminishes this possibility.

The results of P2 and P60 vascular injections further diminish support for the possibility of local leakage in the nerve. After vitreal HRP injections, the pericapillary spaces of P3 nerves were filled throughout Zone 3, well beyond the furthest periaxonal spread

from the vitreal surface (see chapter 2). The vascular HRP injections clearly establish that the intrinsic capillaries of P2 nerves are impermeable to HRP in those regions. These vascular injection experiments offer compelling evidence to support the proposition that vitreally injected HRP spreads directly into the nerve, using the pericapillary spaces as a conduit system. Local extravasation of tracer directly into the pericapillary spaces from intrinsic capillaries does not contribute substantially to the pericapillary filling.

These vascular injection findings are significant in their general relevance to neurobiology and development. They support and extend earlier findings that the blood-brain barrier to circulating HRP is either deficient or absent early in the development of the chick embryo. Thus, after vascularization begins and prior to the closure or completion of the optic nerve capillaries, the parenchyma of the optic nerve and presumably the rest of the CNS, is bathed by circulating materials from the vasculature. It seems obvious therefore, that a variety of developmental events such as neuronal and glial differentiation, myelination, synapse formation, and cell death, may all in part be influenced by substances circulating in the bloodstream. The presence and simultaneous exposure of such factors to the CNS via the circulation opens the possibility of a hormone-like coordination of certain events throughout the CNS.

Another significant aspect of these findigs is the confirmation of a breach in the blood-brain barrier in the lamina cribrosa of the optic nerve. Thus, after the blood-brain barrier is formed the

lamina cribrosa is still constantly exposed to materials from the general circulation. This breach is not based on the permeability characteristics of the intrinsic capillaries of the nerve and thus is not coupled to the timing or extent of vascularization of the nerve. It exists independently of the blood-brain barrier itself.

Due to this breach in the blood-brain barrier, the laminar region of the optic nerve is constantly exposed to large molecular weight materials from the circulation and substances from the perineurial extracellular fluid. The optic nerve is susceptible to a variety of toxins, and other microorganisms that may circulate in the vascular system. The observation that papillitis and retrobulbar neuritis are associated with a variety of bacterial and viral infections might be explained by the microorganisms being deposited in the nerve after leaking from the fenestrated capillaries of the choroid.

CONCLUSIONS

Molecules such as HRP pass into the nerve via patent extracellular spaces that separate the glial foot processes which form the inner limiting membrane. Once past the inner limiting membrane, HRP penetrates into the nerve by: 1) percolating directly through the extracellular spaces and 2) passing into the pericapillary spaces of anterioles and venules of the optic pecten and traveling within the pericapillary conduit system throughout the nerve.

The precise rate of macromolecular passage via these two routes could not be determined from my results. Although the estimated

spread of HRP from the vitreous after 1 hour was less (0.5 mm) than after 4 hours (0.75 mm) at P3, further experiments are needed to determine a rate for this or other ages. At E13 and P3, the distance of periaxonal spread was less than 25% of the spread within the pericapillary conduit system.

A consistent finding in these studies was the existence of HRP-positive inclusions in foot processes and in the perinuclear cytoplasm of glial cells in the nerve. Their presence supports the hypothesis that glial endocytosis of extracellular materials is responsible for the removal of HRP from the periaxonal space. A blockage of extracellular space by hypothetical intercellular occludens junctions was not supported by my findings. Although gap junctions and desmosomes were occasionally seen in the optic nerve, tight junctions (other than endothelial junctions) were never observed.

The spread of HRP into the nerve varied with the age of chick depending on the vascularization of the nerve. Periaxonal spread of tracer from the vitreal surface is a consistent feature of this system. In contrast, passage via the pericapillary conduit system is dependent on formation of the vascular plexus, occurring after E8. Since the periaxonal spread of HRP is fairly constant throughout the period examined, the formation of a pericapillary conduit system (capable of conducting tracer into the retrobulbar nerve, the optic chiasm, and the contralateral nerve) is the major event relative to the extracellular movement of tracers.

Two further observations were generated by study of the vessels of control experiments, dealing with the access of vascularly

circulating HRP to the nerve. First, a breach in the blood-brain barrier at the lamina cribrosa is a common feature of the developing chick optic nerve at all ages. The leakage of vascularly injected HRP from choroidal capillaries and subsequent diffusion into the nerve were not related to the maturation of intrinsic vasculature of the nerve and thus, were constant. Second, the capillaries of E14 optic nerves do not constitute a barrier to vascularly circulating HRP as do P2 and adult CNS capillaries. The physical changes responsible for the altered permeability of these capillaries between E14 and P2 were unclear.

My goal was to determine whether the developing chick eye and optic nerve were suitable models for studies of the retrograde axonal transport of vitreally injected HRP and the developing isthmo-optic projection. Vitreally injected tracer (HRP) spread into the nerve and optic chiasm during the crucial period of isthmo-optic axon arrival at the eye. Thus, this potential artifact is an important consideration for all future studies of embryonic transport.

ACKNOWLEDGEMENTS

I thank Ilene Sugino, Doug Yasumura, Dr. Robert Lisenmeier, Simona Ikeda, and Nancy Lawson for their technical assistance and advice. Matt LaVail graciously and generously allowed me access to excellent EM and photographic facilities. Thanks also to Dave Akers, who assisted in producing photocopies of the figures, and Kathleen Dennett for carefully typing the manuscript.

REFERENCES

Abell, R.B. The permeability of blood capillary sprouts and newly formed blood capillaries as compared to that of older blood capillaries. Amer. J. Physiol. 147:237, 1946.

Anders, J.J. and Brightman, M.W. Assemblies of particles in the cell membranes of developing, mature and reactive astrocytes. J. Neurocytol. 8:777, 1979.

Anderson, D.R. Ultrastructure of human and monkey lamina cribrosa and optic nerve head. Arch. Ophthal. 82(6):800-814, 1969.

Ashton, N. The blood-retinal barrier and vasoglial relationships in retinal disease. Trans. Ophthalmol. Soc. (UK) 85:199, 1965.

Balazs, E.A., Toth, L.E.J., Jutheden, G.M., and Collins, B.A. Cytological and biochemical studies on the developing chicken vitreous. Exp. Eye Res. 4:237, 1965.

Bär, Th. and Wolff, J.R. The formation of capillary basement membranes during internal vascularization of the rat's cerebral cortex. Z. Zellforsch. 133:231, 1972.

Barlow, C.F., Domek, N.S., Goldberg, M.A., Roth, L.J. Extracellular brain space measured by S^{35} sulfate. Arch. Neurol. 5:102, 1961.

Behenson, G. Über die Forbstoffspeicherung in Zentralnervensystem der weissen mans in Verschiedenen Allerzustanden. Z. Zellforsch 4:515, 1927.

Bill, A. Drainage of intraocular fluids. In The Blood-Retinal Barriers, ed. J.G. Cunha-Vaz, Plenum, N.Y., p. 179, 1979.

Ben-Sira, I. and Riva, C.E. Fluorescein diffusion in the human optic disc. Invest. Ophthalmol. Vis. Sci. 14:205, 1975.

Bito, L. and de Rousseau, C.J. Transport functions of the blood-retinal barrier system and the microenvironment of the retina. In The Blood-Retinal Barriers, ed. J.G. Cunha-Vaz, Plenum, N.Y., p. 133, 1979.

Bradbury, M.W.B. Ontogeny of mammalian brain-barrier systems. In Fluid Environment of the Brain (ed.) H.F. Cserr, J.E. Fenstermacher, V. Fencl., Acad. Press Inc. N.Y., p. 81, 1975.

Brightman, M.W. The distribution within the brain of ferritin injected into cerebrospinal fluid compartments. II. Parenchymal distribution. Amer. J. Anat. 117:193, 1965.

Brightman, M.W., Anders, J.J., Schmechel, D., and Rosenstein, J.M. The lability of the shape and the content of glial cells. In Dynamic Properties of Glial Cells, ed. E. Schoffeniels, G. Franck, D.B. Towers, and L. Hertz, Oxford:Pergamon, p. 21, 1978.

Brightman, M.W., Klatzo, I., Olson, Y., and Reese, T.S. The blood-brain barrier to protein tracers under normal and pathological conditions. J. Neurol. Sci. 10:215, 1970a.

Brightman, M.W., Reese, T.S., and Feder, N. Assessment with the electron microscope of the permeability to peroxidase of cerebral endothelium in mice and sharks. In Capillary Permeability, Alfred Benzon Symp. II. (ed. C. Crone and N.A. Lassen), Academic Press, p. 463, 1970b).

Brightman, M.W. and Reese, T.S. Junctions between intimately apposed cell membranes in the vertebrate brain. J. Cell Biol. 40:648, 1969.

Bruns, R.R. and Palade, G.E. Studies on blood capillaries, Part 2 (transport of ferritin molecules across the wall of muscle capillaries). J. Cell Biol. 37:277, 1968.

Bunt, A.H., Lund, R.D. and Lund, J.W. Retrograde axonal transport of horseradish peroxidase by ganglion cells of the albino rat retina. Brain Res. 73:215, 1974.

Caley, D.S. and Maxwell, D.W. Development of the blood vessels and extracellular spaces during postnatal maturation of rat cerebral cortex. J. Comp. Neurol. 138:31, 1970.

Caulfield, J.P. and Farquar, M.G. The permeability of glomerular capillaries to graded dextrans. Identification of the basement membrane as the primary filtration barrier. J. Cell Biol. 63:883, 1976.

Chihara, E. Axoplasmic and nonaxoplasmic transport along the optic pathway of albino rabbits. A theoretical pattern of distribution. Invest. Ophthal. Vis. Sci. 18:339, 1979.

Clarke, E.R. and Clarke, E.L. Microscopic observations on the growth of blood capillaries in the living mammal. Amer. J. Anat. 64:251, 1939.

Clarke, P.G.H. and Cowan, W.M. The development of the isthmo-optic tract in the chick, with special reference to the occurrence and correction of developmental errors in the location and connections of isthmo-optic neurons. J. Comp. Neurol. 167:143, 1975.

Claude, P. and Goodenough, D.A. Fracture faces of zonulae occludentes from "tight" and "leaky" epithelia. J. Cell Biol. 58:390, 1973.

Cliff, W.J. Observations on healing tissue: A combined light and electron microscopic investigation. Trans. Royal Soc. (London) Ser. B. 246:305, 1963.

Cogan, D.G. Vascularization of the cornea. Arch. Ophthalmol. 41:406, 1949.

Cohen, A.I. Is there a potential defect in the blood-brain barrier at the choroidal level of the optic nerve canal? Invest. Ophthal. 12:513, 1973.

Cotran, R.S. and Karnovsky, M.J. Vascular leakage induced by horseradish peroxidase in the rat. Proc. Soc. Exp. Biol. Med. 126:577, 1967.

Coulombre, A.J. Correlations of structural and biochemical changes in the developing retina of the chick. Amer. J. Anat. 96:153, 1953.

Cserr, H.F., Cooper, D.N. and Milhorat, T.H. Flow of cerebral interstitial fluid as indicated by removal of extracellular markers from the rat caudate nucleus. Exp. Eye Res. Suppl. 461, 1977.

Cullen, M.J. and Gulley, R.L. Freeze-fracture studies of the macromolecular organization of glial membranes. Trends in Neurosci. 3:113, 1980.

Cunha-Vaz, J.G. Vitreous fluorophometry. In The Blood-Retinal Barriers, ed. J.G. Cunha-Vaz, Plenum, N.Y., p. 195, 1979.

Cunha-Vaz, J.G. and Maurice, D.M. Fluorescein dynamics in the eye. Doc. Ophthalmol. 26:61, 1969.

Cunha-Vaz, J.G., Shakib, M., and Ashton, N. Studies on the permeability of the blood-retinal barrier. I. On the existence, development, and site of a blood-retinal barrier. Brit. J. Ophthal. 50:441, 1966.

Davson, H. The blood-brain barrier. J. Physiol. (Lond.) 218:337, 1976.

Davson, H. The blood-brain barrier in The Structure and Function of Nervous Tissue (ed. Bourne, G.H.) Vol. IV, Academic Press, N.Y., p. 321, 1972.

Decker, R.S. and Friend, D.S. Assembly of gap junctions during amphibian neurulation. J. Cell Biol. 62:32, 1974.

Delormē, P., Gayet, J., and Grignon, G. Ultrastructural study on trans-capillary exchanges in the developing telencephalon of the chicken. Brain Res. 22:269, 1970.

Dermietzel, R. Junctions in the central nervous system of the cat. IV. Interendothelial junctions of cerebral blood vessels from selected areas of the brain. Cell Tiss. Res. 164:45, 1975.

Dermietzel, R. Junctions in the central nervous system of the cat. III. Gap junctions and membrane-associated orthagonal particle complexes (MOPC) in astrocytic membranes. Cell Tiss. Res. 149:121, 1974.

Donahue, S. and Pappas, G.D. The fine structure of capillaries in the cerebral cortex of the rat at various stages of development. Am. J. Anat. 108:331, 1961.

Ehrlich, P. Das Sanerstoff Bedurfuis des Organismus. Eine forben analytische Studie 1885, pp. 69-72, Hirschwald, Berlin.

Ernest, J.T. and Potts, A.M. Pathophysiology of the distal portion of the optic nerve. II. Vascular relationships. Amer. J. Ophthalmol. 66:380, 1968.

Fenstermacher, J.D. and Patlak, C.S. The exchange of material between cerebrospinal fluid and brain. In: Fluid Environment of the Brain (eds. H.F. Cserr, J.D. Fenstermacher, and V. Fencl), Academic Press, Inc., N.Y., 1975, p. 201.

Ferguson, R.K. and Woodbury, D.M. Penetration of ^{14}C-inulin and ^{14}C-sucrose into brain, cerebrospinal fluid, and skeletal muscle of developing rats. Exp. Brain Res. 7:181, 1969.

Field, E.J. and Brierley, J.B. Retroorbital tissues as a site of outflow of cerebral spinal fluid. Proc. Roy. Soc. Med. 42:447, 1949.

Fine, B.S.V. and Yanoff, M. Ocular Histology, 2nd ed., Harper Row, Hagerstown, Maryland, 1979.

Fischlschweiger, W. and O'Rahilly, R. The ultrastructure of the pecten oculi in the chick. Acta Anat. (Basal) 65:561, 1966.

Flage, T. Permeability properties of the tissues in the optic nerve head region in the rabbit and the monkey. An ultrastructural study. Acta Ophtalmol. 55:652, 1977.

Flage, T. The distribution of intravenously administered peroxidase in the optic nerve head of rabbit and monkey. Acta Ophthalmol. 53:801, 1975.

Flexner, J.B. and Flexner, L.B. Biochemical and physiological differentiation during morphogenesis. XI. The effect of growth on the amount and distribution of water protein, and fat in the liver and cerebral cortex of the fetal guinea pig. Anat. Rec. 106:413, 1950.

Flexner, L.B. and Flexner, J.B. Biochemical and physiological differentiation during morphogenesis. IX. The extracellular and intracellular phases of the liver and cerebral cortex of the fetal guinea pig as estimated from distribution of chloride and radiosodium. J. Cell. Comp. Physiol. 34:115, 1949.

Fowlks, W.L. Meridional flow for the corona ciliaris through the pararetinal zone of the rabbit vitreous. Invest. Ophthalmol. 2:63, 1963.

Franck, G., Grisar, Th., Moonen, G., and Schoffeniels, E. Potassium transport in mammalian astroglia. In Dynamic Properties of Glial Cells (eds. E. Schoffeniels, G. Franck, D.B. Towers, and L. Hertz), Pergamon Press, Oxford, 1978, p.315.

Friederia, H.H.R. The tridimensional ultrastructure of fenestrated capillaries. J. Ultrastruct. Res. 23:444, 1968.

Geijer, C. and Bill, A. Effects of raised intraocular pressure on retinal prelaminar, laminar, and retrolaminar optic nerve blood flow in monkeys. Invest. Ophthal. Vis. Sci. 18:1033, 1979.

Graham, R.C.J. and Karnovsky, M.J. The early stages of absorption of injected horseradish peroxidase in proximal tubules of mouse kidney. Ultrastructural cytochemistry by a new technique. J. Histochem. Cytochem. 14:291, 1966.

Grayson, M.C. and Laties, A.M. Ocular localization of sodium fluorescein: Effects of administration in rabbit and monkey. Arch. Ophthalmol. 85:600, 1971.

Haley, J.E., Wisniewski, H.M. and Ledeen, R.W. Extra-axonal diffusion in the rabbit optic system: A caution in axonal transport studies. Brain Res. 179:69, 1979.

Hamburger, V. and Hamilton, H.L. A series of normal stages in the development of the chick embryo. J. Morph. 88:49, 1951.

Hayreh, S.S. Fluids in the anterior part of the optic nerve in health and disease. Survey of Ophthalmol. 23:1, 1978.

Hayreh, S.S. Optic disc edema in raised intraocular pressure. V. Pathogenesis.Arch. Ophthalmol. 95:1553, 1977.

Hayreh, S.S. Blood supply and vascular disorders of the optic nerve. In: The Optic Nerve. (ed. J. Stanley Cant), C.V. Mosby Co., St. Louis, pp. 59-71, 1972.

Hayreh, S.S. Posterior drainage of the intraocular fluid from the vitreous. Exp. Eye Res. 5:123, 1966.

Hedges, T.R. and Zaren, H.A. The relationship of optic nerve tissue pressure to intracranial and systemic arterial pressure. Am. J. Ophthalmol. 75:90, 1973.

Hogan, M.J., Alvarado, J.A., and Weddell, J.E. Histology of the Human Eye. W.B. Saunders Co., Phil., 1971.

Horton, J.C. and Hedley-White, E.T. Protein movement across the blood-brain barrier in hypervolemia. Brain Res. 169:610, 1979.

Hudspeth, A.J. and Yee, A.G. The intercellular junctional complexes of retinal pigment epithelia. Invest. Ophthalm. Vis. Sci. 12:354, 1973.

Inou, S. and Hogg, J.C. Freeze-Etch study of the tracheal epithelium of normal guinea pigs with particular reference to intercellular junctions. J. Ultrastruct. Res. 61:89, 1977.

Ishikawa, T. Fine structure of retinal vessels in man and macaque monkey. Invest. Ophthalmol. 2:1, 1963.

Jaeger, R.J. and Benevento, L.A. A horseradish peroxidase study of the innervation of the internal structures of the eye. Evidence for a direct pathway. Invest. Ophthalmol. Vis. Sci. 19:575, 1980.

Jaffe, N.S. The vitreous In Clinical Ophthalmology, C.V. Mosby Co., St. Louis, 1969, p.11.

Jones, E.G. On the mode of entry of blood vessels into the cerebral cortex. J. Anat. 106:507, 1970.

Kanwar, Y.S. and Farquar, M.G. Anionic sites in the glomerular basement membrane. In vivo and In vitro localization to the laminae rarae by cationic probes. J. Cell Biol. 81:137, 1979.

Karlsson, V. Observations on the postnatal development of neuronal structures in the lateral geniculate nucleus of the rat by electron microscopy. J. Ultrastruct. Res. 17:158, 1967.

Kreutziger, G.O. Freeze etching of intercellular junctions of mouse liver. Proceedings of 26th meeting of Electron Microscope Soc. of Amer., Claitor's Pub. Div. Baton Rough, p.234.

Kristensson, K. and Wisniewski, H.M. Penetration of protein tracers into the epiretinal portion of the optic nerve in the rabbit eye. J. Neurol. Sci. 30:411, 1976.

Kuffler, S.W. Neuroglial cells: physiological properties and a potassium mediated effect on neuronal activity on the glial membrane potential. Proc. Royal Soc. (Series B) 168:1, 1967.

Kuffler, S.W. and Potter, D.D. Glia in the leech central nervous system: Physiological properties and neuron-glia relationship. J. Neurophysiol. 27:290, 1964.

Kuwabara, T. Species differences in the retinal pigment epithelium. In The Retinal Pigment Epithelium (eds. K.M. Zimm and M.F. Marmor), Harvard University Press, Cambridge, 1979.

Lajtha, A. The development of the blood-brain barrier. J. Neurochem. 1:216, 1957.

Landis, D.M.D. and Reese, T.S. Arrays of particles in freeze-fractured astrocytic membranes. J. Cell Biol. 60:316, 1974.

Lane, N.J. and Treherne, J.E. Peroxidase uptake by glial cells in the desheathed ganglia of the cockroach. Nature (Lond.) 223:861, 1969.

Lasansky, A. The pathway between hyaloid blood and retinal neurons in the toad. Structural observations and permeability to tracer substances. J. Cell Biol. 34:617, 1967.

Laties, A.M. and Rapoport, S.I. The blood-ocular barrier under osmotic stress. Studies on the freeze-dried eye. Arch. Ophthalmol. 94:1086, 1976.

LaVail, J.H. and LaVail, M.M. The retrograde intra-axonal transport of horseradish peroxidase in the chick visual system: A light and electron microscopic study. J. Comp. Neurol. 157:303, 1974.

Lee, J.C. and Olszewski, J. Penetration of radioactive bovine albumin from cerebrospinal fluid into brain tissue. Neurology 10:814, 1960.

Lumb, W.V. Small Animal Anesthesia. Philadelphia, Lea and Febiger, 1963, p.201.

Lyser, K.M. The fine structure of glial cells in the chicken. J. Comp. Neurol. 146:83, 1972.

Majno, G. and Palade, G.E. Studies on inflammation. I. The effect of histamine and serotonin on vascular permeability: An electron microscopic study. J. Biophys. Biochem. Cytol. 11:571, 1961.

Mann, I.C. Differentiation of retinal layers. Brit. J. Ophthalmol. 12:449, 1928.

Mann, I.C. The pecten of gallus domesticus. Quart. J. Microscop. Sci. 68:413, 1924a.

Mann, I.C. The function of the pecten. Brit. J. Ophthalmol. 8:209, 1924b.

Martinez-Palomo, A. and Erlij, D. Structure of tight junctions in epithelia with different permeability. Proc. Nat. Acad. Sci. (U.S.A.) 72:4487, 1975.

Maul, G.G. Structure and formation of pores in fenestrated capillaries. J. Ultrastruct. Res. 36:768, 1971.

Maurice, D.M. Drug exchanges between blood and vitreous. In The Blood-Retinal Barriers (ed. J.G. Cunha-Vaz), Plenum Press, N.Y., 1979, p.165.

Maurice, D.M. Protein dynamics in the eye studied with labeled proteins. Amer. J. Ophthalmol. 47:361, 1959.

Maurice, D.M. The exchange of sodium between the vitreous body and the blood and aqueous humor. J. Physiol. 137:110, 1957.

Max, S.R., Schwab, M., Dumas, M. and Thoenen, H. Retrograde axonal transport of nerve growth factor in the ciliary ganglion of the chick and the rat. Brain Res. 159:411, 1978.

McMahon, R.T., Tso, M., and McLean, I.W. Histological localization of sodium fluorescein in human ocular tissues. Am. J. Ophthalmol. 80:1058, 1975.

McNutt, N.S. Ultrastructure of the myocardial sarcolemma. Circ. Res. 37:1, 1975.

McNutt, N.S. and Weinstein, R.S. Membrane ultrastructure at mammalian intercellular junctions. Prog. Biophys. Molec. Biol. 26:47, 1973.

Minckler, D.S., Bunt, A.H., and Kloch, I.B. Radioautographic and cytochemical ultrastructural studies of axoplasmic transport in the monkey optic nerve head. Invest. Ophthal. Visual Sci. 17:33, 1978.

Minckler, D.S., Bunt, A.H., and Johanson, G.W. Orthograde and retrograde axoplasmic transport during acute ocular hypertension in the monkey. Invest. Ophthalmol. Visual Sci. 16:427, 1977.

Minckler, D.S. and Tso, M. Papilledema produced by cyclo-cryotherapy, an experimental model. Amer. J. Ophthalmol. 82:577, 1976.

Mollgard, K., Malinowska, D.H. and Saunders, N.R. Lack of correlation between tight junction morphology and permeability properties in developing choroid plexus. Nature (Lond.) 264:293, 1976.

Morales, R. and Duncan, D. Specialized contacts of astrocytes with astrocytes and with other cell types in the spinal cord of the cat. Anat. Res. 182:255, 1975.

de la Motte, D.J. Removal of horseradish peroxidase and fluorescein-labelled dextran from CSF spaces of rabbit optic nerve. A light and electron microscopic study. Exp. Eye Res. 27:585, 1978.

Nabeshima, S., Reese, T.S., Landis, D.M.D., and Brightman, M.W. Junctions in the meninges and marginal glia. J. Comp. Neurol. 164:127, 1975.

Okinami, S., Ohkuma, M. and Tsukahara, I. Kundt intermediary tissues as a barrier between the optic nerve and retina. Albrecht von Gaefes Arch. Klin. Exp. Ophthalmol. 201:57, 1976.

Olsson, Y. and Kristensson, K. Permeability of blood vessels and connective tissue sheaths in retina and optic nerve. Acta. Neuropath. (Berl.) 26:147, 1973.

Olsson, Y. and Hossman, K-A. Fine structural localization of exudated protein tracers in the brain. Acta Neuropath. 16:103, 1970.

Olsson, Y., Klatzo, I., Sourander, P., and Steinwall, O. Blood-brain barrier to albumin in embryonic, newborn, and adult rats. Acta Neuropath. 10:117, 1968.

O'Rahilly, R. and Meyer, D.B. The development and histochemistry of the pecten oculi. In: The Structure of the Eye (ed. G.K. Smelser), New York Academic Press, 1961, p.207-219.

Palade, G.E. and Bruns, R.R. Structural modulations of plasmalemmal vesicles. J. Cell Biol. 37:633, 1968.

Palm, E. On the occurrence in the retina of conditions corresponding to the blood-brain barrier. Acta Ophthalmol. 25:29, 1947.

Pappius, H.M. Normal and pathological distribution of water in brain. In: Fluid Environment of the Brain (eds. H.F. Cserr, J.D. Fenstermacher, V. Fencl), Academic Press Inc., N.Y., 1975, p.183.

Peters, A., Palay, S.L., and Webster, H. de F. The Fine Structure of the Nervous System: The Neurons and Supporting Cells. W.B. Saunders Co., Philadelphia, 1976.

Peyman, G.A. and Apple, D. Peroxidase diffusion processes in the optic nerve. Arch. Ophthalmol. 88:650, 1972.

Peyman, G.A. and Bok, D. Peroxidase diffusion in the normal and laser-coagulated primate retina. Invest. Ophthalmol. Vis. Sci. 11:35, 1972.

Peyman, G.A., Spitznas, M., Strastsma, B.R. Peroxidase diffusion in the normal and photocoagulated retina. Invest. Ophthalmol. 10:181, 1971.

Phelps, C.H. The development of glio-vascular relationships in the rat spinal cord: an electron microscope study. Z. Zellforsch. 128:555, 1972.

Pysh, J.J. The development of the extracellular space in the neonatal rat inferior colliculus: An electron microscopic study. Amer. J. Anat. 124:411, 1969.

Quigley, H.A. Gap junctions between optic nerve head astrocytes. Invest. Ophthalmol. Visual Sci. 16:582, 1977.

Quigley, H.A., Guy, J., and Anderson, D.R. Blockade of rapid axonal transport. Effect of intraocular pressure elevation in primate optic nerve. Arch. Ophthalmol. 97:525, 1979.

Radius, R.L. and Anderson, D.R. Distribution of albumin in the normal monkey eye as revealed by Evans blue fluorescence microscopy. Invest. Ophthalmol. Visual Sci. 19:238, 1980.

Rahmann, H. Different modes of substance flow in the optic tract. Acta Neuropath. (Berl.) Suppl. V.:162, 1971.

Rapoport, S.I. Cerebrovascular permeability in the normal brain and following osmotic opening. In: The Blood-Retinal Barriers (ed. J.G. Cunha-Vaz), Plenum Press, N.Y., 1979, p.81.

Raviola, E. The structural basis of the blood-ocular barriers. Exp. Eye Res. Suppl.:p.27, 1977.

Raviola, E. and Raviola, G. A light and electron microscopic study of the pecten of the pigeon eye. Amer. J. Anat. 120:427, 1967.

Reale, E., Luciano, L., and Spitznas, M. Introduction to freeze-fracture method in retinal research. Albrecht v. Gaefes Arch. Klin. Exp. Ophthalmol. 192:73, 1974.

Reese, T.S. and Karnovsky, M.J. Fine structural localization of a blood-brain barrier to exogenous peroxidase. J. Cell Biol. 34:204, 1967.

Rennke, H.G. and Venkatachalam, M.A. Glomerular permeability: In vivo tracer studies with polyanionic and poly cationic ferritins. Kid. Int. 11:44, 1977.

Rennke, H.G., Cotran, R.S., and Venkatachalam, M.A. Role of molecular charge in glomerular permeability. Tracer studies with cationized ferritins. J. Cell Biol. 67:638, 1975.

Rodriguez-Peralta, L.A. Hematic and fluid barriers in the optic nerve. J. Comp. Neurol. 126:109, 1966.

Rodriguez-Peralta, L.A. The blood-optic nerve barrier. Anat. Rec. 145:277, 1963.

Romanoff, A.L. The Biochemistry of the Avian Embryo. New York, Interscience, 1967.

Romanoff, A.L. The Avian Embryo. Structural and Functional Development. New York, MacMillan, 1960.

Roy, S., Hiranoi, A., Kochen, J.A., and Zimmerman, H.M. The fine structure of cerebral blood vessels in chick embryos. Acta Neuropath. (Berl.) 30:277, 1974.

Rush, J.E., Staehlin, L.A. and Ellisman, M.H. Rectangular array of particles on freeze cleaved membranes are not gap junctions. Exp. Cell Res. 86:176, 1974.

Sandison, J.C. Contraction of blood vessels and observations on the circulation in the transparent chamber in the rabbit's ear. Anat. Rec. 54:105, 1932.

Saunders, N.R. Ontogeny of the blood brain barrier. Exp. Eye Res. Suppl. 523, 1977.

Schnaudigel, O. Die Vialfarbung mit Trypanbau am auge. Albrecht von Gaefis Arch. Ophthalmol. 86:93, 1913.

Schneeberger, E.E. and Karnovsky, M.J. The influence of intravascular fluid volume on the permeability of newborn and adult mouse lungs to ultrastructural protein tracers. J. Cell Biol. 49:319, 1971.

Schoefl, G.I. Electron microscopic observations on the regeneration of blood vessels after injury. Annals of N.Y. Acad. Sci. 116(3):789, 1964.

Seaman, A.R. and Storm, H. A correlated light and electron microscopic study on the pecten oculi of the domestic fowl (Gallus domesticus). Exp. Eye Res. 2:163, 1963.

Sellinger, D.Z. and Petiet, P.D. Horseradish peroxidase uptake in vivo by neuronal and glial lysosomes. Exp. Neurol. 38:370, 1973.

Shabo, A.L. and Maxwell, P.S. The subarachnoid space following the introduction of a foreign protein: An electron microscopic study with peroxidase. J. Neuropath. Exp. Neurol. 30:506, 1971.

Shakib, M. and Cunha-Vaz, J.G. Studies on the permeability of the blood-retinal barrier. IV. Role of the junctional complexes of the retinal vessels on the permeability of the blood-retinal barrier. Exp. Eye Res. 5:229, 1966.

Sheffield, J.B. and Fischman, D.A. Intercellular junctions in the developing neural retina of the chick embryo. Z. Zellforsch. 104:405, 1970.

Sherman, S.H., Green, K. and Laties, A.M. The fate of anterior chamber fluorescein in the monkey eye. 1. The anterior chamber outflow pathways. Exp. Eye Res. 27:159, 1978.

Shiose, Y. Electron microscopic studies on blood-retinal barrier and blood-aqueous barrier. Jap. J. Ophthalmol. 14:73, 1970.

Simionescu, N., Simionescu, M., and Palade, G.E. Structural basis of permeability in sequential segments of microvasculature of the diaphram. II. Pathways followed by microperoxidase across the endothelium. Microvasc. Res. 15:17, 1978.

Simionescu, N., Simionescu, M., and Palade, G.E. Permeability of muscle capillaries to small heme-peptides. Evidence for the existence of patent transendothelial channels. J. Cell Biol. 64:586, 1975a.

Simionescu, M., Simionescu, N., and Palade, G.E. Segmental differentiations of cell junctions in the vascular endothelium. J. Cell Biol. 67:863, 1975b.

Smith, R.S. and Rudt, L.A. Ocular, vascular and epithelial barriers to microperoxidase. Invest. Ophthalmol. Vis. Sci. 14:556, 1975.

Spector, R.G. Water content of immature rat brain following cerebral anoxia and ischemia. Brit. J. Exp. Path. 43:472, 1962.

Spitznas, M. and Reale, E. Fracture faces of fenestrations and junctions of endothelial cells in human choroidal vessels. Invest. Ophthalmol. Vis. Sci. 14:98, 1975.

Staehelin, L.A. Three types of gap junctions interconnecting intestinal epithelial cells visualized by freeze etching. Proc. Nat. Acad. Sci. (U.S.A.) 69:1318, 1972.

Sumi, S.M. The extracellular space in the developing rat brain: Its variation with changes in osmolarity of the fixative, method of fixation, and maturation. J. Ultrastruct. Res. 29:398, 1969.

Suran, A.A. and McEwen, W.K. Diffusion studies with ox vitreous body. Amer. J. Ophthalmol. 51:814, 1961.

Suzuki, F. and Nagano, T. Morphogenesis of tight junctions in the peritoneal mesothelium of the mouse embryo. Cell Tiss. Res. 198:247, 1979.

Tschirgi, R.D. Protein complexes and the impermeability of the blood-brain barrier to dyes. Amer. J. Physiol. 163:756, 1950.

Tso, M., Shih, C.-Y, and McLean, I.W. Is there a blood-brain barrier at the optic nerve head? Arch. Ophthalmol. 93:815, 1975.

Tsukahara, I. and Yamashita, H. An electron microscopic study on the blood-optic nerve and fluid-optic nerve barrier. Albrecht von Gaefes Arch. Klin. Exp. Ophthalmol. 196:239, 1975.

Turner, P.T. and Harris, A.B. Ultrastructure of exogenous peroxidase in cerebral cortex. Brain Res. 74:305, 1974.

Van Harreveld, A. The extracellular space in the vertebrate central nervous system. In: The Structure and Function of Nervous Tissue. Vol. IV. Bourne Acad. Press, N.Y. and London, 1972, p.447.

Vaugn, J.E. An electron microscopic analysis of gliogenesis in rat optic nerves. Z. Zelforsch. 94:293, 1969.

Vaugn, J.E. and Peters, A. Electron microscopy of the early postnatal development of fibrous astrocytes. Amer. J. Anat. 121:131, 1967.

Vernadakis, A. and Woodbury, D.M. Cellular and extracellular spaces in developing rat brain: Radioactive uptake studies with chloride and inulin. Arch. Neurol. 12:284, 1965.

Wagner, H.-J., Pilgrim, Ch., Brandl, J. Penetration and removal of horseradish peroxidase injected into the cerebrospinal fluid. Role of cerebral perivascular spaces, endothelium and microglia. Acta Neuropath. (Berl.) 27:299, 1974.

Wakai, S. and Hirokawa, N. Development of the blood-brain barrier to HRP in the chick embryo. Cell Tiss. Res. 195:195, 1978.

Walls, G.L. The vertebrate eye and its adaptive radiation. Hafner, N.Y., 1942.

Warwick, R. Eugene Wolff's Anatomy of the Eye and Orbit, 7th Ed., W.B. Saunders Co., Philadelphia and Toronto, 1976.

Westergaard, E. The blood-brain barrier to horseradish peroxidase under normal and experimental conditions. Acta Neuropathol. (Berl.) 39:181, 1977.

Weysse, A.W. and Burgess, W.S. Histogenesis of the retina. Amer. Nat. 40:611, 1906.

White, F.P. Protein synthesis in the rat telencephalic slices: High amounts of newly synthesized protein found in association with brain capillaries. Neurosci. 5:173, 1980.

Williams, M.C. and Wissig, S.L. The permeability of muscle capillaries to horseradish peroxidase. J. Cell Biol. 66:531, 1975.

Wissig, S.L. Identification of the small pore in muscle capillaries. Acta Physiol. Scand. Suppl. 463:33, 1979.

Wollam, D.H.M. and Millen, J.W. The perivascular spaces of the mammalian central nervous system and their relation to the perineuronal and subarachnoidal spaces. J. Anat. 89:193, 1955.

Wood, J.G., Jean, D., Whitaker, J.N., McLaughlin, B.J. and Albers, R.W. Immunocytochemical localization of the sodium, potassium activated ATPase in Knifefish brain. J. Neurocytol. 6:571, 1977.

Yamashita, H., Mikii, H., Tsukahara, I. and Ogawa, K. A histochemical study on the blood-optic nerve and fluid-optic nerve barrier. Acta Histochem. Cytochem. 6:163, 1973.

Yoshimoto, H. and Murata, M. A freeze-fracture study on chorio-capillaries in spontaneously hypertensive rats. Ophthalmic Res. 11:177, 1979.

FIGURE LEGENDS

Figure 1 Electron micrographs of the inner limiting membrane (ilm)

A. Vitreal surface of E6 embryo, 4 hrs after vitreal HRP injection. A series of glial end feet form the inner limiting membrane. The processes contain numerous particles (presumed to be glycogen) and larger, HRP-positive inclusions (arrows). The basal lamina at the vitreal surface is masked by HRP reaction product in the vitreal space (vit). HRP (barred arrows) has spread to the extracellular space between the glial processes of the ilm and surrounds ganglion cell axons in the optic fiber layer. Bar = 0.5 μm.

B. Vitreal surface of an uninjected chick at P3. The glial cell processes are separated by patent extracellular spaces. The periodic globular deposits in the basal lamina are found in tissue post-fixed in reduced osmium. Bar = 0.5 μm.

Figure 2 Electron micrographs of the E5.5 retina.

A. The pigment epithelia (P.E.) and neural retinal layers are separated by the patent ventricular space (V). This embryo received HRP intravitreally, 1 hr earlier. Reaction product is visible in the extracellular spaces between retinal elements (arrow) and adhering to cytoplasmic extensions (barred arrow) which project from both PE and neural retinal cells into the ventricular space. M - nucleus of a mitotic cell. Bar = 1.0 μm.

B. An electron micrograph of the retina of an uninjected E6 embryo. Cytoplasmic extensions protrude into the patent

ventricular space. Zonulae adhaerentes (arrows) are present between adjacent neural retina cells. Occasionally elements of the PE and neural retina are joined by gap junctions. Bar = 0.2 μm.

Figure 3 Junctional complexes between cells of the retinal pigment epithelium.

A. An arc-shaped gap junction (gj) and a tight junction (tj) between adjacent PE cells are shown. Bar = 0.1 μm.

B. Pigment epithelial junction of P3 retina, 1 hr after vitreal HRP injection. Reaction product fills the retinal extracellular space (arrow) but it is not present in the extracellular space beyond the PE tight junction (barred arrow). Bar = 0.1 μm.

Figure 4 Light micrographs of the E6 retina and optic nerve.

A. The patent ventricular space extends from the retina into the optic nerve. Numerous mitotic profiles (M) are present in the proliferative zone adjacent to the ventricle in the retina and the nerve. (10 μm thick, thionine-stained paraffin section) Bar = 50 μm.

B. Some cellular elements of the nerve are arranged longitudinally (arrow). Also apparent is the loosely organized cellular cluster at the vitreal surface of the optic nerve head (Bergmeister's papilla), and the cellular rays which radiation from the papilla into the nerve. (Toluidine blue-stained plastic section of the retina and optic nerve) Bar = 100 μm.

Figure 5

A. At E13, numerous scleral trabeculae extend from the pecten and perineurial connective tissue into the nerve. The space separating the neural retina from the perineurial connective tissue is an artifact of preparation. (Toluidine blue-stained, 2 μm thick, plastic section) Bar = 200 μm.

B. The optic nerve head of a P3 chick. Zone 1 (retinal lamina), extends from the vitreal surface to the level of the pigment epithelium. Zone 2 (choroidal and scleral laminae), extends from Zone 1 to the outer level of the cartilagenous cuff (CC). Zone 3 (retrobulbar portion) extends from Zone 2 to the optic chiasm. Vascular septae extend posteriorly into the nerve (arrows). In some cases, their continuity with scleral trabeculae at the lamina cribrosa (barred arrows) can be appreciated. (Toluidine blue-stained, 2 μm thick, section) Bar = 200 μm.

Figure 6 Photomicrographs of the optic pecten.

A. The choroid fissure near the optic nerve head. Bergmeister's papilla (bp), the loosely arranged tissue situated between folds of the optic cup has protruded into the vitreal space. (10 μm thick, thionine-stained, paraffin section) Bar = 50 μm.

B. A segment of a single E13 pecten fold. Note the scattered, disorganized arrangement of immature vascular elements (arrows) and pigmented interstitial cells (barred arrows). (2 μm thick, toluidine blue-stained plastic section) Bar = 10 μm.

C. A P3 pecten fold. Open-lumen capillaries are clearly discernible (arrows). Dense, pigmented interstitial cells are segregated, filling the gaps separating vascular elements (barred arrows). (2 μm thick, toluidine blue-stained plastic section) Bar = 10 μm.

Figure 7 Electron micrographs of P3 pecten capillaries and interstitial cells.

A. Cellular elements in a P3 pecten fold. Two capillaries, whose endothelial walls feature numerous luminal and abluminal cytoplasmic processes, are shown. The perinuclear region contains numerous cytoplasmic organelles such as rough endoplasmic reticulum (RER), Golgi complexes (G), and mitochondria (MIT). The processes forming the capillary luminal walls are often attenuated (lg arrow). The adventitiae separating the capillaries contains a finely dispersed arrangement of collagen fibrils in addition to an interstitial cell. A basal lamina forms the boundary of the pecten fold at the vitreal space and surrounds the interstitial cell. Bar = 0.5 μm.

B. The region of apposition of two pecten interstitial cells is often the site of focal junctions between the adjacent cells (arrows). Bar = 0.2 μm.

C. A pecten capillary endothelial cell of a P3 chick in which luminal cytoplasmic extensions are apparent. Omega figures suggest vesicle fusions at the luminal and abluminal surfaces (arrows). Tight junctions (tj) are seen between adjacent endothelial processes. Bar = 0.5 μm.

Figure 8

A and B. Ink-filled blood vessels are apparent in the perineurial connective tissue and in the optic nerve head of an E8 embryo injected vascularly with India ink. A set of four short branches of this perineurial plexus (arrows) extend to the network of vessels at the base of the pecten. In B, the vascular connection between perineurial and pecten vessels is also present (arrow), in addition to faintly filled vessels present in the optic nerve (barred arrows). (150-200 μm thick, thionine-stained, frozen sections) Bar = 200 μm.

C. Ink-filling of vessels of an E10 nerve reveals numerous vessels radiating from pial vessels (pv) and vessels in the perineurial connective tissue surrounding the lamina cribrosa. Bar = 200 μm.

D. By E16, the vascular invasion has resulted in a dense branching and anastomosing network of vessels throughout the nerve. Bar = 500 μm.

Figure 9 Electron micrographs of E13 optic nerve capillaries.

A. Four endothelial processes (end) joined by tight junctions form an open capillary lumen which contains a nucleated red blood cell (rbc). The electron-dense cell at the lower right is presumed to be a developing glial cell (gl) whose processes have begun wrapping around the vascular cells. Later, these processes will form the perivascular glial sheath. Bar = 1.0 μm.

B. A capillary at E13. Two thick endothelial processes, joined by tight junctions bound a lumen which is occupied by several cytoplasmic projections. Several glial processes form a partial sheath around the vascular cells. No basal laminae are apparent in either A or B. Bar = 0.5 μm.

C. A typical example of membrane fusion between the endothelial cell processes of an E13 embryonic optic nerve capillary. Bar = 0.1 μm.

Figure 10 Electron micrographs of the vascular unit in uninjected P3 nerves.

A. A P3 capillary and other concentrically arranged elements are demonstrated. Capillary endothelial processes (end) joined by a tight junction outline the boundary of a round capillary lumen. A vascular basal lamina (vbl) situated at the abluminal endothelial surface, also encloses processes of cells in the pericapillary space (pcs). The pericapillary space is bounded by a sheath of astrocytic processes (Ast) identifiable by the presence of bundles of astrocytic filaments, and its associated glial basal lamina (gbl). Bar = 0.1 μm.

B. Endothelial processes of a comparable P3 capillary are joined by tight junctions with multiple sites of membrane fusion (arrows). Bar = 0.1 μm.

C and D. Astrocytic processes forming the pericapillary sheath are occasionally joined by junctional specializations such as desmosomes (C) and gap junctions (D). No occludens junctions were found. Bar = 0.1 μm.

Figure 11 Electron micrographs of capillaries of the choriocapillaris.

A. A segment of the luminal wall of a P3 choroid capillary demonstrating fenestrae (a) with a single diaphram and central knob (barred arrow), and transendothelial pores with double diaphrams (b). Bar = 0.1 μm.

B. When cut tangentially, the endothelial openings appear as electron-lucent circular profiles with a diffuse central density (arrow). Bar = 0.1 μm.

C. The endothelial junction of the P3 choriocapillaris capillary features points of membrane fusion (arrow). Bar = 0.1 μm.

D. At E6, the membrane fusion sites at endothelial junctions (barred arrows) appear to be circumvented (arrow) by vesicles at the luminal and abluminal surfaces. Bar = 0.1 μm.

E. At P3, a vesicle fusing simultaneously with the luminal surface and the abluminal end of the endothelial cleft, circumvents the endothelial tight junction (barred arrows). Bar = 0.1 μm.

Figure 12 The retrobulbar region of the optic nerve of a P3 chick.

A. Photomicrograph showing clear capillary lumens surrounded by darkly staining pericapillary connective tissue. Glial cells are present both adjacent to vascular elements (arrows), and in clusters segregated from vascular elements (barred arrows). (2 μ m thick, toluidine blue-stained plastic section) Bar = 20 μm.

B. Electron micrograph showing a perivascular astrocyte (barred arrow) and a cluster of extravascular glial cells [containing astrocytes (A) and oligodendrocytes (O)] situated among both myelinated (mn) and unmyelinated (un) nerves. Bar = 2.0 μm.

Figure 13

A. The optic nerve head of an E5.5 embryo, 1 hr after HRP injection into the vitreous. Note dense, diffuse, reaction product at the vitreal surface diminishing with distance in the nerve. A region in which enzyme substrate failed to penetrate is located near the vitreal surface (*). Unstained, 10 μm thick plastic section. Bar = 200 μm.

B. Electron micrograph from Zone 2 of an E5.5 embryo, 4 hrs after intravitreal injection. The developing glial cell (gl) contains numerous HRP-positive inclusions (arrow). Reaction product appears adsorbed to the surface of axonal and glial profiles (barred arrow). Bar = 0.5 μm.

Figure 14 E13 optic nerves, 1 hr after intravitreal HRP injection.

A. Diffuse reaction product extends from the vitreal surface into Zones 1 and 2. HRP-filled vascular septae (arrows) extend from a region of diffuse extracellular staining into Zone 3. As in fig. 13A, the asterisk marks a region in which substrate failed to penetrate. (Unstained, 10 μm thick plastic section) Bar = 200 μm.

B. Electron micrograph of Zone 2. The marker appears within the pericapillary space (pcs) and surrounds axons in the nerve parenchyma (arrows). Astrocytic processes (Ast) that form the boundary of the pericapillary space also contain HRP-positive inclusions (I). Endothelial junctions (tj) of the developing capillary (C) create an irregular capillary lumen (L). Bar = 1.0 μm.

Figure 15 P3 optic nerve head, 1 hr after intravitreal HRP injection.

A. Diffuse reaction product extends past the region of poor substrate penetration (*) through Zones 1 and 2 and into the proximal portion of Zone 3. As in E13, nerves after similar injections, HRP-filled vascular septae extend beyond the zone of diffuse tracer penetration into Zone 3. Bar = 200 μm.

B. Reaction product highlights vascular septae surrounding vessels of the optic chiasm after vitreal HRP injection. (Unstained, 10 μm thick, plastic sections) Bar = 200 μm.

Figure 16 Electron micrographs of P3 optic nerves, 1 hr after intravitreal HRP injections.

A. A glial cell in Zone 2 is surrounded by myelinated and unmyelinated axons. Reaction product fills the extracellular space surrounding all cellular elements of this zone (arrows) and glial cytoplasmic inclusions (barred arrows). Bar = 1.0 μm.

B. An HRP-filled pericapillary space (pcs) in Zone 3. Reaction product has collected in the periaxonal space (arrow) outside the pericapillary astrocytic processes (Ast).

Dense HRP-positive inclusions are present within astrocytic processes (barred arrows). Bar = 1.0 μm.

Figure 17 Left optic nerve of P3 chick, 4 hrs after intravitreal injection in the right eye.

A. Reaction product has accumulated in the choroid and in the scleral trabeculae (arrows) radiating into the retrobulbar nerve. (Unstained, 10 μm plastic section) Bar = 200 μm.

B. Zone 2 of the left optic nerve. The marker (arrow) has collected near the astrocytic sheath processes (Ast). Reaction product also is present between the axonal surfaces and the astrocytic processes (barred arrow). Bar = 0.5 μm.

Figure 18 Diagram of the optic nerve of a P3 chick in which HRP was injected into the vitreal chamber.

The large arrows near the vitreal surface indicate the route of access of HRP by direct diffusion through the periaxonal spaces of the optic nerve. The small arrows illustrate the route of access of HRP into the periaxonal spaces via the pericapillary spaces after either 1) diffusion into these pericapillary spaces from the vitreous, or 2) escape from fenestrated capillaries of the choroid (that anastomose with pecten vessels) and percolation through the pericapillary spaces bounded by astrocytic end feet (inset).

Figure 19 Micrographs of E14 optic nerves after vascular HRP injection.

A. The optic nerve head of an E14 embryo which was fixed immediately after cardiac injection of HRP. Note the dense, diffuse reaction product in all three zones of the nerve and especially dense accumulation in the scleral connective tissue (sct). Reaction product densely fills vascular septae (arrows) in all zones (including the optic chiasm) in which the substrate has penetrated. (Unstained, 10 μm thick plastic section) Bar = 50 μm.

B and C. Electron micrographs from Zone 2 of an E14 embryo, 1 hr (B), and 4 hrs (C), after vitelline vein, HRP injection. Reaction product is adsorbed to the glial basal lamina of the pericapillary sheath (lg arrows), is present in organelles within astrocytic process inclusions (B), and in the astrocyte perinuclear cytoplasm (C) (barred arrows). Marker also has gained access to periaxonal spaces where it is adsorbed to glial and axonal surfaces (sm arrows).
Bar = 1.0 μm.

D. Four hours after vascular HRP injections, the perinuclear cytoplasm of many glial cells in the nerve are filled with numerous HRP-positive inclusions. Bar = 1.0 μm.

Figure 20

A. A micrograph of P2 optic nerve head, after intracardiac injection of HRP. The reaction product accumulates in the choroid, in the scleral trabeculae radiating into the nerve

(arrow), and in vascular septae within the nerve (barred arrows). (Unstained, 10 μm plastic section) Bar = 200 μm.

B. Electron micrograph of the choriocapillaris of a P2 chick, 1 hr after vascular injection. Reaction product is densely deposited at the luminal and abluminal surfaces of the capillary walls, on collagen fibrils in Bruch's membrane, and surrounding the basal processes of cells of the adjacent PE. Note reaction product filling pore-shaped spaces in the choroid capillary wall (arrow) and in continuity across an endothelial junction (barred arrow). Bar = 0.5 μm.

C. Electron micrograph of the endothelial junction of an intrinsic optic nerve capillary after vascular HRP injection in a P2 chick. Reaction product is deposited at the luminal surface, but is blocked from passing between adjacent endothelial processes by the tight junction between the processes (arrow). Bar = 0.1 μm.

Figure 21 P2 optic nerve capillaries, 1 hr after vascular HRP injection.

A. The convoluted lumen of a capillary is highlighted by reaction product. The tortuous nature of the luminal space of this capillary makes it difficult to identify the round, HRP-filled profiles (adjacent to the lumen) as closed vesicles or transversely sectioned continuities of the luminal space. The reaction product present in the luminal and pericapillary spaces is separated by the tight junctions which seal the capillary luminal space. Bar = 1.0 μm.

B. An open-lumen capillary after vascular HRP injection. The pericapillary and periaxonal spaces (barred arrows) are outlined by reaction product. Note the numerous HRP-positive organelles in the cell located in the pericapillary space. Bar = 1.0 μm.

FIGURE ABBREVIATIONS

Ast.	astrocytic process
ax.	axon
BM.	Bruch's membrane
bp	Bergmeister's papilla
C	developing capillary
CC	cartilagenous suff
ch	choroid
end	endothelial cell
G	golgi complex
gj	gap junction
I	HRP inclusion
IC	interstitial cell
ilm	inner limiting membrane
L	lumen
M	mitotic nucleus
mit	mitochondria
OC	optic chiasm
ON	optic nerve
OP	optic pecten
PE	pigment epithelium
pv	pial vessels
r	retina
rer	rough endoplasmic reticulum
sct	scleral connective tissue
tj	tight junction
v	ventricular space
vit	vitreal space
*	area of poor substrate penetration

FIGURE 1

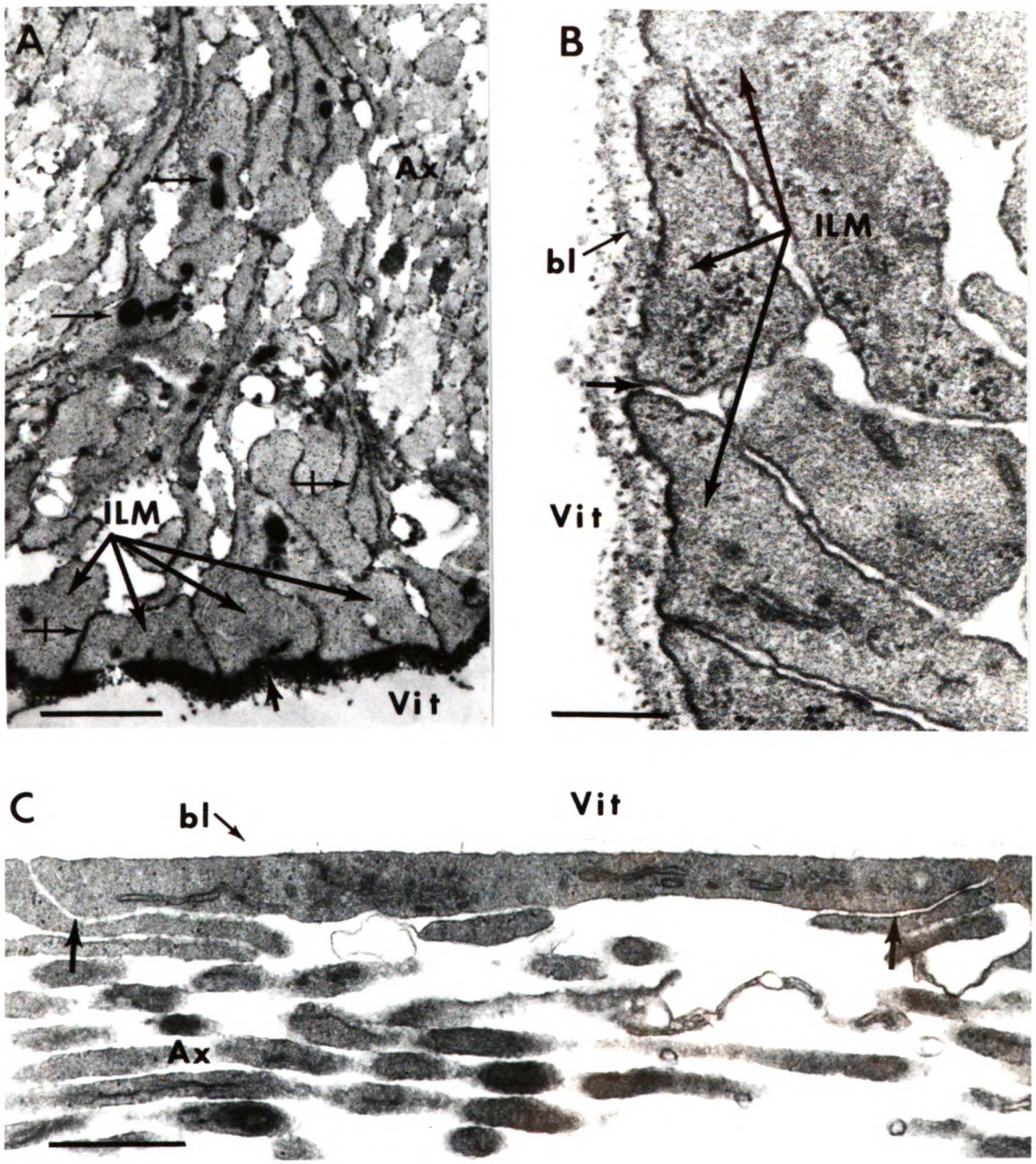

FIGURE 2

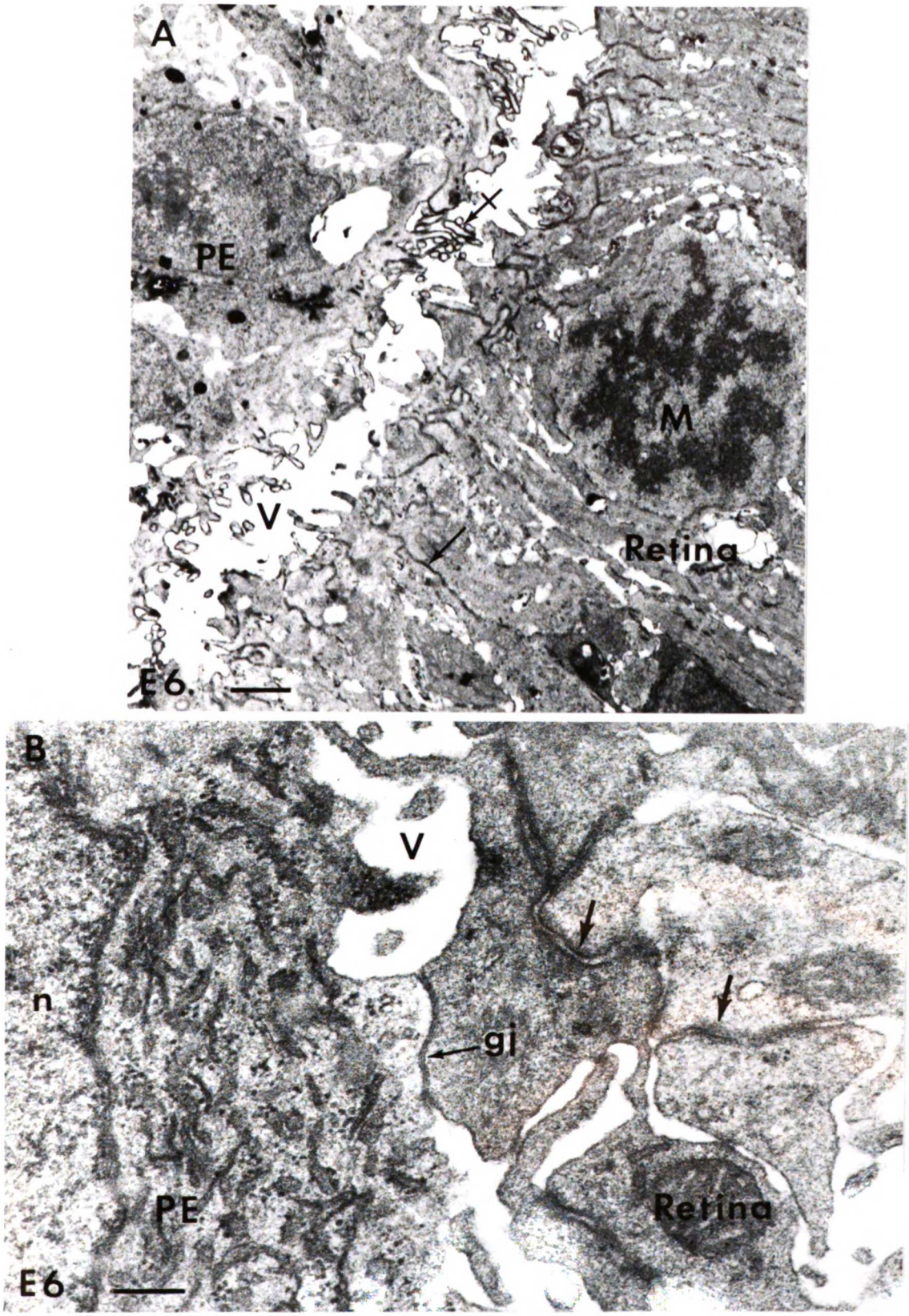

FIGURE 3

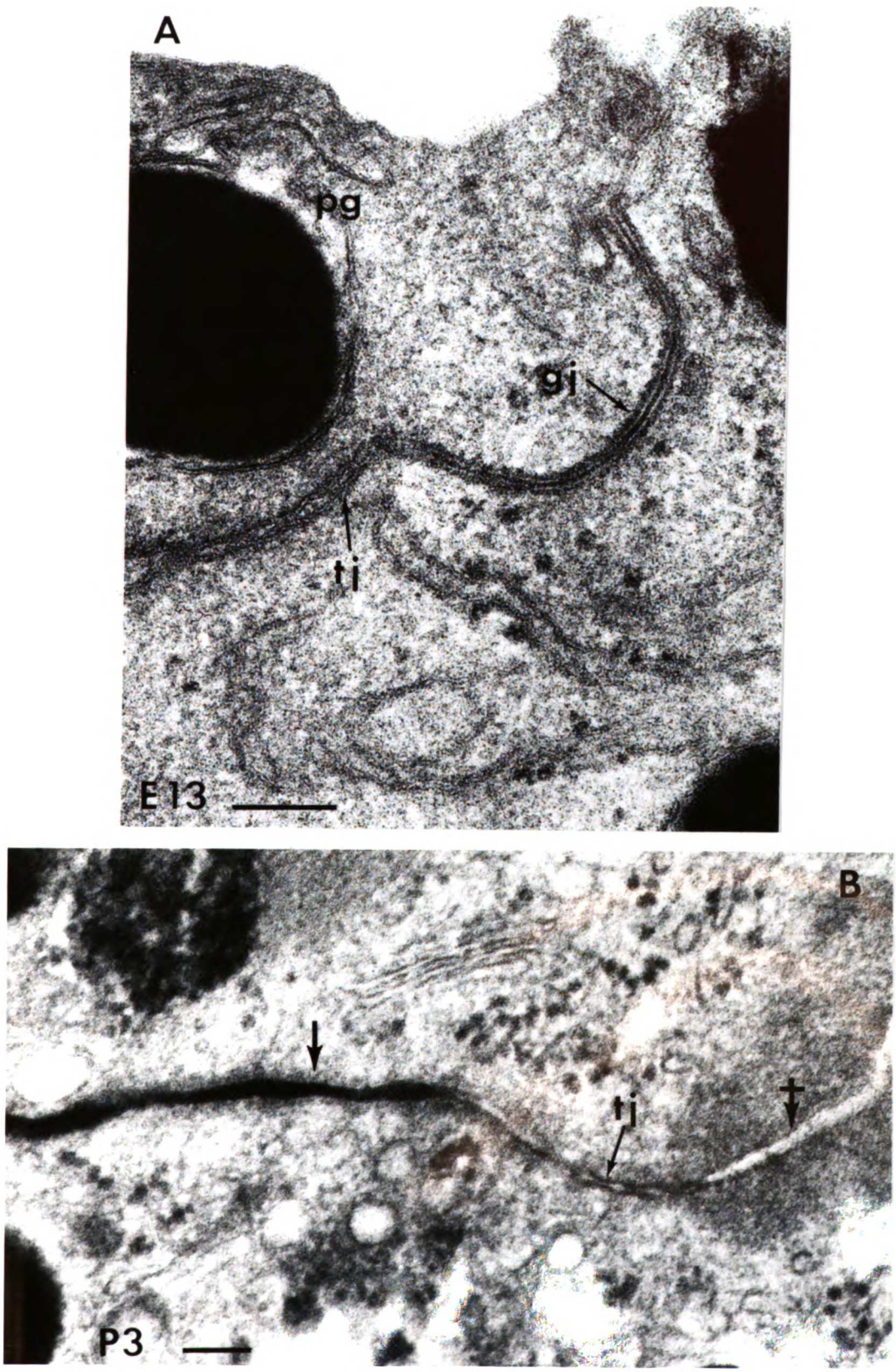

FIGURE 4

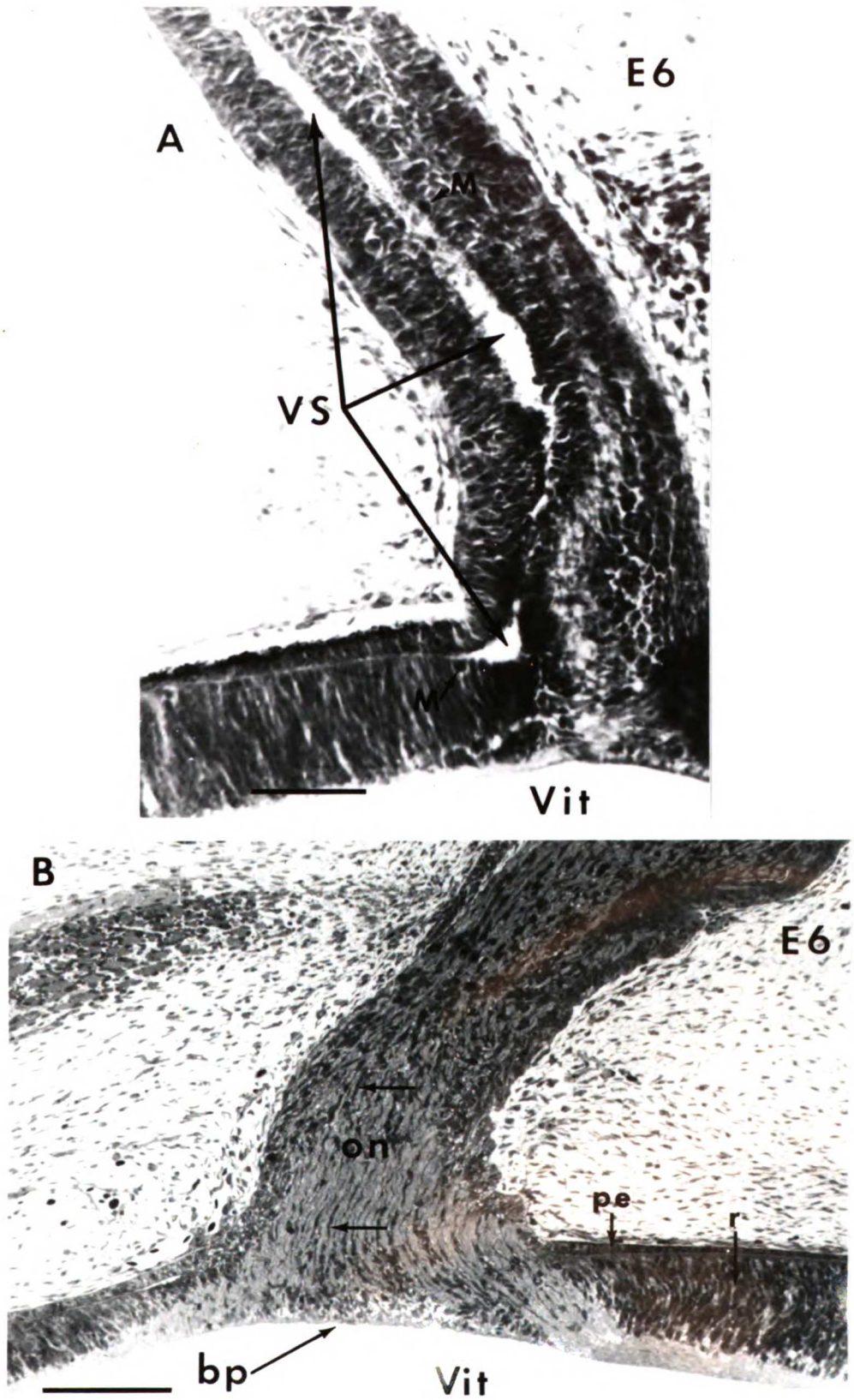

FIGURE 5

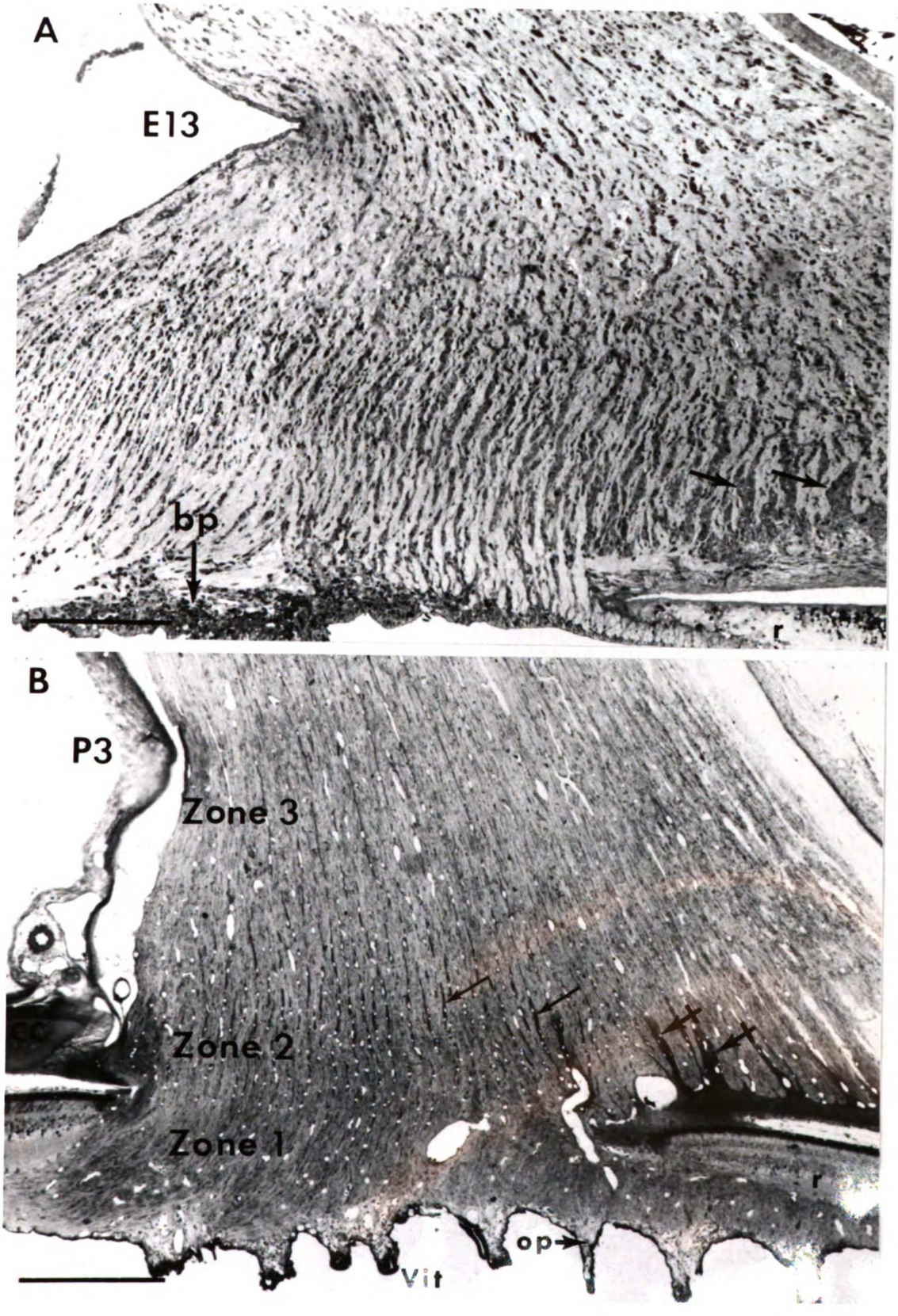

FIGURE 6

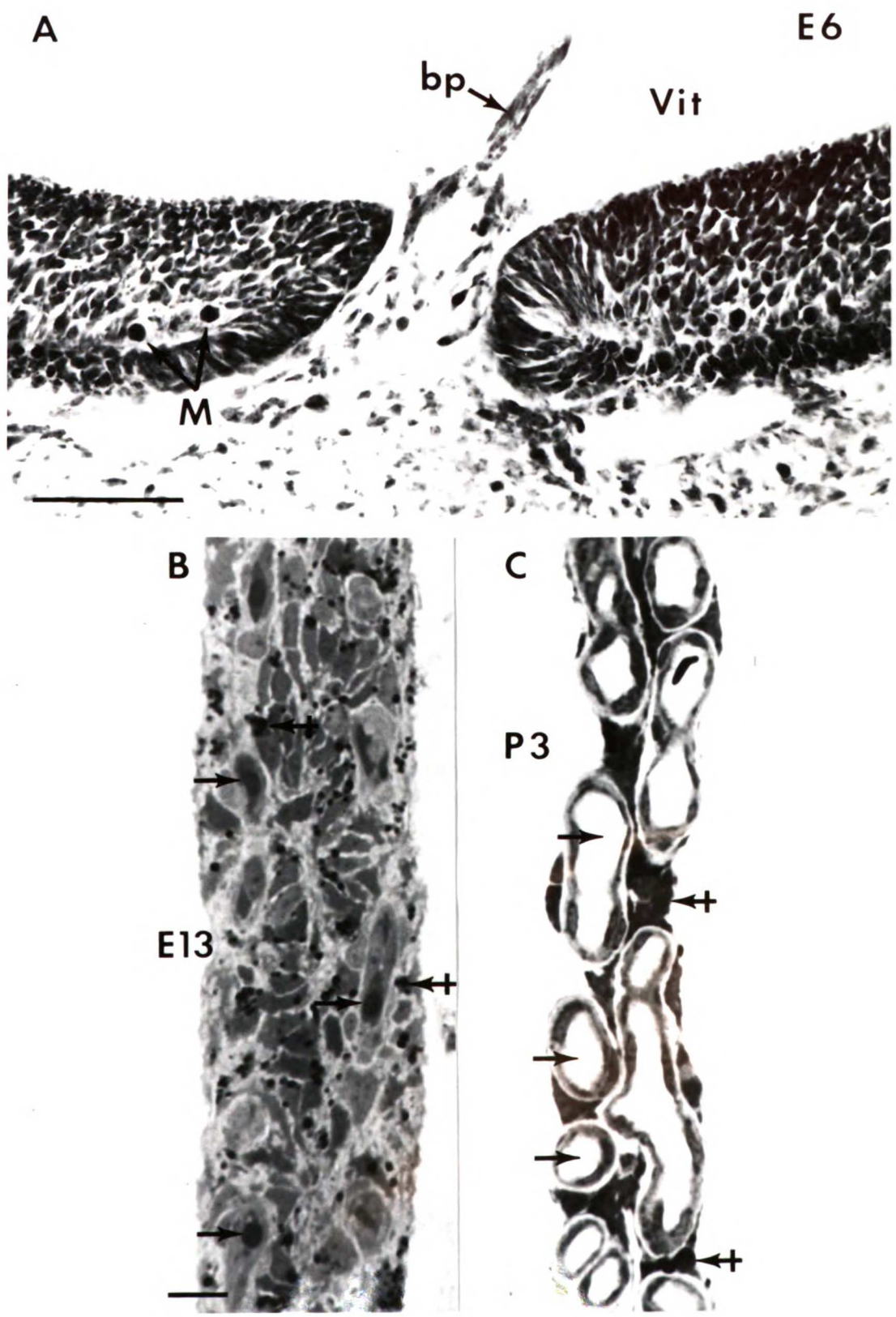

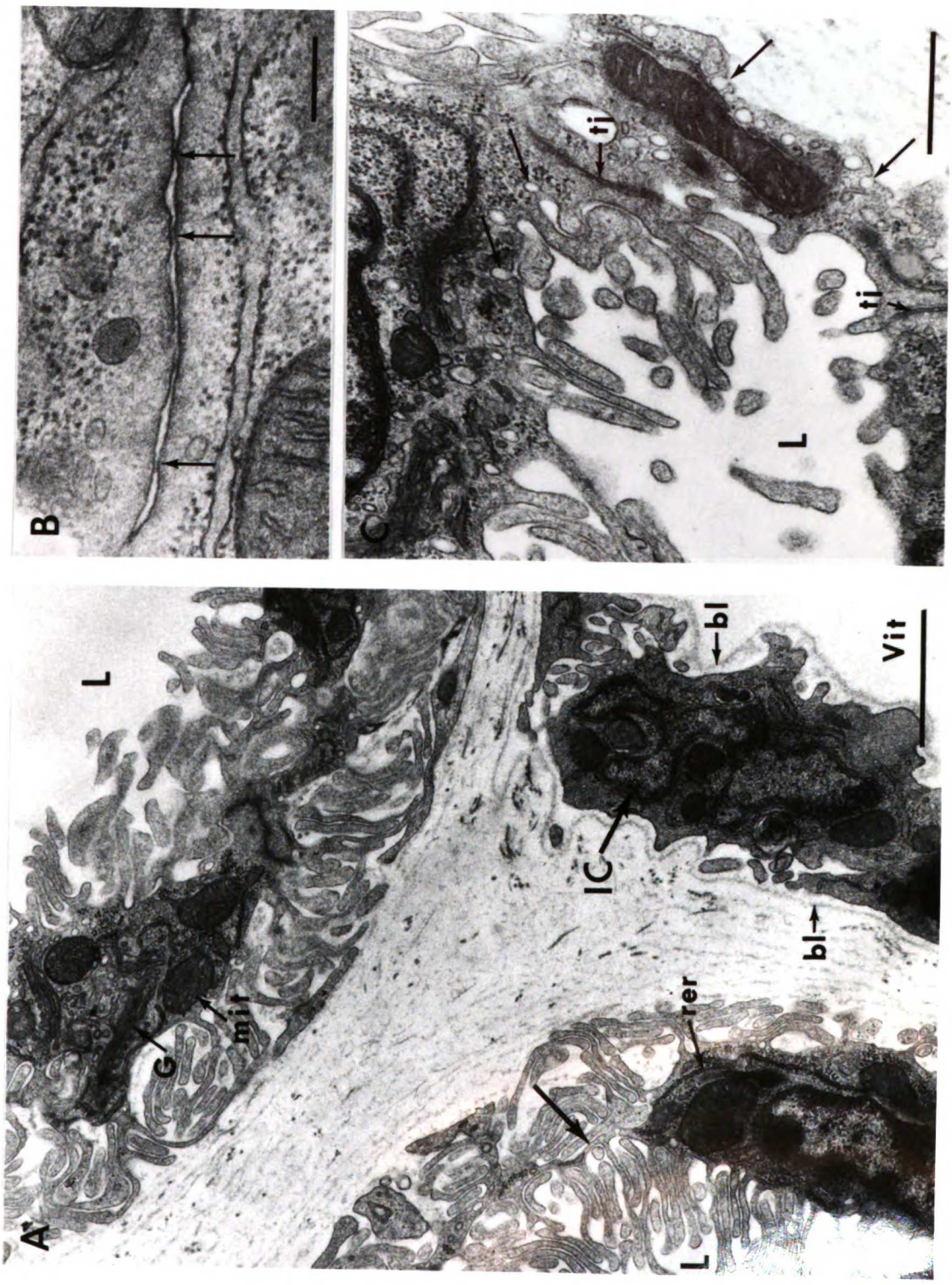

FIGURE 7

FIGURE 8

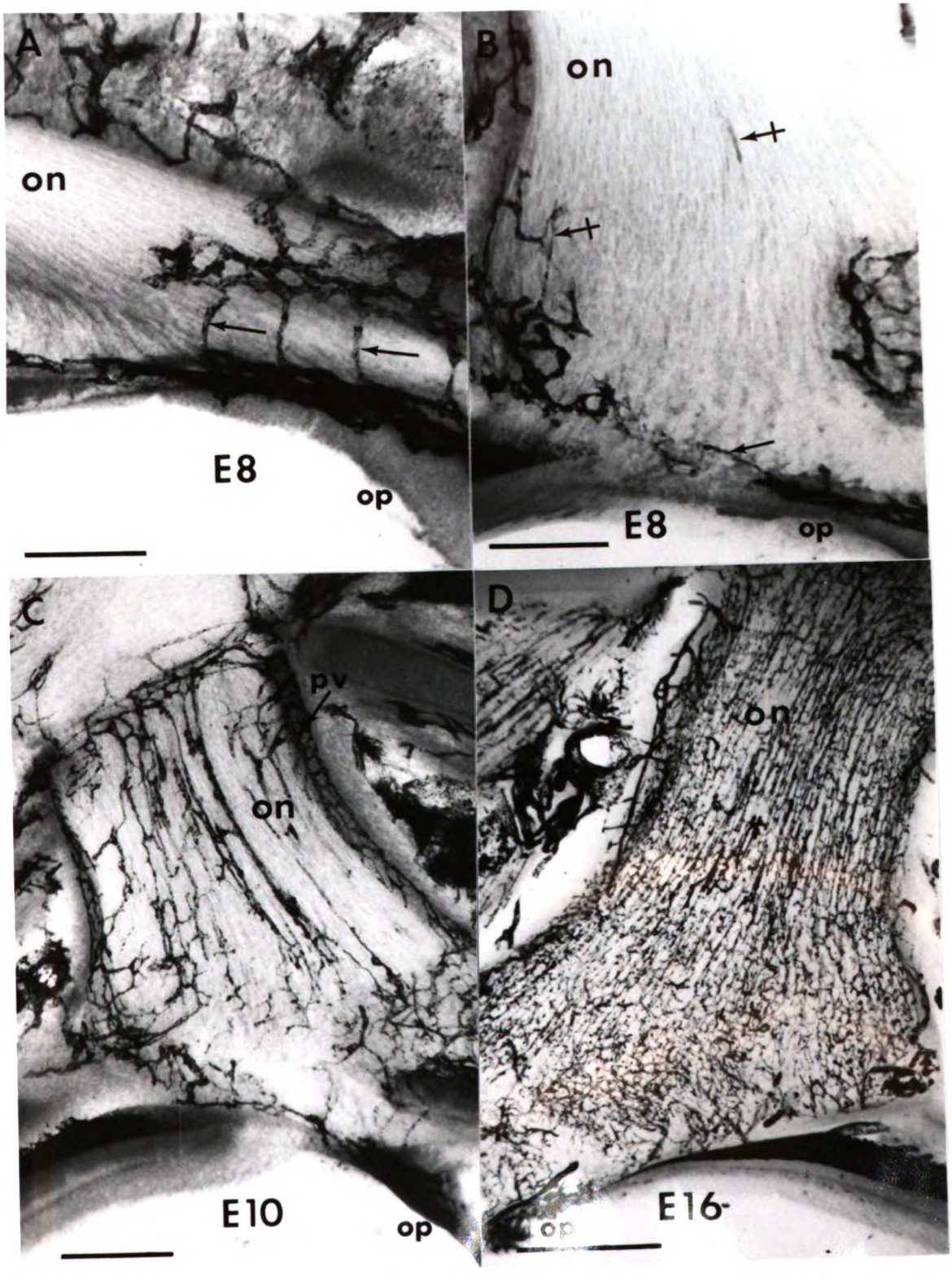

FIGURE 9

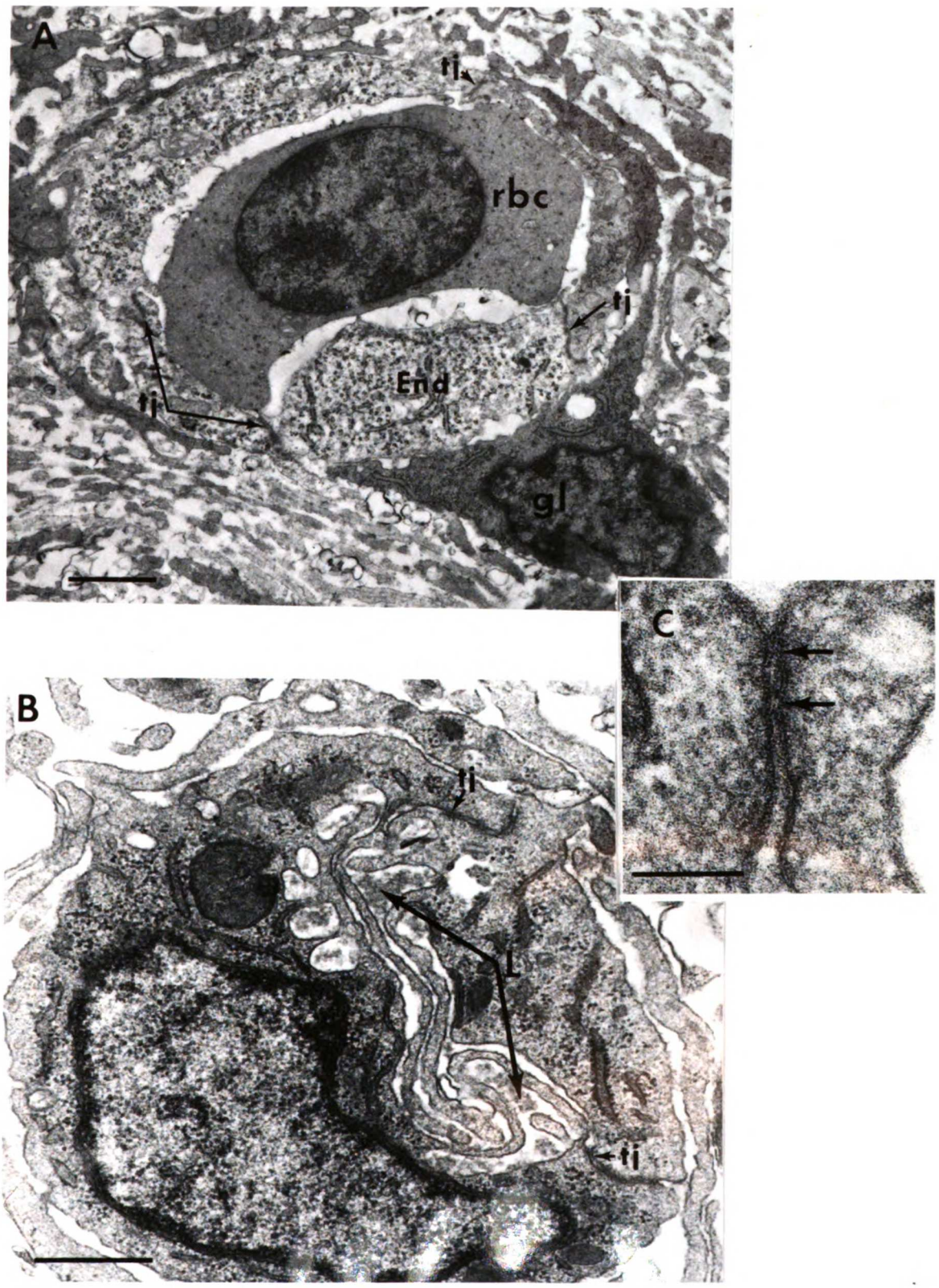

FIGURE 10

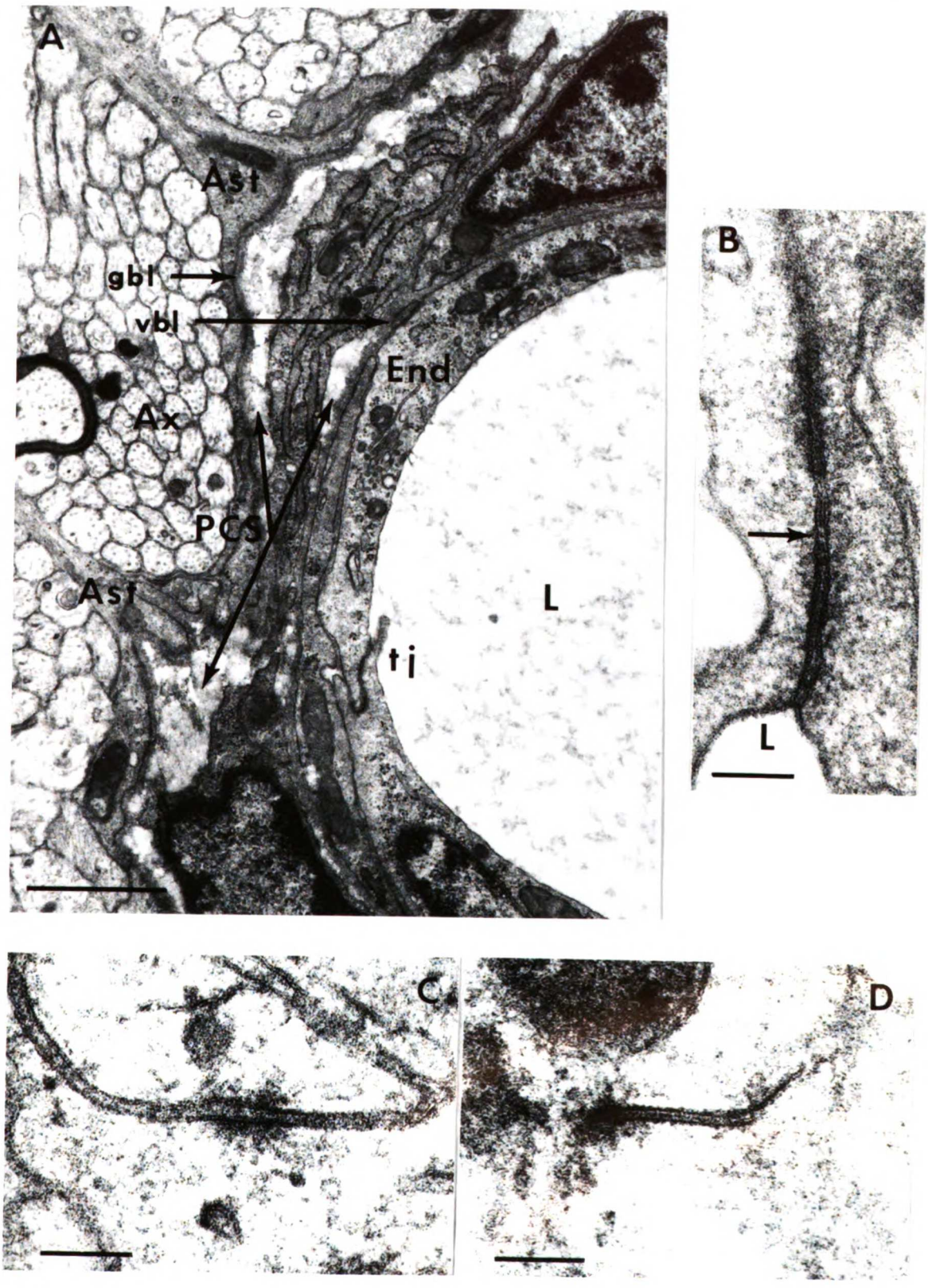

FIGURE 11

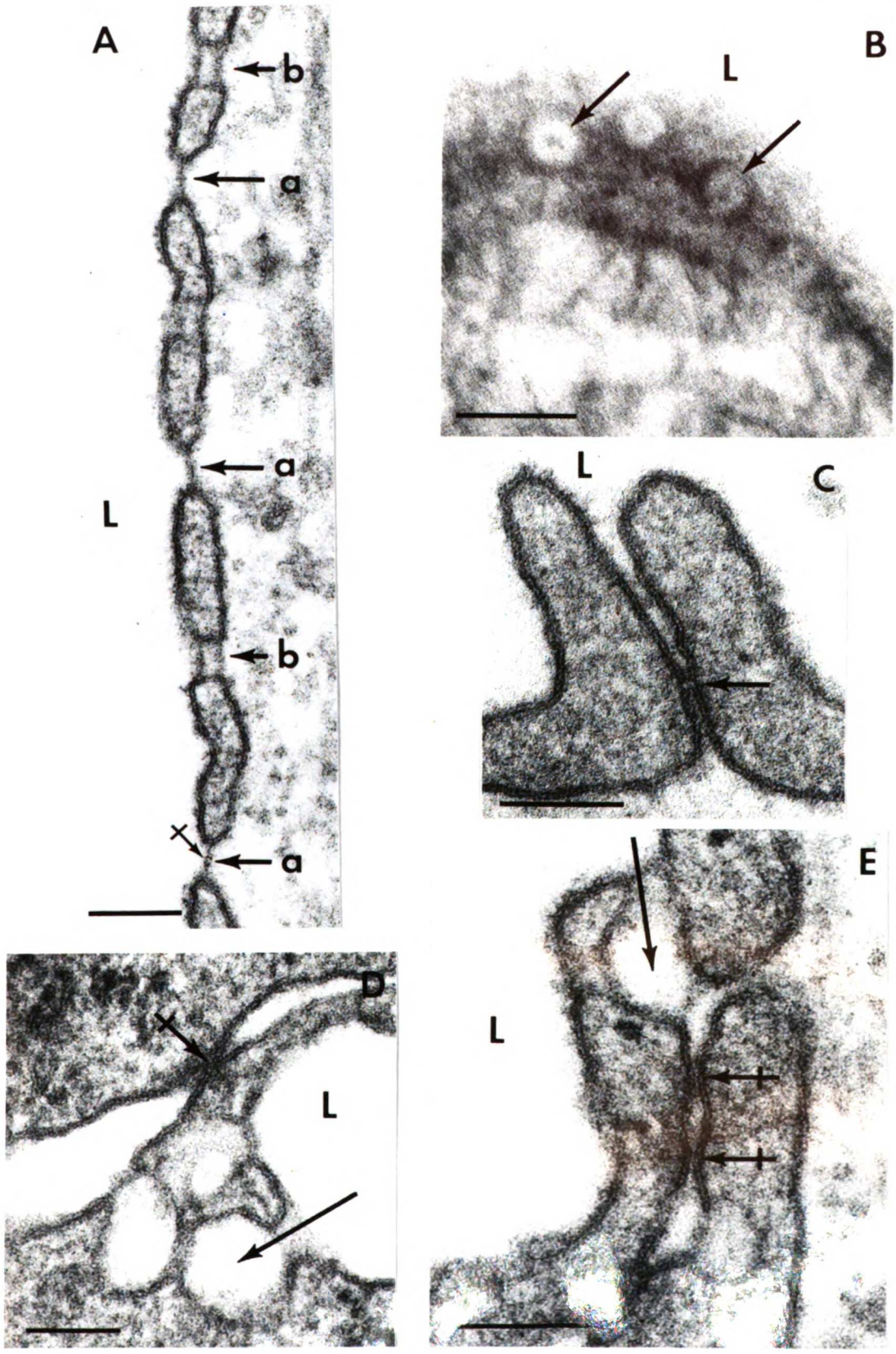

FIGURE 12

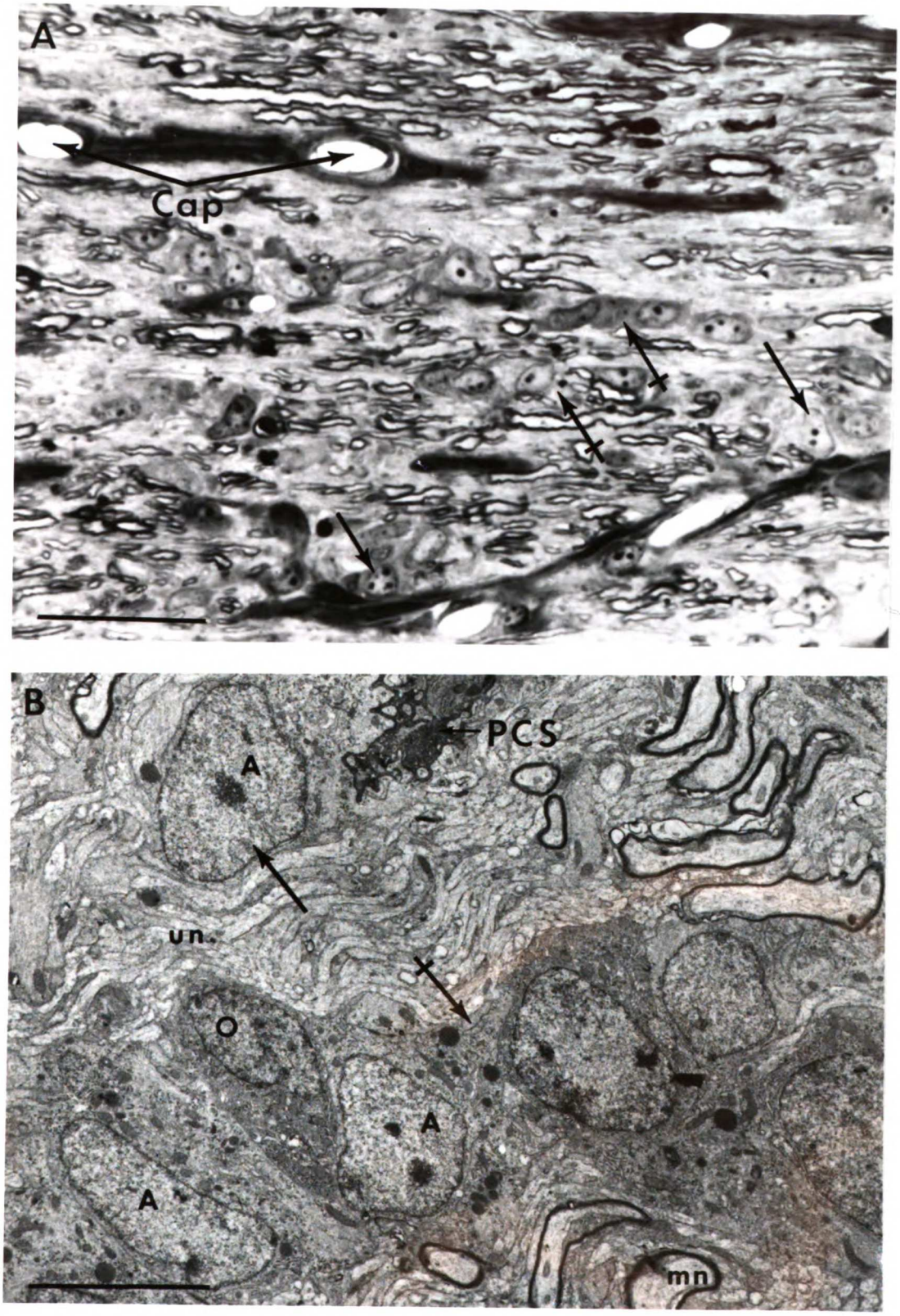

FIGURE 13

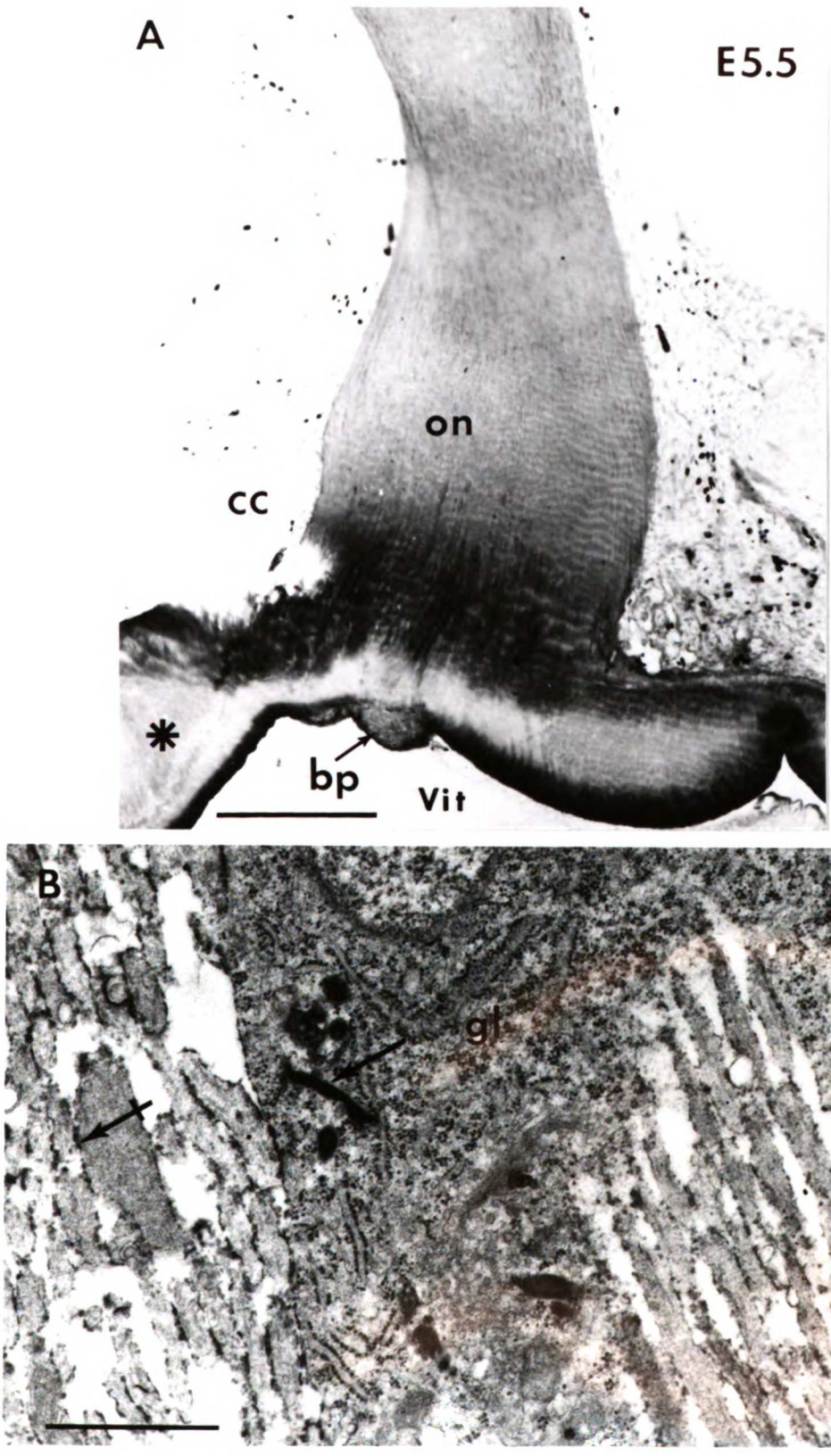

FIGURE 14

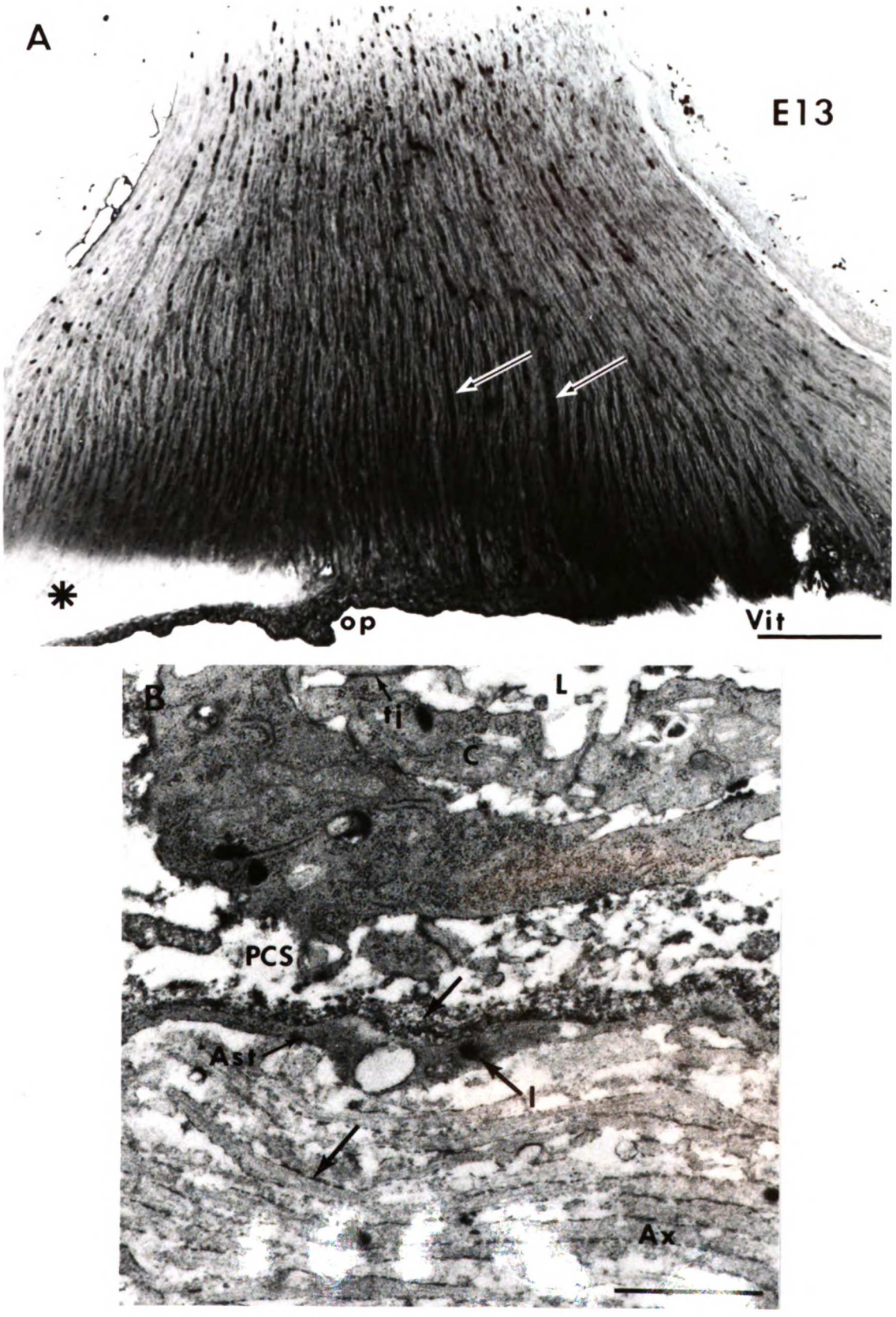

FIGURE 15

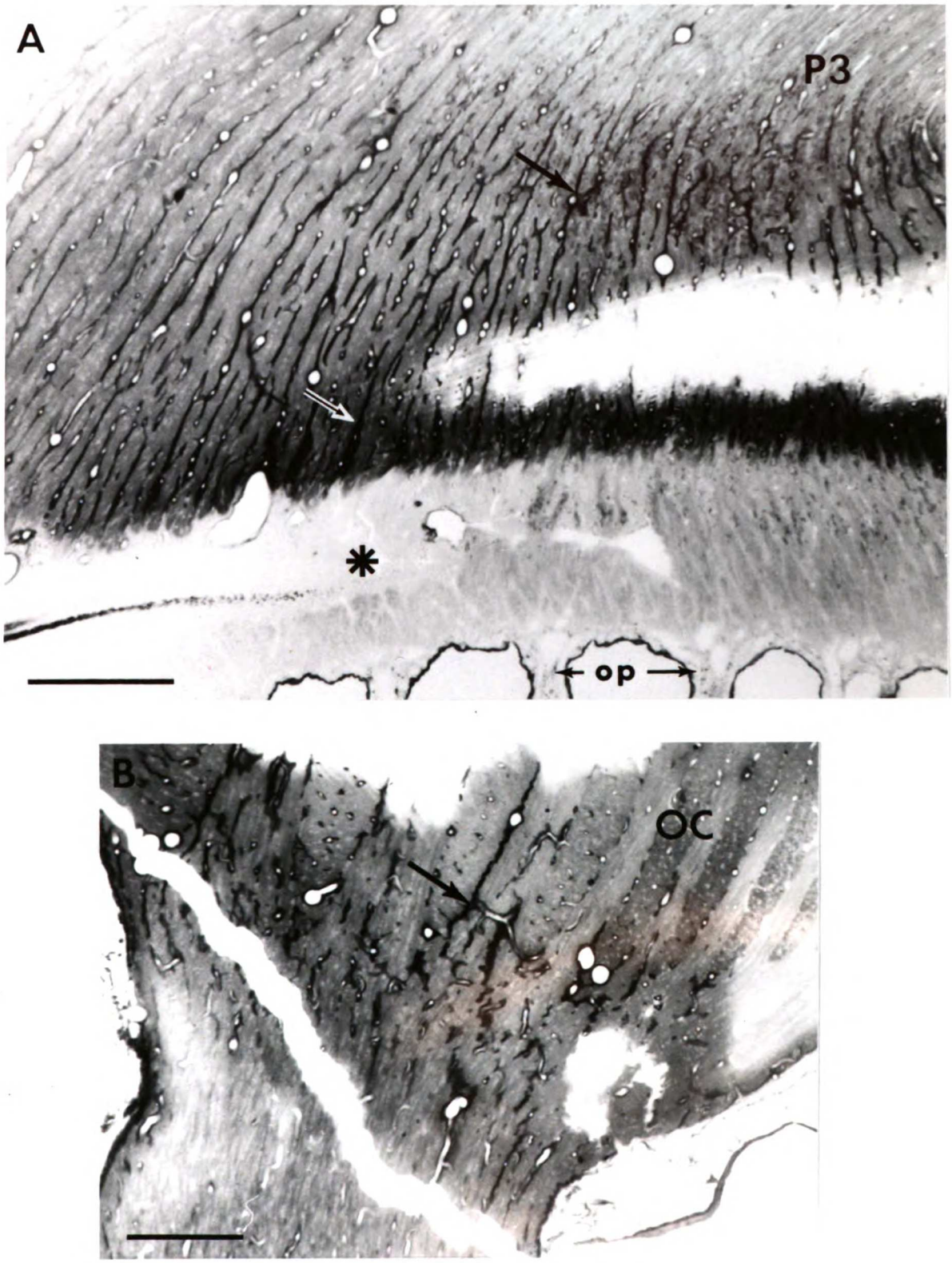

FIGURE 16

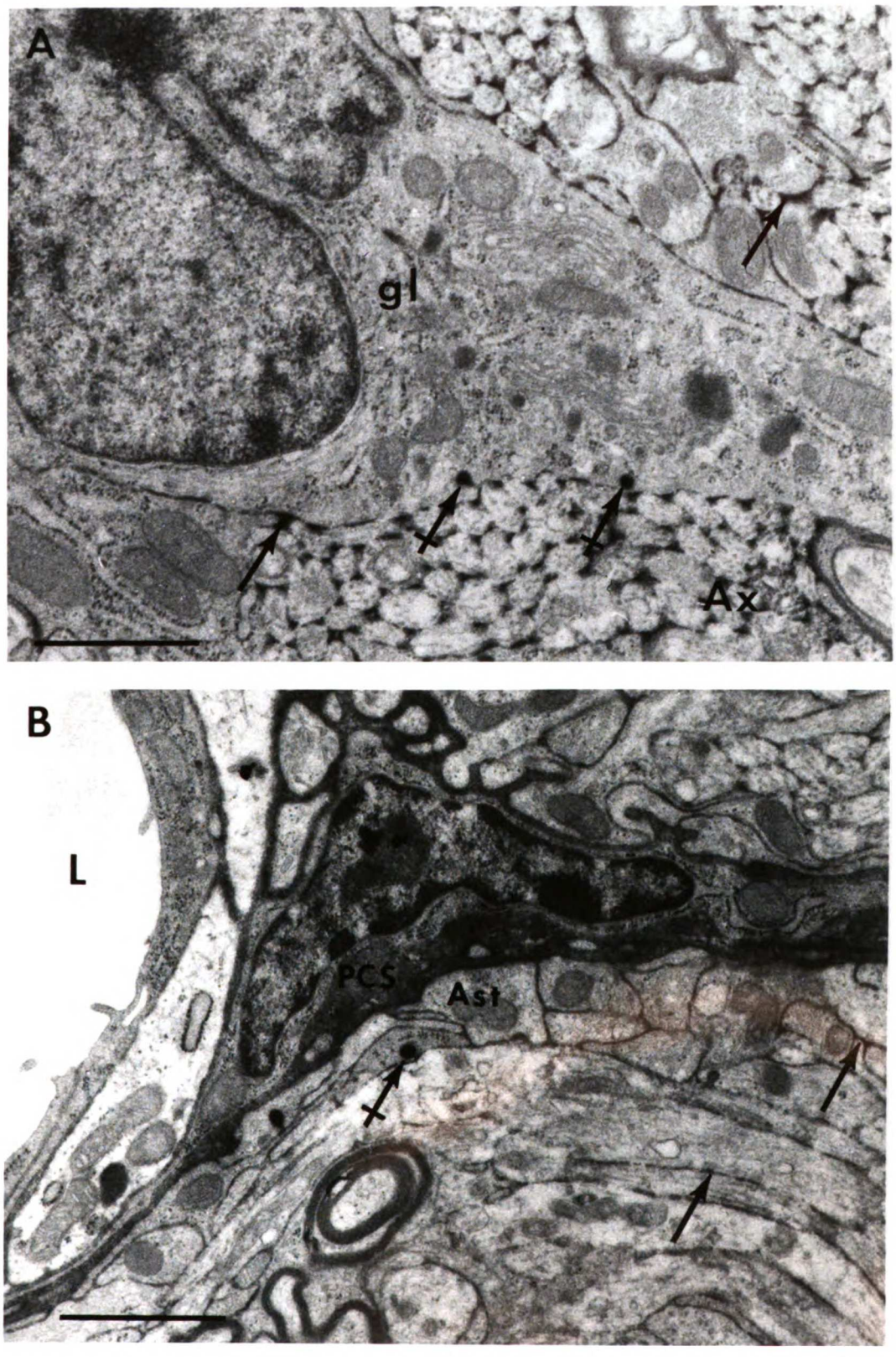

FIGURE 17

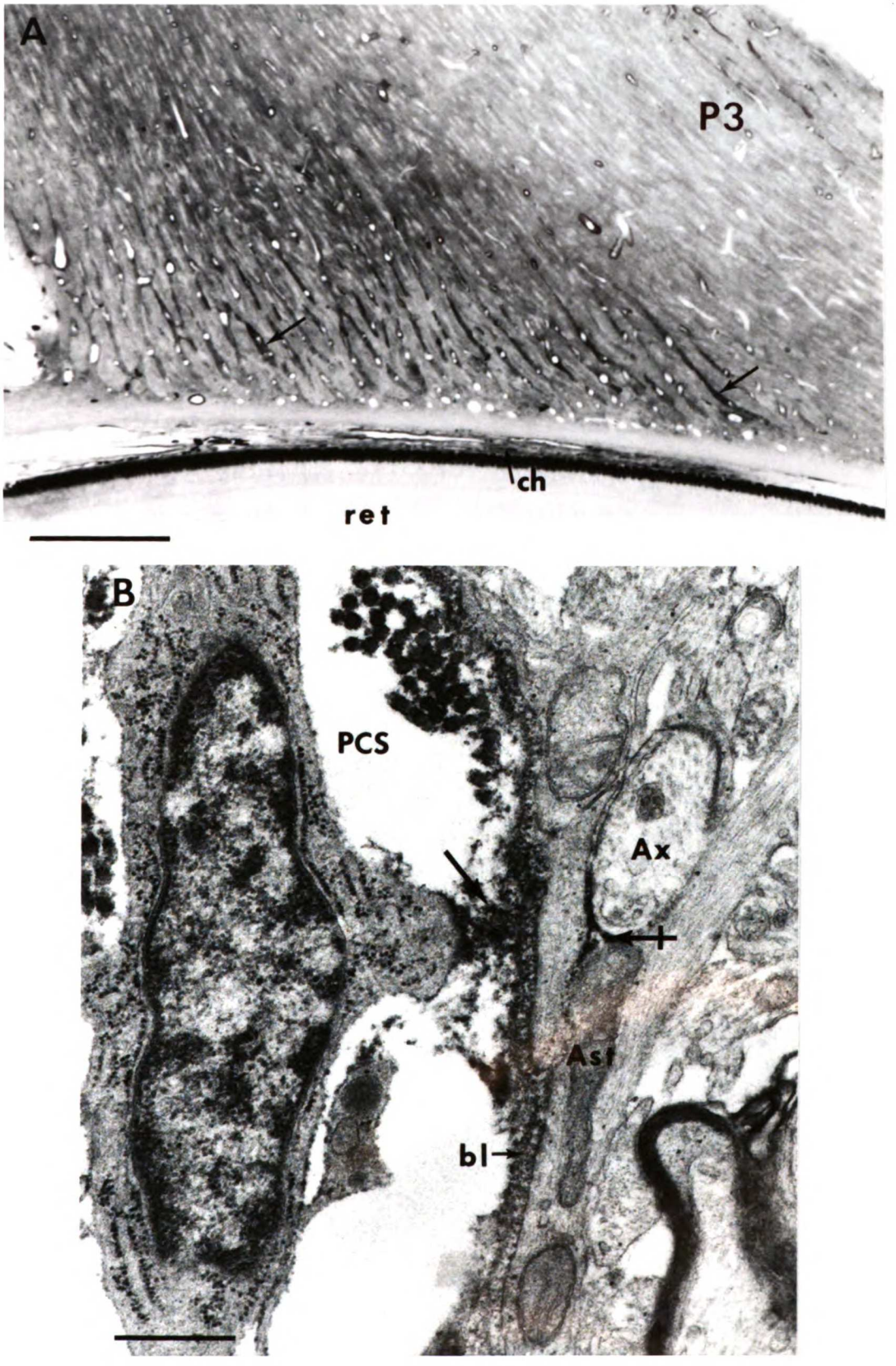

FIGURE 18

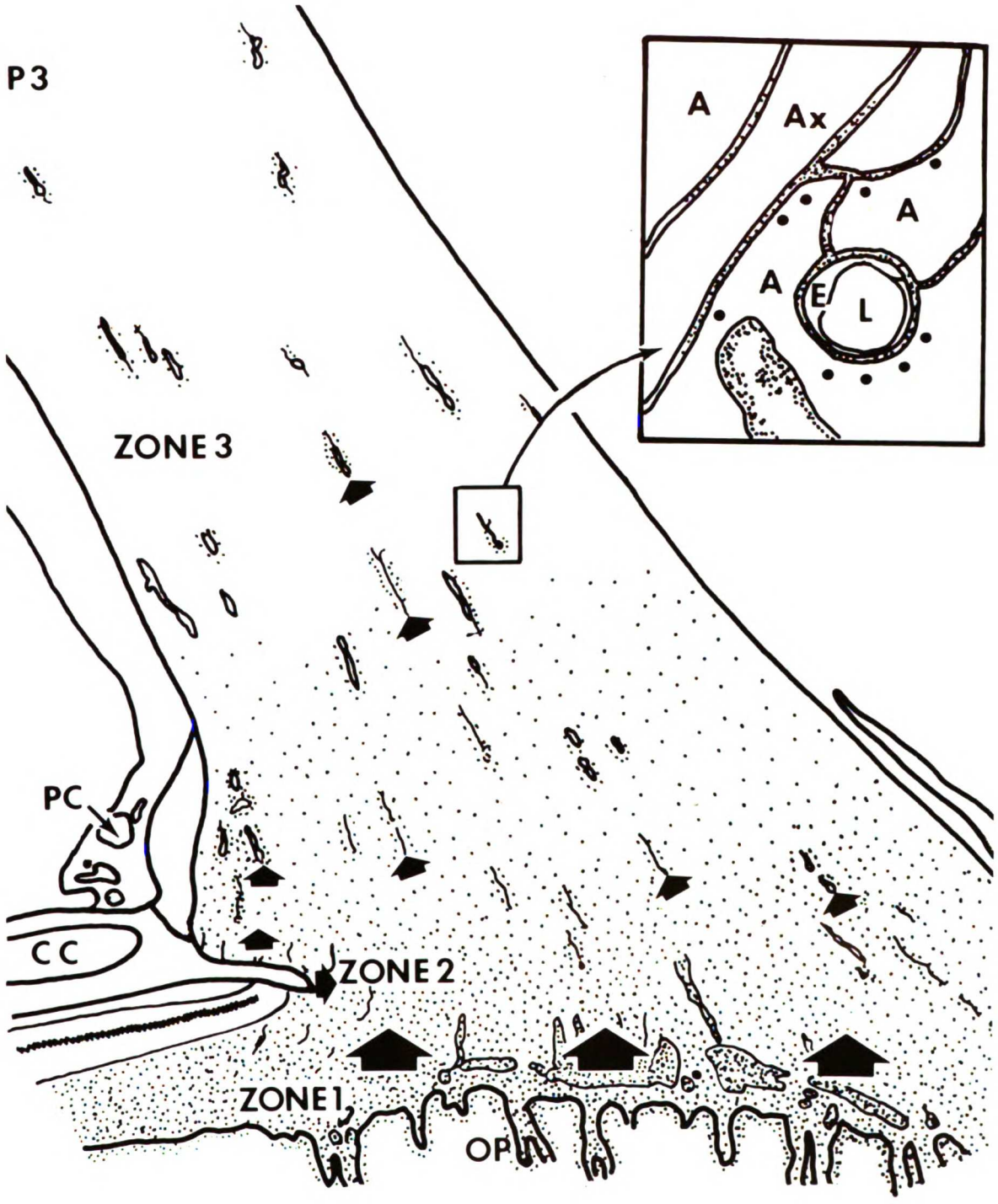

FIGURE 19

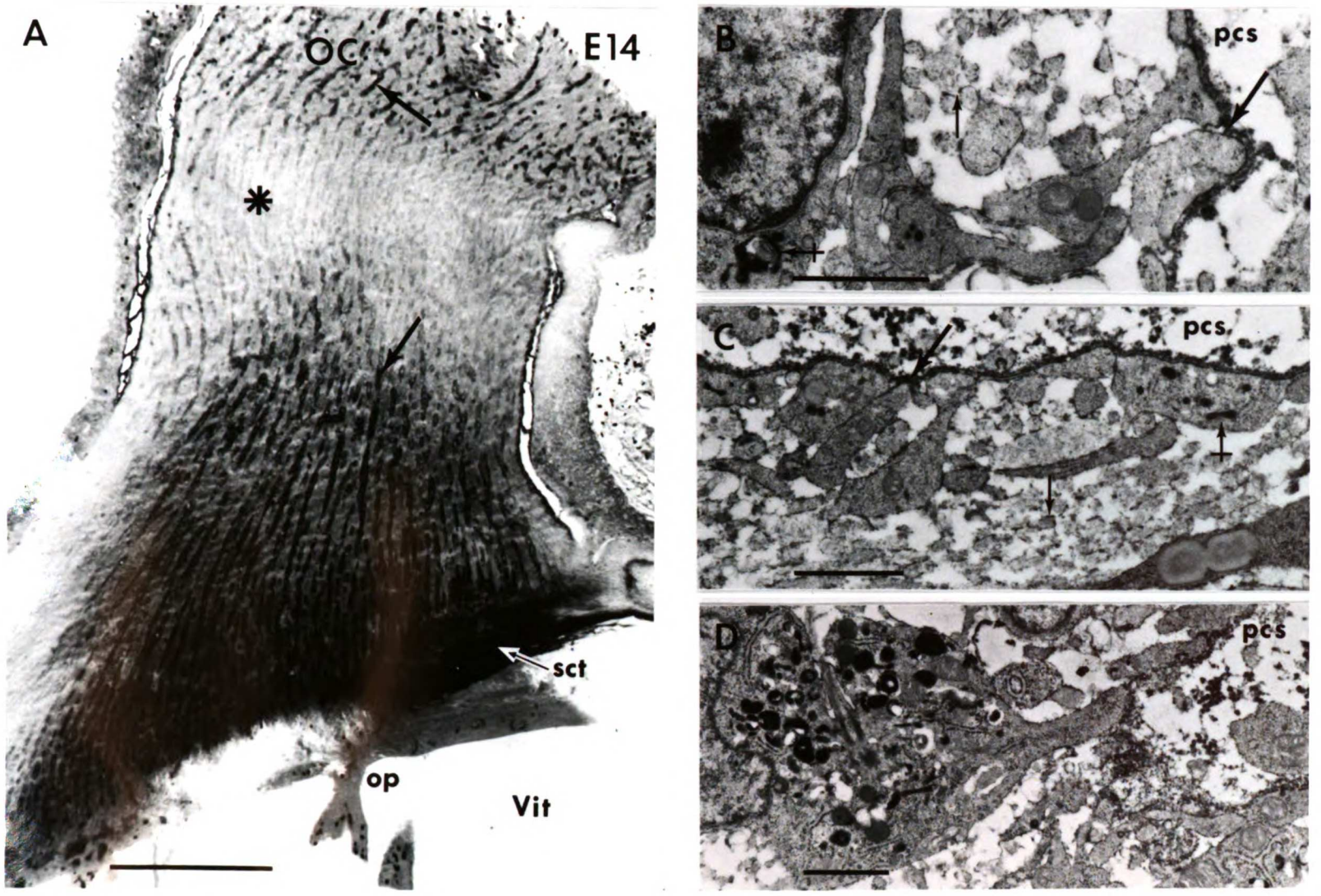

FIGURE 20

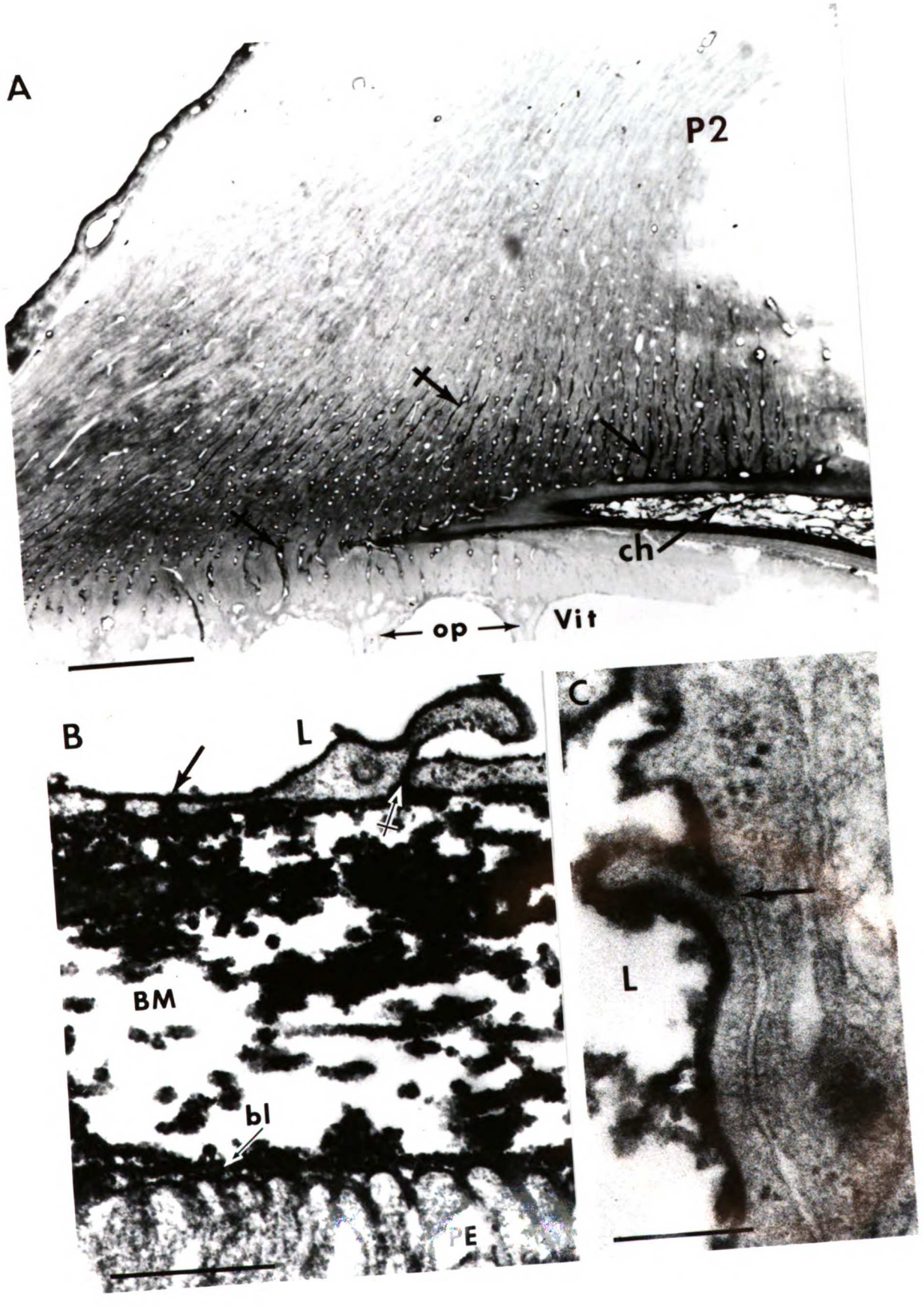

FIGURE 21

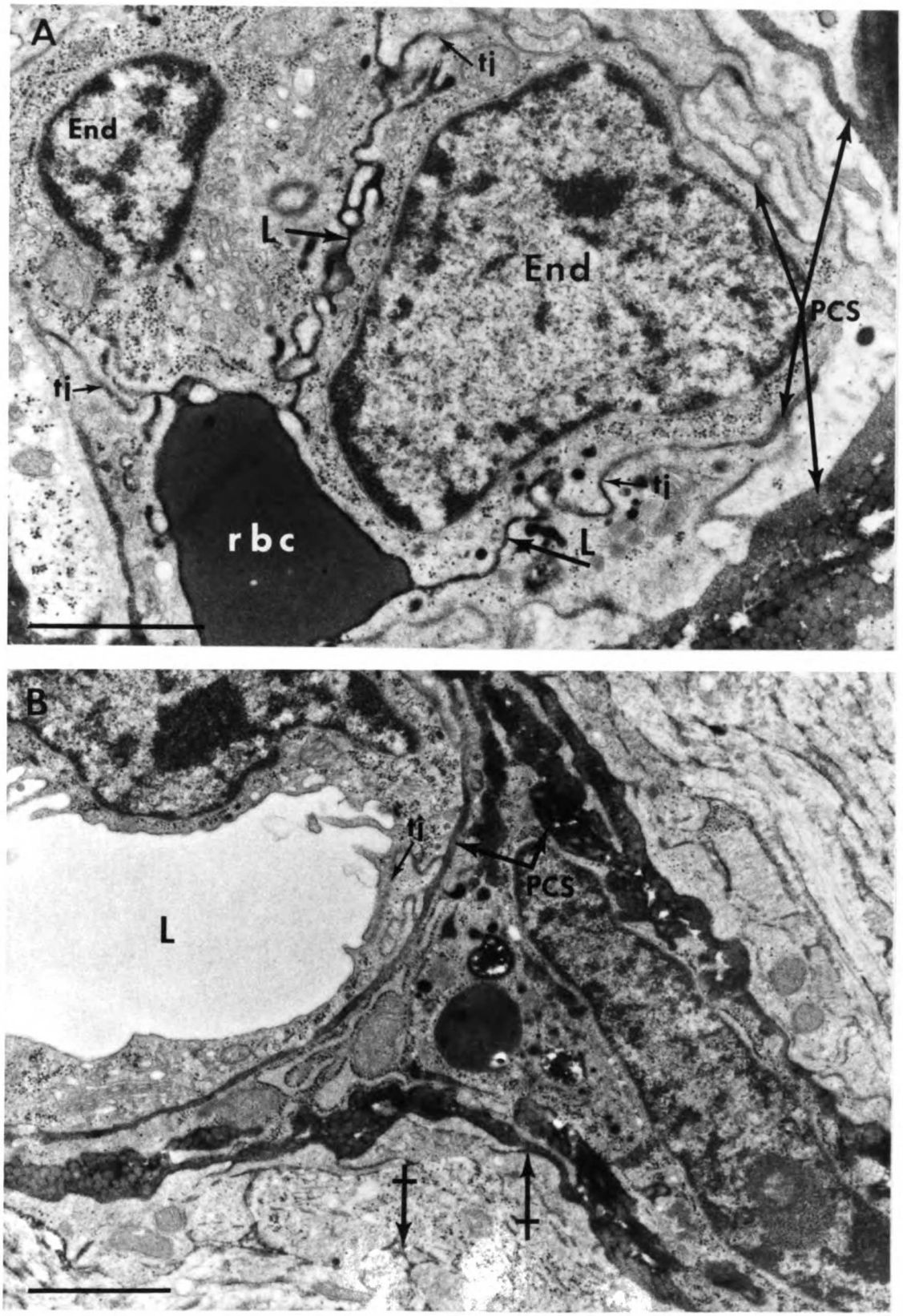

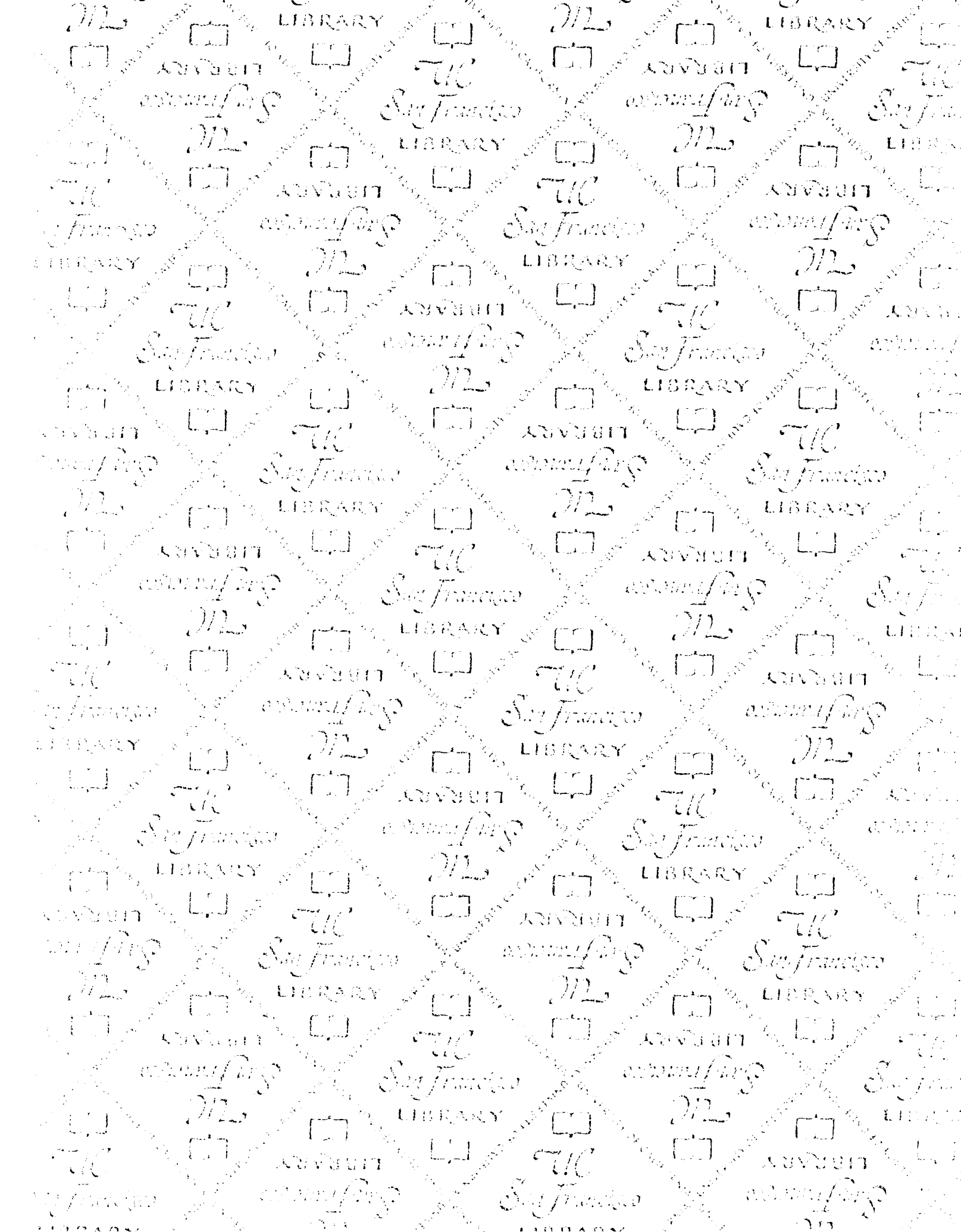
SF
San Francisco
LIBRARY